FINAL REPORT

TRANSFER FUNCTIONS IN MATHEMATICAL SIMULATION FOR RELIABILITY PREDICTION

F491-2
AF 30(602)2376

PREPARED FOR

RELIABILITY TECHNIQUES GROUP
APPLIED RESEARCH LABORATORY
ROME AIR DEVELOPMENT CENTER
AIR FORCE SYSTEMS COMMAND
UNITED STATES AIR FORCE
GRIFFISS AIR FORCE BASE
NEW YORK

FOREWORD

This effort is part of an overall program whose object is the investigation, development and application of techniques which may be utilized to predict electronic circuit and system reliability, both initial (time zero) and time dependent. The investigation of prediction techniques and tools (i. e., linearization, Monte Carlo, computer poles and zeros analysis, regression analysis) conducted by the contractor during a preliminary phase of the program is described in RADC-TR-61-299, "Mathematical Simulation for Reliability Prediction".

It was the purpose of the second and current phase to develop transfer functions for selected circuits and to investigate means for deriving system transfer functions by combining the transfer functions of constituent circuits. In follow on, in-house work now underway, RADC is using the above circuits to empirically evaluate each of the prediction techniques investigated in phase one.

In order to assure that the circuit functions chosen would be appropriate to typical circuit functions encountered in Air Force ground systems, the RADC preferred functional divisions (Report RADC-TR-59-243) were chosen as test vehicles. Utilization of these particular circuit functions lead to the additional advantage that the transfer functions developed and the predictions of performance characteristics (initial and time dependent) will lend themselves readily to form the nucleus of a library of preferred circuit transfer functions with predicted initial and time dependent performance characteristics.

ABSTRACT

This report presents the results of the second phase of the study program for the development of techniques for predicting the reliability of electronic systems from statistical information about the performance of system components. The transfer functions which have been developed in this phase are mathematical models of the actual systems to be evaluated. They are used to determine system performance when component characteristics vary from nominal values as a result of:

(1) Manufacturing and handling

(2) Degradation due to age

(3) Internal and external random stresses

This report concludes that the simulation techniques used are the most efficient for the purpose and have the following distinct advantages.

(1) They provide a means of determining the sensitivity of circuits and systems to the variations noted above. When circuits and systems become complex, then the simpler conventional methods (e. g., differentiation) are no longer feasible for determining circuit sensitivity. At this point, mathematical simulation techniques provide the most efficient and indeed the only means of analyzing and evaluating system performance.

(2) They provide a means of determining not only the tolerance limits but also the shape of the underlying frequency distribution of the particular components used in the circuit or system under investigation.

(3) They provide an unambiguous definition of failure.

(4) They provide a means of assessing the relative merits of competing systems.

(5) They allow the transfer function to be expressed conveniently in matrix form so that conventional routines available to modern computers can be utilized. Hence, the analytical expressions of system performance, necessary even for the most rudimentary statistical design techniques are unnecessary. (Such analytical expressions are laborious to form).

(6) They can be used to optimize a system for a given cost.

The circuits analyzed in this report will not only serve as vehicles to substantiate the findings of the first contractual phase, but will in addition serve as a nucleus for a library of preferred designs with defined lifetime characteristics.

CONTRIBUTORS

Rome Air Development Center, Reliability Techniques Group:

Edward Krzysiak
Jerome Klion
Lester Gubbins:

Sylvania Waltham Laboratory:

Irving Bosinoff - Project Manager
Dr. Kurt Arbenz
Thomas Crowder
Donald Fradette
Amiel Goodman
Juliette Herman
Richard Jacobs
Barbara Prutsalis
James Rizik
T. Senecal
Emery Todd

TABLE OF CONTENTS

LIST OF ILLUSTRATIONS

LIST OF ILLUSTRATIONS (Continued)

LIST OF ILLUSTRATIONS (Continued)

LIST OF TABLES

LIST OF TABLES (Continued)

SECTION I

INTRODUCTION

1.1 DISCUSSION OF BASIC CONCEPTS

1.1.1 Transfer Functions

A transfer function is a mathematical function in an equation which relates the characteristics of system performance to the characteristics of component performance and to system inputs. This is expressed mathematically by:

$$z_i = F_t(x_1, x_2 \cdots x_n, y_1, y_2 \cdots y_n) \tag{1}$$

where the z_i represent system performance characteristics, the x_i represent component characteristics, the y_i represent inputs into the system, and F_t is the transfer function.

One elegant method for actually solving for the transfer functions describing a particular circuit is that presented in [1, 2]. Here one writes the circuit equations in compact matrix form, for example:

$$\begin{bmatrix} a_{11} & a_{12} \cdots a_{1n} \\ a_{21} & a_{22} \cdots a_{2n} \\ \cdot & \cdot \quad \cdot \\ \cdot & \cdot \quad \cdot \\ \cdot & \cdot \quad \cdot \\ a_{n1} & \quad a_{nn} \end{bmatrix} \begin{bmatrix} z_1 \\ z_2 \\ \cdot \\ \cdot \\ \cdot \\ z_n \end{bmatrix} = \begin{bmatrix} b_1 \\ b_2 \\ \cdot \\ \cdot \\ \cdot \\ b_n \end{bmatrix} \tag{2}$$

The n by n square matrix, called the "transformation matrix", consists of elements which are functions of values of the various system components, such as resistance, capacitance, inductance, etc.

The individual elements of the transformation matrix are functions of the nominal values of the component parameters and are derived from the circuit equations describing the particular circuit; examples of such derivations may be found in Sections III and IV. The b_i are voltage or current constants also obtained from the circuit equations. The elements z_i of the third matrix are the individual transfer functions describing system performance. Following Gabriel Kron, we may say that the transformation matrix dominates the whole problem of reliability prediction. Indeed, once this matrix is known, the task of finding the unknown transfer functions can be made entirely automatic - a mere mechanical routine. If the transfer matrix is non-singular, then the unknown transfer matrix [z] can be found by:

$$[z] = [A]^{-1} [B] \tag{3}$$

Equation (3) thus enables one to find the z_i described in (1) in a convenient and compact form.

This basic procedure of finding transfer functions can be used to perform any one of three different types of circuit analysis:

1. DC Analysis: The performance criteria are the quiescent currents and voltages.

2. AC Analysis: The performance criteria are the functional relationships between amplitude, phase and frequency.

3. Transient Analysis: The performance criteria are rise and decay time, pulse width, overshoot, etc. Such characteristics are called transient responses.

These three types of analysis together with the use of the transfer functions to perform them can be applied at any level of system or circuit complexity. Specifically, transfer functions can be applied to analyze the performance of an individual circuit, of a subsystem composed of individual circuit, of a system composed of subsystems, and so on ad infinitum.

1.1.2 Monte Carlo

If a system is made up of a large number of components whose characteristics are described in terms of statistical measures, e.g., distribution functions, and whose characteristics may change in time in a probabilistic way, then the system performance criteria may also be determined in a probabilistic way as

functions of the distributions of component characteristics. Thus, the problem of reliability prediction consists in determining the probability distributions of measures of component performance. The functions relating system performance to component characteristics can be found in two ways, analytically (see Appendix IV) or synthetically.

Given the cumulative distribution functions of various characteristics of the components of a system, an integral equation can be formed which relates the corresponding density functions to cumulative distribution functions of characteristics of over-all system performance. When the system or the circuit is relatively simple, i. e., when the underlying density functions are normal and the components are either all in series or all in parallel, then the integral equation can be solved by analytic means (see Appendix IV). However, as soon as the circuit becomes in any way more complex, or if the underlying density functions are no longer normal, then analytic means are no longer practical and statistical methods. of solving this integral equation must be applied. The statistical sampling methods used to solve such integral equations are called Monte Carlo methods or mathematical simulation methods. Examples of the use of this method can be found in Section III and Section IV of this report, as well as in [3]. For a general introduction to Monte Carlo methods, see also [4].

Before concluding, it may help to consider an example of the application of Monte Carlo methods to the solution of an area integral. Suppose a closed curve to be traced on a plane surface in the form of a square, as shown below. On this surface, a coordinate system is superimposed. A source of pairs of random numbers is available, any pair corresponding to a point on the square, with the condition that the random pairs are uniformly distributed. This means that a random point may fall anywhere on the surface with equal likelihood. If these random pairs are classified into two groups according to whether they fall inside or outside of the closed curve, then the ratio of the area inside the curve to the total area is approximated by the ratio of the points falling inside the curve to the total number of random points. The accuracy of this approximation can be increased by increasing the number of random pairs. This example could obviously be extended to three or more dimensions. This illustrates the connection between Monte Carlo methods and integrals, since integrals are used to express areas, volumes, etc. [11].

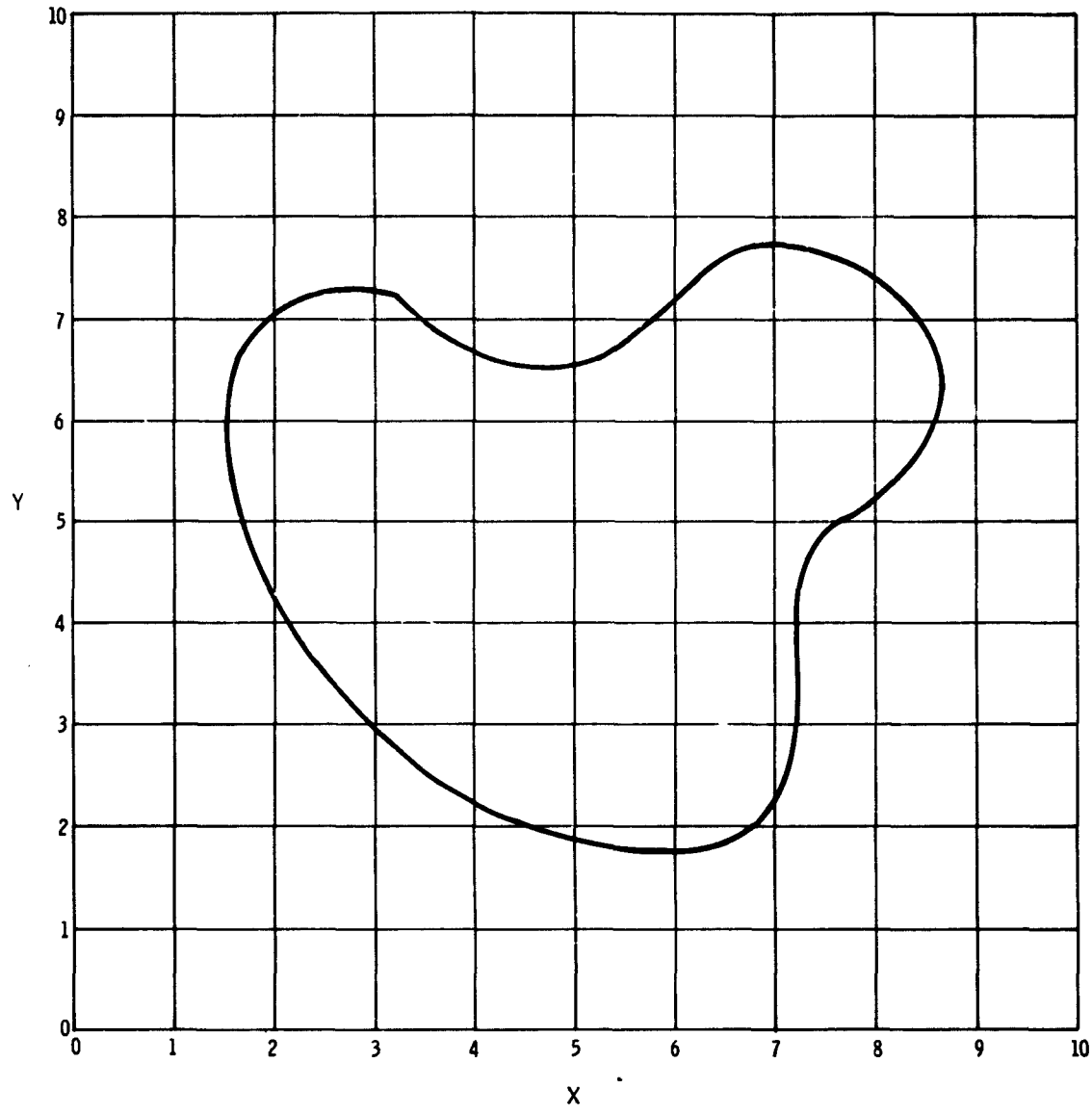

Figure 1. Statistical Solution of Area Integral

SECTION II

PROCEDURES AND COMPUTER APPLICATIONS

2.1 INTRODUCTION

In this section a description is to be found of the actual manner in which concepts and techniques of transfer functions and Monte Carlo methods are applied in a reliability analysis of a circuit or a system of circuits. Next, the role of the computer in this analysis is described followed by the flow charts used in the computer programs, together with relevant explanations as to their use. Finally, there is a formalized description of these procedures suitable for enumerating specifications in contract use.

2.2 GENERAL PROCEDURE

The following is a brief description of the procedure for performing a reliability prediction as outlined in the block diagram in Figure 2.

Step 1: Deterministic Analysis

A set of performance criteria is first received which specifies how the system is to perform. Based on these criteria, a circuit is then selected, preferably from a catalog of standard circuits of proved performance and reliability. An equivalent circuit is then formed which represents the schematic and which is then analyzed so as to yield the circuit equations. From these equations the transfer function is then formed. In many cases these functions can be formulated in the form of a matrix. This matrix is set up with the specified nominal values of the circuit and solved by the computer. At this point, if it is impossible or inconvenient to find an equivalent circuit; or to set up the circuit equations; or to solve the matrices, a regression analysis may be alternatively used to determine the transfer functions. Substituting the nominal values of the component characteristics into the transfer functions, one then obtains the nominal values of the system performance measures represented by each transfer function. The nominal values of the system performance measures are then compared with the nominal system performance criteria. If no suitable agreement occurs, then a new circuit must be chosen and the entire procedure repeated until suitable agreement

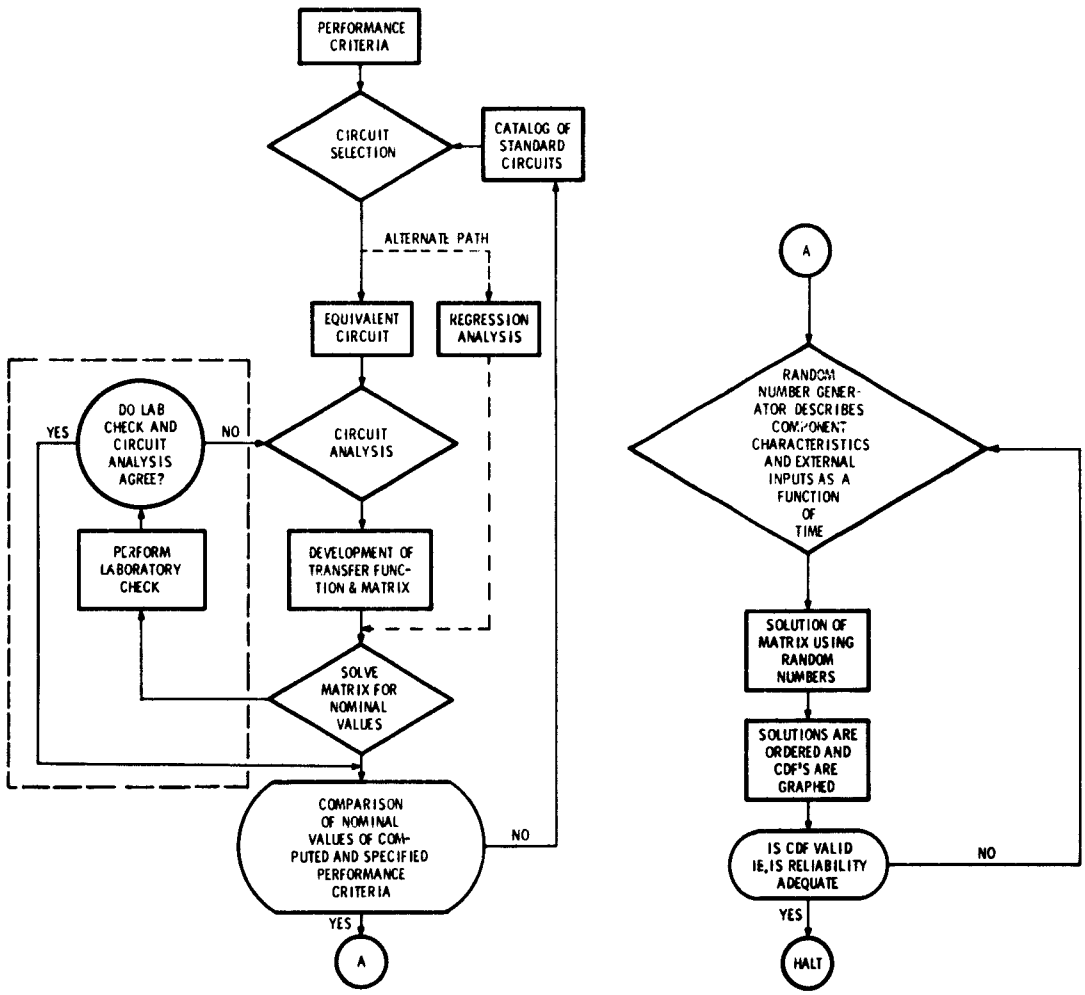

Figure 2. Procedure for Performing Reliability Prediction

is obtained. At this point, an optional experimental check of the calculated nominal values may be undertaken. The computations as well as the laboratory experiments must be repeated until computed and experimental nominal values of performance measures agree.

Step 2: Probabilistic Analysis

Once it has been ascertained that the transfer functions are correct, the computations correct, and the laboratory experiments accurate, so that all nominal values for system performance agree, then the next stage of analysis begins. Random variations in the component characteristics will give rise to random variations in the system performance measures. At this stage, random numbers are first generated according to the rule which describes the random variation in the component characteristics, i.e., the generation of these random numbers simulates the random variation which the component characteristics are subject to. These generated random numbers are then substituted into the transfer functions, which are then evaluated and, in turn, yield sets of random numbers whose variations can be described by a cumulative distribution function (see Appendix I). [5, 6] This cumulative distribution function describes the resulting random variations in the system performance measures. This process can be repeated at intervals to give a description of how the system operates in time. At this point, the cumulative distribution functions describing the system performance measures can be examined to see if they are in accordance with the specified performance criteria. If they are not, the components are changed and the Monte Carlo process described above is repeated until the performance criteria are finally satisfied.

2.3 COMPUTER APPLICATIONS

In this section a description is to be found of the role of the computer in the analysis of the performance of circuits and systems, and in the efficient treatment of the transfer functions, both in the deterministic phase of analysis and in the probabilistic phase of analysis using random numbers. Following this there is a generalized flow chart which, together with relevant explanations, describes the computer program in a general way applicable to any of the circuits or systems discussed. With slight modifications, it can be rearranged to apply to any of the specific circuits or systems in this report.

2.3.1 Role of Computer

In the mathematical simulation procedures the computer plays an indispensable part. In the probabilistic stage of analysis where random numbers are generated and substituted in the transfer functions of a solution, it is impractical to do the work manually. The time-saving speed of the computer is also most desirable in the solution of the matrices in the deterministic stage. The speed and convenience of using the computer not only save time and money, but also take Monte Carlo methods out of the realm of theoretical possibility into practical reality.

A further advantage in the use of computers in this analysis is that one obtains, so to speak, a built-in reference library which completely describes the system and to which one has immediate access. A documented record of circuit performance exists on cards or tape and information retrieval techniques can be used to ascertain immediately the particular characteristics of system or component performance. Given a particular amplifier placed in a particular configuration, for example, one can immediately find the gain, bandwidth and associated distributions.

2.3.2 Generalized Flow Chart and Explanation

Figure 3 shows a generalized flow chart which (with suitable modifications) can be applied to any one of the specific circuits or systems in this report. The general computer routine in the flow chart is as follows: Initially, the machine is prepared for operation by rewinding the magnetic tape and setting the counter to the appropriate number. Next, the various sets of random numbers are generated in accordance with the underlying frequency distributions of the component parameters. This involves a proper adjustment of the random numbers, i.e., fitting them into the proper scale, e.g., 0 to 1, 2.5 to 4.6, 900 to 1100, and ascertaining whether they fall within the proper range within the scale, if the distribution is to be truncated. Next, the random numbers are used to generate and solve the matrix involved in the problem. The solutions are converted for the plotter and the answers written on the magnetic tape. The large loop on the left indicates that the above steps are repeated one at a time for each single random number and that the process comes to a halt only after all the generated random numbers have been utilized (counter = 0). [19]

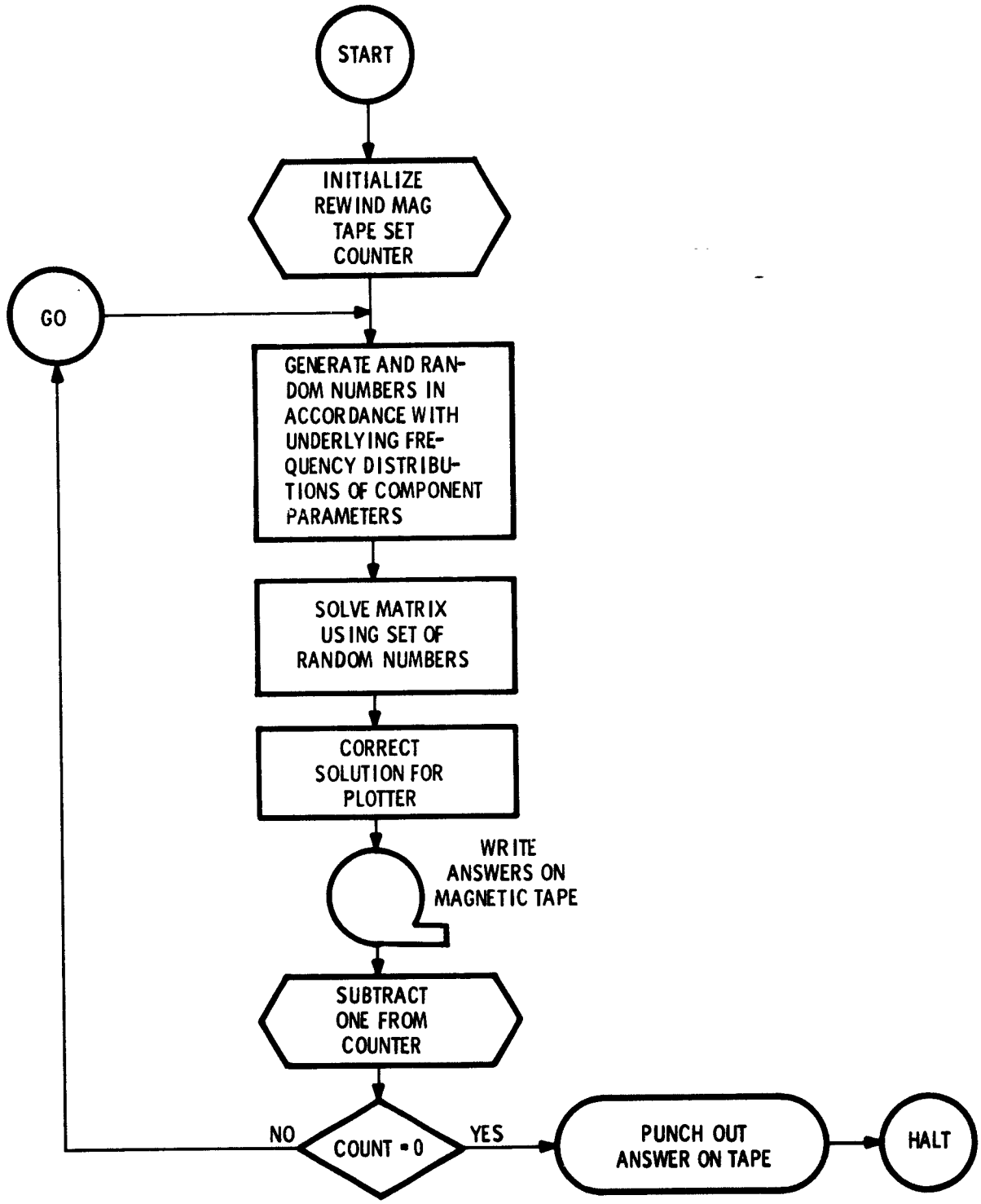

Figure 3. Generalized Flow Chart

2.4 FORMAL PROCEDURE FOR RELIABILITY ANALYSIS

Step 1. A standard circuit or a system composed of standard circuits is selected to satisfy the required performance criteria. In other words, the circuit configuration or particular arrangement of the components is chosen, as opposed to the specific or nominal values and their respective tolerances. If two or more competing circuits exist and are capable of performing similar functions, an analysis may be made of them in order to determine the circuit or system capable of best meeting the requirements.

Step 2. Next, the transfer functions describing each critical performance criterion such as bandwidth, rise time, quiescent current and voltage, noise figure, etc., are generated. The transfer functions are constructed in the following manner:

> First, equivalent circuits are constructed from the schematics, and the mathematical equations describing the equivalent circuits are formulated. From these circuit equations, the matrices contained in the equation for the transfer function $[Z] = [A]^{-1}[B]$ can then be formed.

In cases where it is not technically or economically feasible to define the transfer function analytically, it may be defined experimentally using regression analysis techniques.

Step 3. Next, the matrix equation obtained in Step 2 must be solved by the computer using the specified nominal values of the component characteristics.

Step 4. Once the solution is obtained mathematically, an experimental check on the accuracy of the transfer function may be made in the laboratory by constructing the actual circuit, taking measurements of specified performance criteria and comparing these experimental values with the values obtained analytically from the transfer functions.

Note: It is important to note at this time that the concept of failure must be clearly defined since such a definition is essential for the application of mathematical simulation procedures. In this program, the following definition applies:

A failure is a cessation of ability to perform a specified function or functions within previously established limits on specific performance characteristics, i.e., referring to the cumulative distribution function plotted in Figure 4, a failure is any unit that falls in the shaded area.

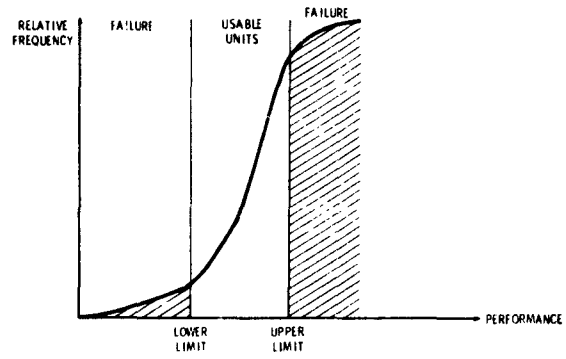

Figure 4. Cumulative Distribution Function of Critical Performance Limits - Used to Define Failures

Step 5. Random numbers are generated according to the rule which describes the random variation in component characteristics, i.e., the generation of these random numbers simulates the random variation which the component characteristics are subject to. These variations may be due to external stresses, e.g. temperature, vibration, humidity, etc., as well as internal stresses.

Note: Random number tables for frequently occurring distrubutions which represent a large class of those elements comprising electronic circuits and systems are available in reference [3], which describes the generation of random numbers having the following distributions:

1. Uniform
2. Exponential
3. Weibull
4. Normal (Gaussian)
5. Log Normal
6. Poisson
7. Chi-Square with even degrees of freedom

For cases where it is not known if any of the above sets of random numbers describe the component, empirical cumulative distribution functions can be generated. The values of the actual components to be used in the system are measured and then ordered to form cumulative distribution functions. These values can then be used directly or can be obtained from a curve that has been fitted to these points.

Step 6. The appropriate random numbers are then substituted into the transfer function, which is then evaluated on the computer. This process results in cumulative distribution functions describing system performance measures[17,18].

Step 6a. If the results of Step 6 are not satisfactory, the components used in Step 5 must be replaced or alternatively the basic design must be modified so that system performance is less dependent on component tolerance (e.g., add feedback, temperature stabilization, etc.).

Step 7. Repeat steps 1 through 6 as required.

SECTION III

CIRCUIT APPLICATIONS

3.1 INTRODUCTION TO CIRCUIT APPLICATIONS

It is the purpose of this section to present an individual circuit analysis of each of the circuits that make up the systems represented in Figures 5 and 6. The Timing Network is composed of conventional circuits chosen from the list of preferred circuits included in the RADC Technical Report - RADC-TR-59-243. The Error Sensing and Readout System is composed of microminiature circuits. Microminiature circuits were chosen since they are of a "state of the art" nature and consequently relatively little is known of their reliability. Therefore, with the cooperation of the Sylvania Microelectronics Laboratory, it was decided to include these circuits as a portion of the Mathematical Simulation Program.

It is possible to present three different analyses of any circuit: namely DC, AC or transient. However, since the purpose of this program is to prove the feasibility of a technique, the main emphasis has been placed on the DC or quiescent current and voltage portions. The techniques, as described below are also applicable to the AC and transient analyses. The major difference in the approach is due to the fact that the equations derived in the AC or transient analyses are time dependent or differential equations, whereas the DC analysis yields algebraic equations. However, it is possible to change these time dependent expressions into algebraic expressions by use of the Laplace Transformation and then, once the solution is obtained, transform it back into the time domain. [10]

The technique which has been referred to above is outlined as follows: Once the circuit or system is chosen, a complete analysis is performed. This is realized, in the DC treatment, by describing the circuit or system with a set of nodal and/or mesh equations. These equations are arranged and a transformation matrix is formed. Contained in this matrix are all of the critical circuit parameters as well as all of the individual components and/or various combinations of these components which will, if varied, cause a change in the value of the corresponding parameter or parameters. The matrix is then solved for the nominal values of the components by means of a computer. At this point it is desirable to

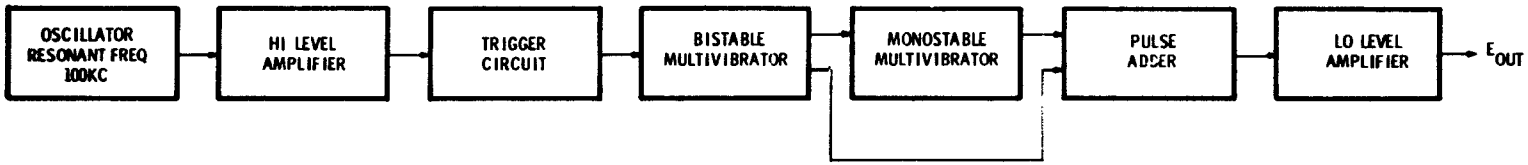

1. THE RESONANT FREQUENCY OF THE OSCILLATOR (100KC) MAY BE OBTAINED BY ADJUSTING THE TIMING CKT
2. FOR THE MONOSTABLE PULSEWIDTH (100 μ SEC)

$$t_p = 31 \times 10^3 C$$

$$100 \times 10^{-6} = 31 \times 10^3 C$$

$$C = 3.3 \times 10^{-9} \approx 0.003 \mu F$$

Since C = C4 + CX (SEE SCHEMATIC)
WHERE CX IS AN EXTERNAL CAPACITOR
AND C4 = 33 $\mu\mu$ F

$$CX = C - C4 = 3.3 \times 10^{-9} - 33 \times 10^{-12} \approx 3.27 \times 10^{-9}$$

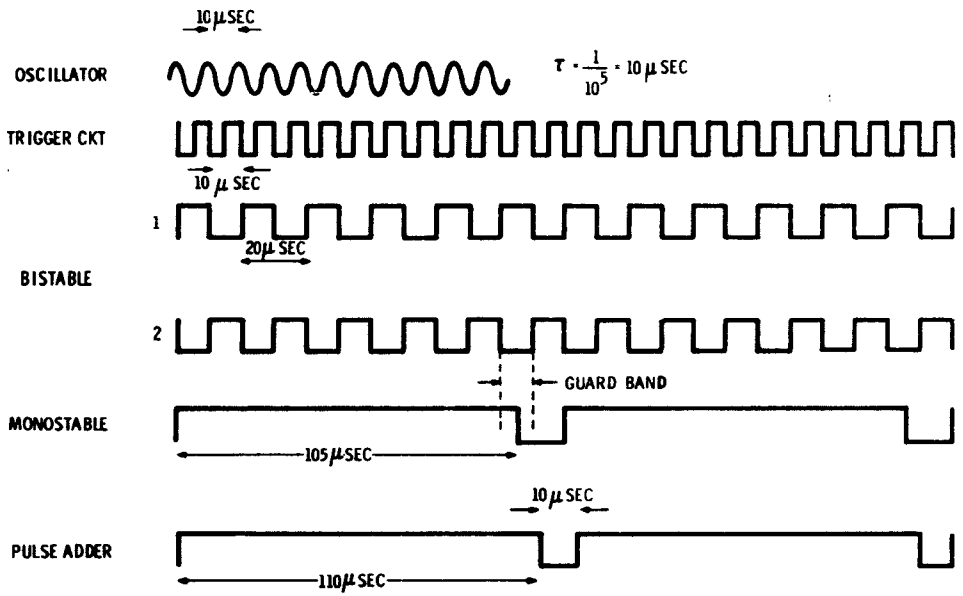

Figure 5. Timing Network

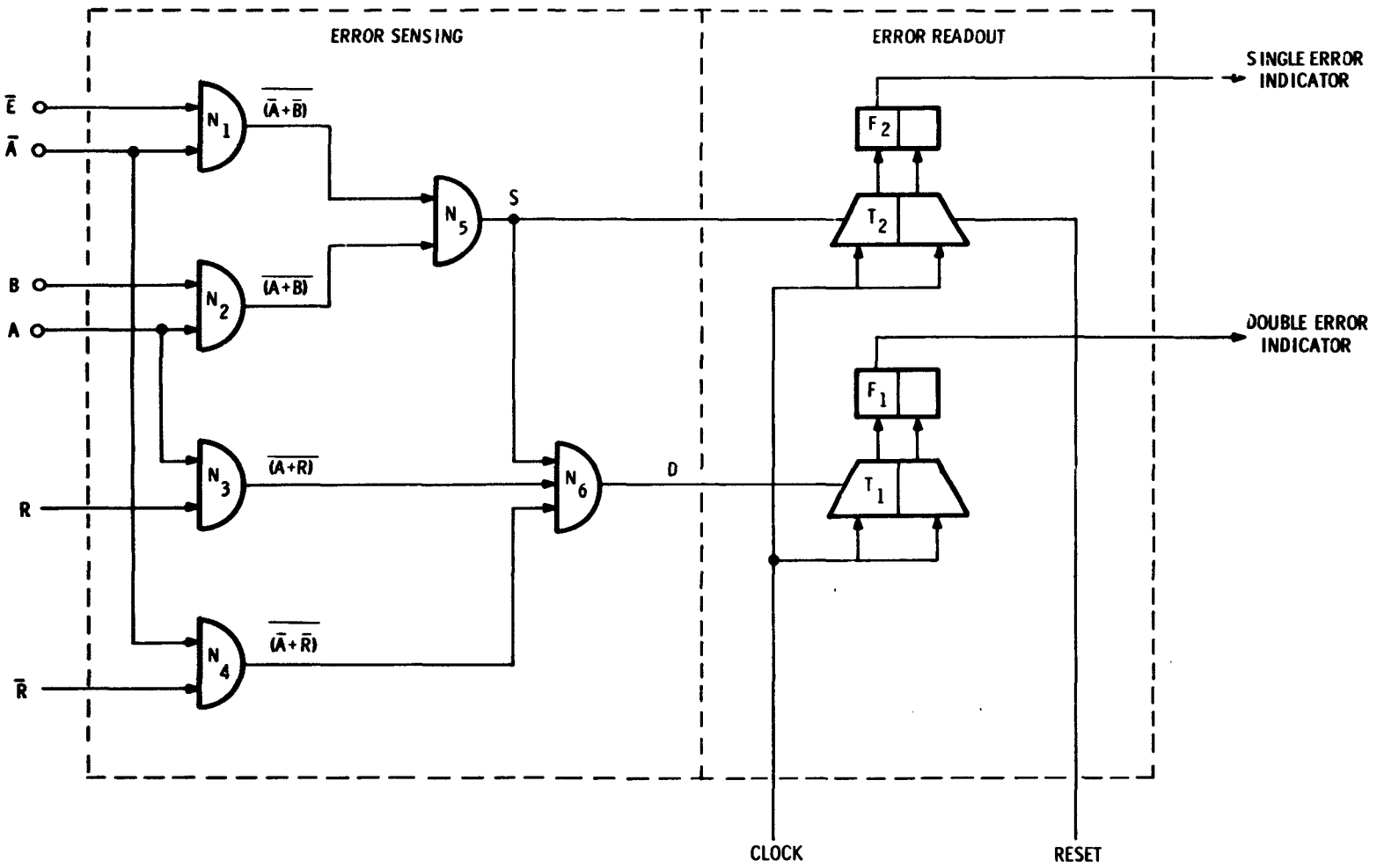

Figure 6. Error Sensing and Readout System

verify the accuracy of the transfer function by measuring the circuit parameters on a breadboard of the particular circuit or system. A comparison of the empirical and analytical values will accomplish the verification. This is the extent to which this section covers this technique; however, Section IV will present the complete solution, the remainder of which is briefly described below.

Sets of random numbers are generated that correspond to the various parts of the circuit or system. The type of random numbers depend upon the type of distribution of the part or parts; i.e., normal, uniform, etc. These random numbers are substituted into the various matrices and the effects on the performance noted. In this manner, it is possible to isolate the most critical parts and, therefore, circuit redesign or maintainability steps may be taken. It is also possible to repeat the above procedure at some time or times in the future by generating new sets of random numbers based upon known characteristics of the particular parts, thus obtaining a prediction of circuit reliability.

3.2 TRANSFER FUNCTIONS OF CONVENTIONAL CIRCUITS

This section presents the transfer functions of a number of circuits chosen from the list of preferred circuits included in the RADC Technical Report - RADC-TR-59-243. [9] The circuits chosen for analyses are preferred circuits of the highest reliability (failure rate wise) which have undergone extensive life test. Reference Report RADC-TR-59-243, "Reliable Preferred Solid State Functional Divisions", and the RADC Reliability Notebook in which it is included. In this report there is some philosophy about the circuits which you may find helpful.

3.2.1 Transfer Function of the Trigger Circuit

This subsection presents an analysis of an emitter coupled binary circuit, commonly known as the Schmitt Trigger, in terms of its transfer functions. [7] The expressions derived are those for the circuit appearing on page 47 of the RADC Technical Report, RADC-TR-59-243. The solutions are in the form of matrices of algebraic equations for the quiescent currents and voltages.

The circuit as analyzed is shown in Figure 7 and functions as a general purpose multivibrator or squaring assembly. The transistors Q_2 and Q_3 perform as emitter followers isolating the timing circuit from external loads; and Q_1 and Q_4, coupled through the common emitter resistor R_7 perform the squaring function. The circuit will accept a sine wave, complex wave, or rectangular input signal and present two DC coupled complementary signals at the output terminals.

A complete solution of the circuit indicates that neither transistor when operating was in a saturated condition. A verification of this fact may be received by an examination of the computer solutions of the base currents for both cases see Tables 2 and 3. From the solutions, it may be seen that the base currents are all negative indicating an impossible situation. As a check on the accuracy of the transfer functions, a breadboard circuit was set up and the various voltages were measured. As may be seen from Table 1, the measured and calculated values compare very closely, thus, confirming the accuracy of the transfer functions.

TABLE 1

COMPARISON OF CALCULATED VS. MEASURED VALUES OF TRIGGER CIRCUIT

A

Q_4 NON-SATURATED, Q_1 OFF			
	V_{E2}	V_{E3}	V_{E4}
CALCULATED	22.1	8.8	7.4
MEASURED	22.5	8.8	8.0

B

Q_1 NON-SATURATED, Q_4 OFF					
	V	V_1	V_{E1}	V_{E2}	V_{E3}
CALCULATED	10.0	-0.7	8.6	8.7	22.3
MEASURED*	11.0	-0.7	9.0	8.6	22.5

*Measured with a positive DC trigger of 12 v.

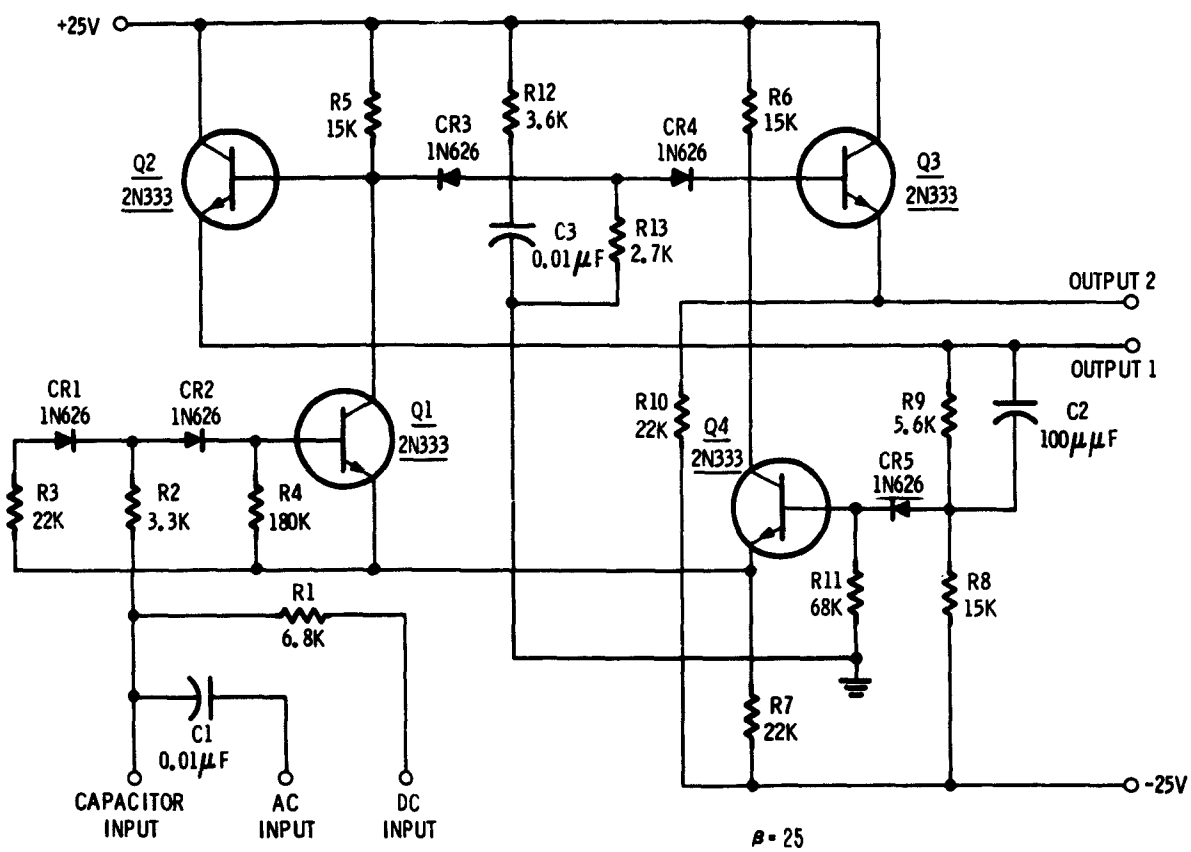

Figure 7. Trigger Circuit Schematic

Quiescent Current and Voltage for Q_1 Off

When the condition exists that Q_1 is off and Q_4 is in either the saturated or non-saturated state, Q_1, CR_3 and the associated circuitry are removed from the circuit because of reverse biasing. Figure 8 is the equivalent circuit used for the circuit analysis and Figures 9 and 10 are the equivalent circuits for a transistor in the non-saturated and saturated state respectively. A 0.6V drop was assumed across the diodes CR_4 and CR_5 due to forward biasing. Utilizing the nodes indicated in Figure 8, the circuit equations were derived for the state in which Q_4 is saturated and are presented below.

$$\frac{V_{E2}}{R_5} + \frac{I_{C2}}{\beta_2} = \frac{24.4}{R_5} \tag{4}$$

$$V_{E2}\left(\frac{1}{R_{L1}} + \frac{1}{R_9}\right) + V_{E4}\left(-\frac{1}{R_9}\right) + I_{C2}\left(-1 - \frac{1}{\beta_2}\right) = \frac{1.2}{R_9} \tag{5}$$

$$V_{E2}\left(\frac{1}{R_9}\right) + V_{E4}\left(-\frac{1}{R_9} - \frac{1}{R_8} - \frac{1}{R_{11}}\right) - I_{B4} = \frac{1.2}{R_9} + \frac{26.2}{R_8} + \frac{0.6}{R_{11}} \tag{6}$$

$$V_{E3}\left(\frac{1}{R_6} + \frac{1}{R_{12}} + \frac{1}{R_{13}}\right) + I_{C4}(1) + I_{C3}\left(\frac{1}{\beta_3}\right) = \frac{24.4}{R_6} + \frac{23.8}{R_{12}} - \frac{1.2}{R_{13}} \tag{7}$$

$$V_{E4}\left(-\frac{1}{R_7}\right) + I_{C4} + I_{B4} = \frac{25}{R_7} \tag{8}$$

$$V_{E3}\left(-\frac{1}{R_{L2}} - \frac{1}{R_{10}}\right) + I_{C3}\left(1 + \frac{1}{\beta_3}\right) = \frac{25}{R_{10}} \tag{9}$$

$$V_{E3}(1) + V_{E4}(-1) = -0.4 \tag{10}$$

The matrix used for the computer solution of this state is presented in equation 11. The computer solution of this matrix is included in Table 2. For the situation where Q_4 is non-saturated, it may be easily seen by referring

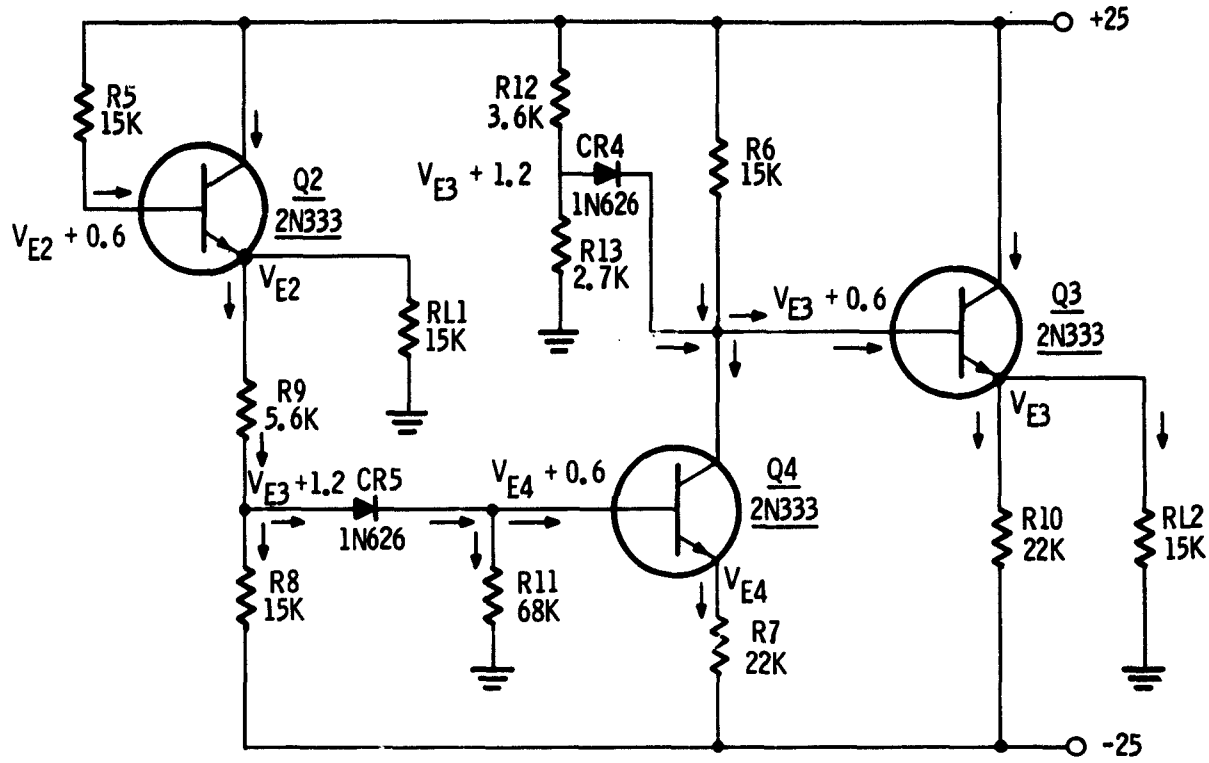

Figure 8. Equivalent Trigger Circuit for Q_1 off and Q_4 on

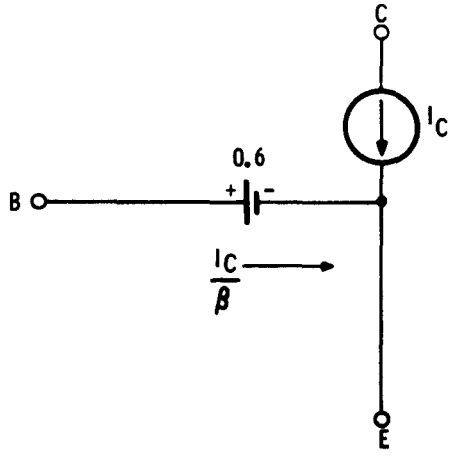

Figure 9. Equivalent Circuit for Transistors in Active Region

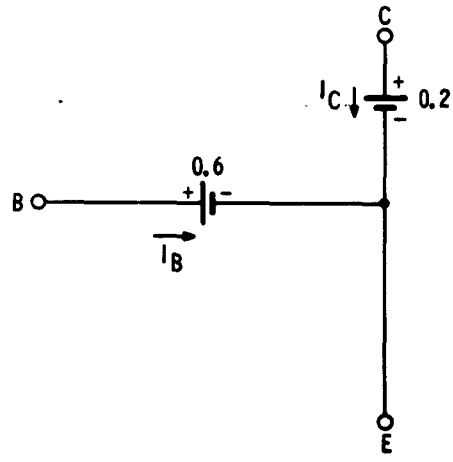

Figure 10. Equivalent Circuit for Transistors in Saturation

$$
\begin{bmatrix}
\frac{1}{R_5} & 0 & 0 & \frac{1}{\beta_2} & 0 & 0 & 0 \\
\frac{1}{R_4}+\frac{1}{R_9} & 0 & -\frac{1}{R_9} & -1-\frac{1}{\beta_2} & 0 & 0 & 0 \\
\frac{1}{R_9} & 0 & -\frac{1}{R_9}-\frac{1}{R_8}-\frac{1}{R_{11}} & 0 & 0 & 0 & -1 \\
0 & \frac{1}{R_6}+\frac{1}{R_{12}}+\frac{1}{R_{13}} & 0 & 0 & \frac{1}{\beta_3} & 1 & 0 \\
0 & 0 & -\frac{1}{R_7} & 0 & 0 & 1 & 1 \\
0 & -\frac{1}{R_{12}}-\frac{1}{R_{10}} & 0 & 0 & 1+\frac{1}{\beta_3} & 0 & 0 \\
0 & 1 & -1 & 0 & 0 & 0 & 0
\end{bmatrix}
\begin{bmatrix} V_{E2} \\ V_{E3} \\ V_{E4} \\ I_{C2} \\ I_{C3} \\ I_{C4} \\ I_{B4} \end{bmatrix}
=
\begin{bmatrix} -\frac{24.4}{R_5} \\ \frac{1.2}{R_9} \\ \frac{1.2}{R_9}+\frac{26.2}{R_8}+\frac{0.6}{R_{11}} \\ \frac{24.4}{R_6}+\frac{23.8}{R_{12}}-\frac{1.2}{R_{13}} \\ \frac{25}{R_7} \\ \frac{25}{R_{10}} \\ -0.4 \end{bmatrix}
\qquad (11)
$$

to Figures 9 and 10 that the matrix for this case may be written directly from the matrix of equation 11. When Q_4 is non-saturated, the base current I_{B4} is directly proportional to $1/\beta_4$ times the collector current I_{C4}. Therefore, the matrix for Q_4 (non-saturated) may be written as shown in equation 12. The computer solution for this matrix is shown in Table 3.

TABLE 2

COMPUTER SOLUTION OF TRIGGER CIRCUIT

(Q_1 OFF, Q_4 SATURATED)

V_{E2}	V_{E3}	V_{E4}	I_{C2}	I_{C3}	I_{C4}	I_{B4}
22.3	8.3	8.7	0.004	0.002	0.002	-0.0002

TABLE 3

COMPUTER SOLUTION OF TRIGGER CIRCUIT

(Q_1 OFF, Q_4 NON-SATURATED)

V_{E2}	V_{E3}	V_{E4}	I_{C2}	I_{C3}	I_{C4}
22.1	88	24	0.003	0.002	0.001

Quiescent Current and Voltage for Q_4 Off

When the circuit receives a sufficient positive DC trigger to cause Q_4 to be cut off and Q_1 to conduct, the equivalent circuit represented in Figure 11 applies. In this case, Q_4, CR_1 and CR_4 are ignored due to reverse biasing. The first situation to be explored is when Q_1 is saturated and the equations for this case, utilizing the circuit indicated in Figure 11, are presented in equations 13 through 20.

$$
\begin{bmatrix}
\frac{1}{R_5} & 0 & 0 & \frac{1}{\beta_2} & 0 & 0 \\
0 & \frac{1}{R_6}+\frac{1}{R_{12}}+\frac{1}{R_{13}} & 0 & 0 & \frac{1}{\beta_2} & 1 \\
\frac{1}{R_9} & 0 & -\frac{1}{R_9}-\frac{1}{R_8}-\frac{1}{R_{11}} & 0 & 0 & -\frac{1}{\beta_3} \\
\frac{1}{R_{L1}}+\frac{1}{R_9} & 0 & -\frac{1}{R_9} & -1-\frac{1}{\beta_3} & 0 & 0 \\
0 & -\frac{1}{R_{L2}}-\frac{1}{R_{10}} & 0 & 0 & 1+\frac{1}{\beta_3} & 0 \\
0 & 0 & -\frac{1}{R_7} & 0 & 0 & 1+\frac{1}{\beta_3}
\end{bmatrix}
\begin{bmatrix} V_{E2} \\ V_{E3} \\ V_{E4} \\ I_{C2} \\ I_{C3} \\ I_{C4} \end{bmatrix}
=
\begin{bmatrix}
\frac{24.4}{R_5} \\
\frac{24.4}{R_6}+\frac{23.8}{R_{12}}-\frac{1.2}{R_{13}} \\
\frac{26.2}{R_8}+\frac{1.2}{R_9}+\frac{0.6}{R_4} \\
\frac{1.2}{R_9} \\
\frac{25}{R_{10}} \\
\frac{25}{R_7}
\end{bmatrix}
\qquad (12)
$$

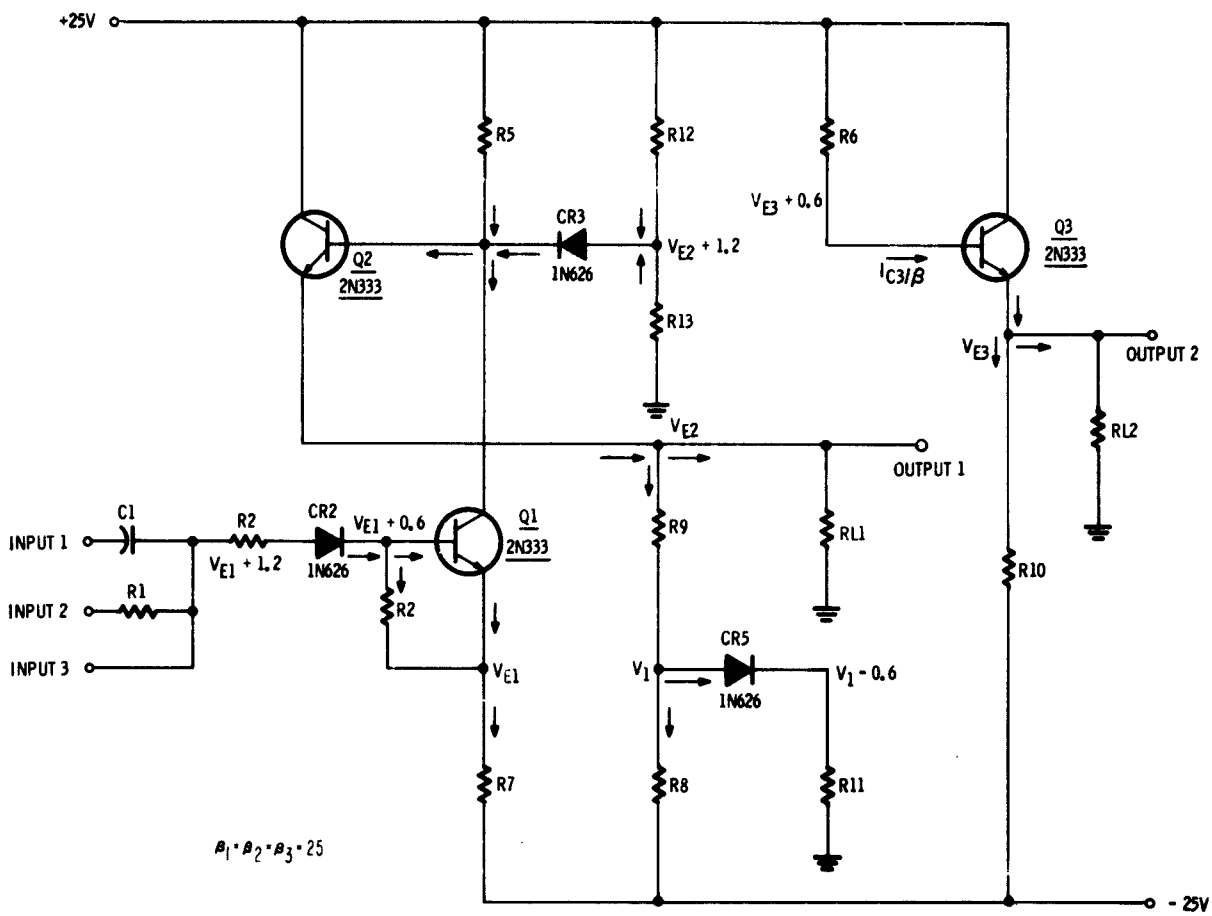

Figure 11. Equivalent Circuit for Q_4 off and Q_1 on

$$V_{E1}\left(\frac{1}{R_2}\right) + {}_{B1} = \frac{V - 1.2}{R_2} - \frac{0.6}{R_4} \tag{13}$$

$$V_{E1}\left(\frac{1}{R_7}\right) - I_{C1} - I_{B1} = \frac{0.6}{R_4} \tag{14}$$

$$V_{E2}\left(\frac{1}{R_5} + \frac{1}{R_{12}} + \frac{1}{R_{13}}\right) \quad I_{C1} + \frac{I_{C2}}{\beta_2} = \frac{24.4}{R_5} + \frac{23.8}{R_{12}} - \frac{1.2}{R_{13}} \tag{15}$$

$$V_{E2}\left(\frac{1}{R_9} + \frac{1}{R_{L1}}\right) - V_1\left(\frac{1}{R_9}\right) - I_{C2}\left(1 + \frac{1}{\beta_2}\right) = 0 \tag{16}$$

$$V_{E2}\left(\frac{1}{R_9}\right) - V_1\left(\frac{1}{R_9} + \frac{1}{R_8} + \frac{1}{R_{11}}\right) = \frac{25}{R_8} - \frac{0.6}{R_{11}} \tag{17}$$

$$V_{E1}(1) + V_{E2}(-1) = 0.4 \tag{18}$$

$$V_{E3}\left(\frac{1}{R_6}\right) + I_{C3}\left(\frac{1}{\beta_3}\right) = \frac{24.4}{R_6} \tag{19}$$

$$V_{E3}\left(-\frac{1}{R_{10}} + \frac{1}{R_{L2}}\right) + I_{C3}\left(1 + \frac{1}{\beta_3}\right) = \frac{25}{R_{10}} \tag{20}$$

Its corresponding matrix is shown in equation 21. The computer solutions for this matrix for values of V=1 to 10 volts are in Table 4. As was stated before, it is possible to write the matrix for the non-saturated condition directly. However, in this case, the equations are as shown in equations 22 through 28. The matrix for this set of equations is presented in equation 29 and its computer solution in Table 5.

$$
\begin{bmatrix}
-\frac{1}{R_9}-\frac{1}{R_8}-\frac{1}{R_{11}} & 0 & \frac{1}{R_9} & 0 & 0 & 0 & 0 & 0 \\
0 & \frac{1}{R_7} & 0 & 0 & -1 & 0 & 0 & -1 \\
0 & 1 & -1 & 0 & 0 & 0 & 0 & 0 \\
0 & 0 & 0 & \frac{1}{R_6} & 0 & 0 & \frac{1}{\beta_3} & 0 \\
0 & 0 & \frac{1}{R_5}+\frac{1}{R_{12}}+\frac{1}{R_{13}} & 0 & 1 & \frac{1}{\beta_2} & 0 & 0 \\
-\frac{1}{R_9} & 0 & \frac{1}{R_9}+\frac{1}{R_{L1}} & 0 & 0 & -1-\frac{1}{\beta_2} & 0 & 0 \\
0 & 0 & 0 & -\frac{1}{R_{10}}-\frac{1}{R_{L2}} & 0 & 0 & 1+\frac{1}{\beta_3} & 0 \\
0 & \frac{1}{R_2} & 0 & 0 & 0 & 0 & 0 & 1
\end{bmatrix}
\begin{bmatrix} V_1 \\ V_{E1} \\ V_{E2} \\ V_{E3} \\ I_{C1} \\ I_{C2} \\ I_{C3} \\ I_{B1} \end{bmatrix}
=
\begin{bmatrix}
\frac{25}{R_8}-\frac{0.6}{RT1} \\
\frac{0.6}{R_4} \\
0.4 \\
\frac{24.4}{R_6} \\
\frac{24.4}{R_5}+\frac{23.8}{R_{12}}-\frac{1.2}{R_{13}} \\
0 \\
\frac{25}{R_{10}} \\
\frac{V}{R_2}-\frac{0.6}{R_4}-\frac{1.2}{R_2}
\end{bmatrix}
\qquad (21)
$$

Where V = 1, 2, ... 9, 10

TABLE 4

COMPUTER SOLUTION OF TRIGGER CIRCUIT FOR Q_4 OFF AND Q_1 SATURATED

V_1	V_{E1}	V_{E2}	V_{E3}	I_{C1}	I_{C2}	I_{C3}	I_{B1}	V
- 1.152	7.469	7.07	22.3	.00266	.00193	.0035	- .00233	1
- 1.133	7.753	7.35		.00246	.00196		- .00211	2
- 1.113	8.036	7.64		.00226	.002		- .00189	3
- .937	8.320	7.92		.00205	.00203		- .00168	4
- .742	8.604	8.20		.00185	.00206		- .00146	5
- .547	8.887	8.49		.00164	.00210		- .00124	6
- .352	9.171	8.77		.00144	.00213		- .00103	7
- .157	9.455	9.05		.00123	.00216		- .00081	8
.038	9.739	9.34		.00103	.00220		- .00037	9
.232	10.022	9.62	22.3	.000826	.00223	.0035	- .00037	10

$$V_{E1}\left(\frac{1}{R_2}\right) + I_{C1}\left(\frac{1}{\beta_1}\right) = \frac{V - 1.2}{R_2} - \frac{0.6}{R_4} \tag{22}$$

$$V_{E1}\left(-\frac{1}{R_7}\right) + I_{C1}\left(1 + \frac{1}{\beta_1}\right) = \frac{25}{R_7} - \frac{0.6}{R_4} \tag{23}$$

$$V_1\left(-\frac{1}{R_9}\right) + V_{E2}\left(\frac{1}{R_9} + \frac{1}{R_{L1}}\right) + I_{C2}\left(-1 - \frac{1}{\beta_2}\right) = 0 \tag{24}$$

$$V_{E2}\left(\frac{1}{R_5} + \frac{1}{R_{12}} + \frac{1}{R_{13}}\right) + I_{C1}(1) + I_{C2}\left(\frac{1}{\beta_2}\right) = \frac{24.4}{R_5} + \frac{23.8}{R_{12}} + \frac{1.2}{R_{13}} \tag{25}$$

$$V_1\left(-\frac{1}{R_9} - \frac{1}{R_8} - \frac{1}{R_{11}}\right) + V_{E2}\left(\frac{1}{R_9}\right) = \frac{25}{R_8} - \frac{0.6}{R_{11}} \tag{26}$$

$$V_{E3}\left(\frac{1}{R_6}\right) + I_{C3}\left(\frac{1}{\beta_3}\right) = \frac{24.4}{R_6} \tag{27}$$

$$V_{E3}\left(-\frac{1}{R_{10}} - \frac{1}{R_{12}}\right) + I_{C3}\left(1 + \frac{1}{\beta_3}\right) = \frac{25}{R_{10}} \tag{28}$$

The analysis, as presented above, is typical of the analyses of the remaining circuits. All equations necessary for the complete description of the relationships between the components and the respective circuit performance characteristics are defined in the matrix equations. Thus, all required tools are available for a Monte Carlo Mathematical Simulation.

3.2.2 Transfer Functions of a Variable Frequency Oscillator

This study of the performance of a variable frequency oscillator will be limited to an analysis of the oscillator's frequency as a function of its components.

$$
\begin{bmatrix}
0 & \frac{1}{R_2} & 0 & 0 & \frac{1}{\beta_1} & 0 & 0 \\
0 & -\frac{1}{R_7} & 0 & 0 & 1+\frac{1}{\beta_1} & 0 & 0 \\
-\frac{1}{R_9} & 0 & \frac{1}{R_9}+\frac{1}{R_{L1}} & 0 & 0 & -1-\frac{1}{\beta_2} & 0 \\
0 & 0 & \frac{1}{R_5}+\frac{1}{R_{12}}+\frac{1}{R_{13}} & 0 & 1 & \frac{1}{\beta_2} & 0 \\
-\frac{1}{R_8}-\frac{1}{R_9}-\frac{1}{R_{11}} & 0 & \frac{1}{R_9} & 0 & 0 & 0 & 0 \\
0 & 0 & 0 & \frac{1}{R_6} & 0 & 0 & \frac{1}{\beta_3} \\
0 & 0 & 0 & -\frac{1}{R_{10}}-\frac{1}{R_{L2}} & 0 & 0 & 1+\frac{1}{\beta_3}
\end{bmatrix}
\begin{bmatrix} V_1 \\ V_{E1} \\ V_{E2} \\ V_{E3} \\ I_{C1} \\ I_{C2} \\ I_{C3} \end{bmatrix}
=
\begin{bmatrix}
\frac{V-1.2}{R_2}-\frac{0.6}{R_4} \\
\frac{25}{R_7}-\frac{0.6}{R_4} \\
0 \\
\frac{24.4}{R_5}+\frac{23.8}{R_{12}}-\frac{1.2}{R_{13}} \\
\frac{25}{R_8}-\frac{0.6}{R_{11}} \\
\frac{24.4}{R_6} \\
\frac{25}{R_{10}}
\end{bmatrix}
\qquad (29)
$$

TABLE 5

COMPUTER SOLUTION OF TRIGGER CIRCUIT FOR Q_4 OFF AND Q_1 NON-SATURATED

V_1	V_{E1}	V_{E2}	V_{E3}	I_{C1}	I_{C2}	I_{C3}	V
- .004	-.353	9.28	22.3	.001	.002	.003	1
- .046	-.641	9.22	22.3	.001	.002	.003	2
- .087	1.64	9.16	22.3	.001	.002	.003	3
- .129	2.63	9.10	22.3	.001	.002	.003	4
- .170	3.62	9.09	22.3	.001	.002	.003	5
- .212	4.62	8.98	22.3	.001	.002	.003	6
- .253	5.61	8.92	22.3	.001	.002	.003	7
- .295	6.61	8.85	22.3	.001	.002	.003	8
- .336	7.60	8.79	22.3	.001	.002	.003	9
- .378	8.60	8.73	22.3	.001	.002	.003	10

A schematic of the oscillator is shown in Figure 12 and its equivalent circuit is shown in Figure 13. Table 6 presents the performance criteria for the oscillator.

TABLE 6[8]

PERFORMANCE CRITERIA OF VARIABLE FREQUENCY OSCILLATOR

Requirements	Maximum	Design Center	Minimum
Frequency range 1	250 kc	----	50 kc
Frequency range 2	1 mc	----	250 kc
Frequency range 3	5 mc	----	1 mc
Frequency range 4	10 mc	----	5 mc
Power Output	4 mw	3 mw	2 mw
Output Impedance	50	----	----
Load Impedance	----	----	50 Ω
Output Voltage, 50-ohm Load Open Circuit	----	0.4 v	----
Frequency Stability, Power Supply	1% v DC	----	----
DC Supply Voltage	----	-12 v	----
Operating Temperature	50°C	25°C	0°C

It has been shown that if a circuit is provided with a sufficient amount of regenerative feedback, a transistor circuit will serve as a generator of periodically varying waves. A variety of feedback circuits which differ in detail are available for the production of self-sustained oscillations. Characteristic of these circuits is a feedback network through which a portion of the output is fed back into the input circuit having such phase and amplitude that self-excitation results. The analysis of such feedback oscillators will be simplified with the application of the following two points: [12, 15, 16, 25]

1. The response of a circuit is oscillatory if the poles of the transfer functions are complex conjugates. The oscillation will be sustained with constant amplitude if the real parts of these poles are 0.

2. The voltage amplification or transfer function of a feedback amplification with voltage feedback is:

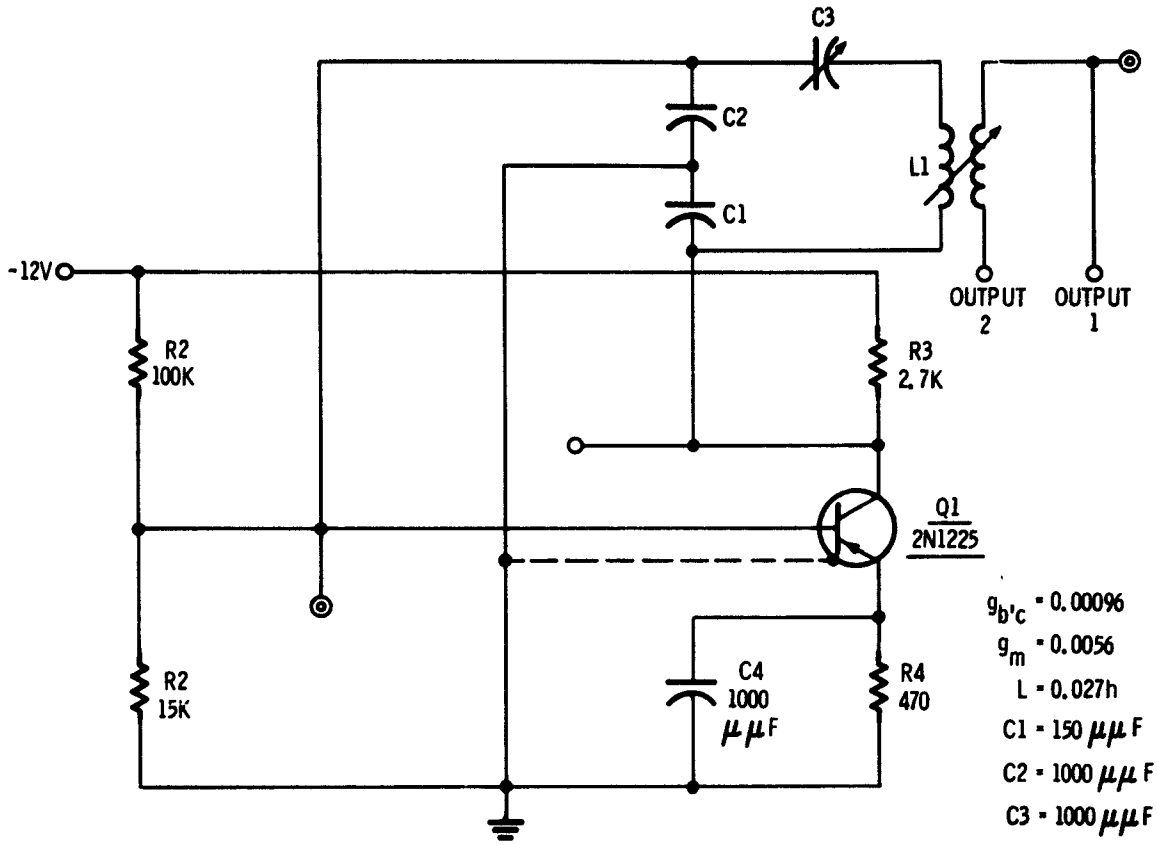

NOTE: THIS CIRCUIT IS CONTAINED IN RADC REPORT TR59-243, DEC. 15,

Figure 12. Variable Frequency Oscillator Schematic

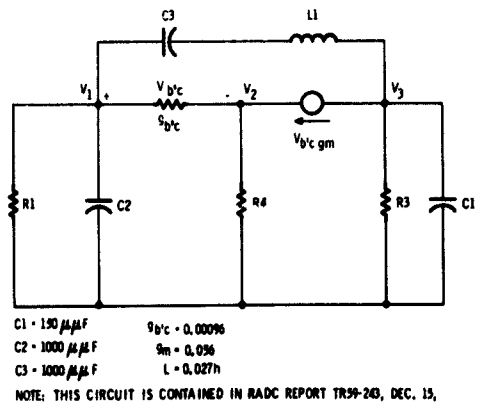

Figure 13. Equivalent Circuit of Variable Frequency Oscillator at 50 kc

$$A_c = \frac{A_o}{1 - A_o}$$

The poles of this function are the roots of the denominator: $1 - A_o = 0$.

The procedure for analyzing the feedback oscillator is as follows:

1. Draw the complete Class A equivalent circuit (this is shown in Figure 13):
   a. Replace by-pass capacitors by short circuits
   b. Replace radio frequency chokes with open circuits
   c. Indicate tube or transistor capacitances
   d. Draw the circuit as an open loop amplifier
2. Compute the over-all amplification of the open loop circuit as a function of the frequency (p). This will equal the feedback factor: A_o.
3. Let $\beta A_o - 1 = 0$.
4. This equation will appear as a polynomial in (p) with unity as the coefficient of the highest power of (p).
5. For oscillations to occur there must be a pair of conjugate roots with zero real parts. These two conditions yield two design equations.

From Figure 13 a nodal analysis allows the following equations to be written:

$$V_1 g_1 + (V_1 - V_2) g_{b'e} + \frac{V_1 - V_3}{pL + \frac{1}{pC_3}} + V_1 pC_2 = 0 \qquad (30)$$

$$(V_2 - V_1) g_{b'e} + V_2 g_4 - (V_1 - V_2) g_m = 0 \qquad (31)$$

$$\frac{(V_3 - V_1)}{pL + \frac{1}{pC_3}} + (V_1 - V_2) g_m + V_3 g_3 + V_3 pC_1 = 0 \qquad (32)$$

The following is the coefficient matrix of the above equation:

$$\begin{bmatrix} (g_1 + g_{b'e} + \frac{pC_3}{p^2LC_3+1} + pC_2) & (-g_{b'e}) & (\frac{-pC_3}{p^2C_3L+1}) \\ (-g_{b'e} - g_m) & (g_4 + g_{b'e} + g_m) & 0 \\ (\frac{-pC_3}{p^2LC_3+1} + g_m) & (-g_m) & (\frac{pC_3}{p^2LC_3+1} + g_3 + pC_1) \end{bmatrix} = \Delta$$

The gain is $\frac{V_3}{V_1} = \beta A_o = 1$ (33)

since $V_3 = \frac{\Delta_1}{\Delta}$ (34)

where Δ_1 is the coefficient matrix with the coefficients of V_3 replaced by the constant terms of equations (30, 31, and 32) respectively. Then the gain, $\frac{V_3}{V_1}$ may be written as:

$$\frac{V_3}{V_1} = \frac{\Delta_1}{V_1\Delta} \tag{35}$$

combining equations (33 and 35) we have

$$\frac{\Delta_1}{V_1\Delta} - 1 = 0 \tag{36}$$

multiplying equation (36) by $V_1\Delta$ and

$$\Delta_1 - V_1\Delta = 0 \tag{37}$$

Since $\Delta_1 = 0$ because column 3 in the matrix is all zeros and V1 cannot equal zero, then $\Delta = 0$. (38)

We now solve the coefficient matrix and from equation (38) we set the matrix equal to zero. Solving the matrix, we have

$$[g_{b'e}g_4g_3 + g_1g_3g_{b'e} + g_1g_3g_4 + g_1g_3g_m] + [g_{b'e}g_4C_1 + C_3g_{b'e}g_4 + C_2g_{b'e}g_3 +$$

$$C_2g_3g_4 + g_1g_{b'e}C_1 + C_3g_1g_{b'e} + g_1g_4C_1 + C_3g_1g_4 + C_3g_{b'e}g_3 + C_3g_3g_4 +$$

$$(C_2g_3 + g_1C_1 + C_3g_1 + C_3g_3 + C_3g_4)g_m]P + [C_1C_2g_{b'e} + C_2C_3g_{b'e} + C_1C_2g_4 +$$

$$C_2C_3g_4 + C_1C_3g_{b'e} + C_1C_3g_4 + g_{b'e}g_4g_3C_3L + g_1g_3g_{b'e}C_3L + g_1g_3g_4C_3L + \quad (39)$$

$$(C_1C_2 + C_2C_3 + C_3C_1 + g_1g_3C_3L)g_m]\,P^2 + [g_{b'e}g_4C_1C_3L + g_{b'e}g_3C_2C_3L +$$

$$C_2C_3g_3g_4L + g_1g_{b'e}C_1C_3L + g_1g_4C_1C_3L + (C_2C_3g_3L + g_1C_1C_3L)g_m]\,P^3 +$$

$$[C_1C_2C_3g_{b'e}L + C_1C_2C_3g_4L + C_1C_2C_3L\ g_m]\,P^4 = 0$$

The circuit values for this matrix are shown in Table 1 and substituting these constants in the above equation (39) and combining terms will result in equation (40) below.

$$[0.08457248618 \times 10^{-8} + 2.8 \times 10^{-8}\ g_m]$$

$$+[0.7996937653 \times 10^{-14} + 3.060708003 \times 10^{-12}\ g_m]\,P$$

$$+[3.5191363382 \times 10^{-20} + 4.769320769 \times 10^{-18}\ g_m]\,P^2 \quad (40)$$

$$+[0.1233719939 \times 10^{-24} + 0.1311538462 \times 10^{-22}\ g_m]\,P^3$$

$$+[0.1251125203 \times 10^{-30} + 0.405 \times 10^{-28}\ g_m]\,P^4 = 0$$

The first technique utilized to solve equation (40) for the resonant frequency (p) was graphical in nature. A computer program was developed to solve the above equation and a search was made for the value of g_m that would result in a pair of complex conjugate roots on the imaginary axis. Figure 14 is a graph of some of the roots of equation (40). Figure 15 is the same data presented on an

expanded scale. This graph intersected the imaginary axis when the value of g_m was 0.0086 and $p = j381,300$. Since $p = j\omega$ and $\omega = 2\pi f$, the frequency of oscillation may be found by equation $2\pi fj = 381,300j$. Divide both sides by j

$$2\pi f = 381,300$$

$$f = \frac{381,300}{6.28} = 60,717 \text{ CPS} \qquad (41)$$

A second method for solving equation (40) is the utilization of the Routh-Hurwitz criterion. The technique is as follows for a 4th order equation, after dividing equation (40) by 10^{-8} the 4th order equation appears as equation (42)

$$(.125 \times 10^{-22} + .405 \times 10^{20}\, g_m)p^4 + (.123 \times 10^{-16} + .131 \times 10^{-14}\, g_m)p^3$$
$$+ (3.52 \times 10^{-12} + 4.77 \times 10^{-10}\, g_m)p^2 + (.800 \times 10^{-6} + \qquad (42)$$
$$3.06 \times 10^{-4}\, g_m)p + (.0846 + 2.8\, g_m) = 0$$

This equation is of the same form as equation (43).

$$1 - A\,B = ap^4 + bp^3 + cp^2 + dp + e = 0 \qquad (43)$$

The formal procedure is as follows:

1. Form the array from the coefficients

p^4	a	c	e
p^3	b	d	
p^2	A	B	
p^1	C		
p^0	D		

$$A = \frac{bc - ad}{b}, \quad B = \frac{be - a(0)}{b} = e$$
$$C = \frac{Ad - bB}{A}, \quad D = \frac{cB - A(0)}{c} = B \qquad (44)$$

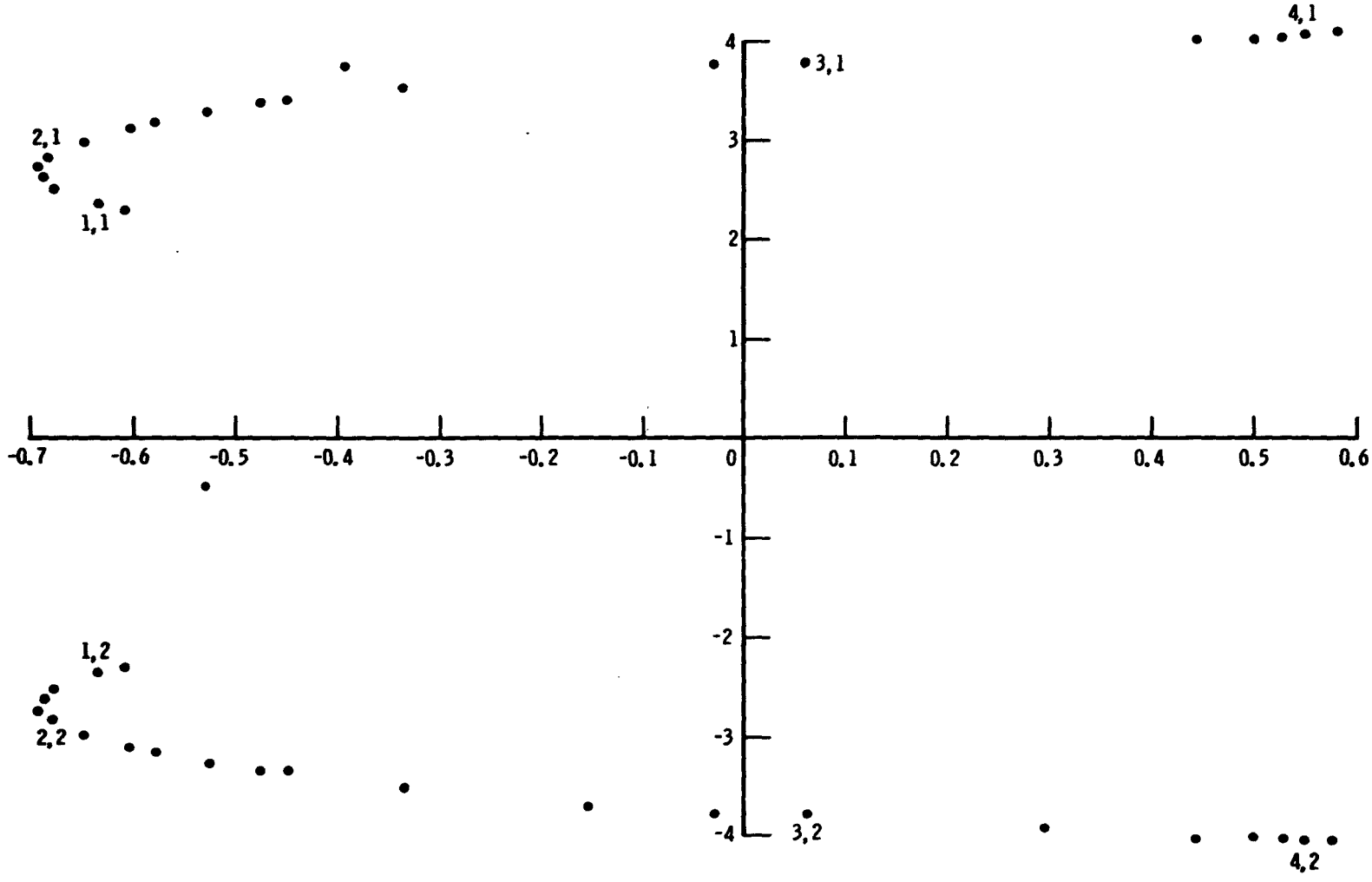

Figure 14. Pole Location vs. g_m for Variable Frequency Oscillator

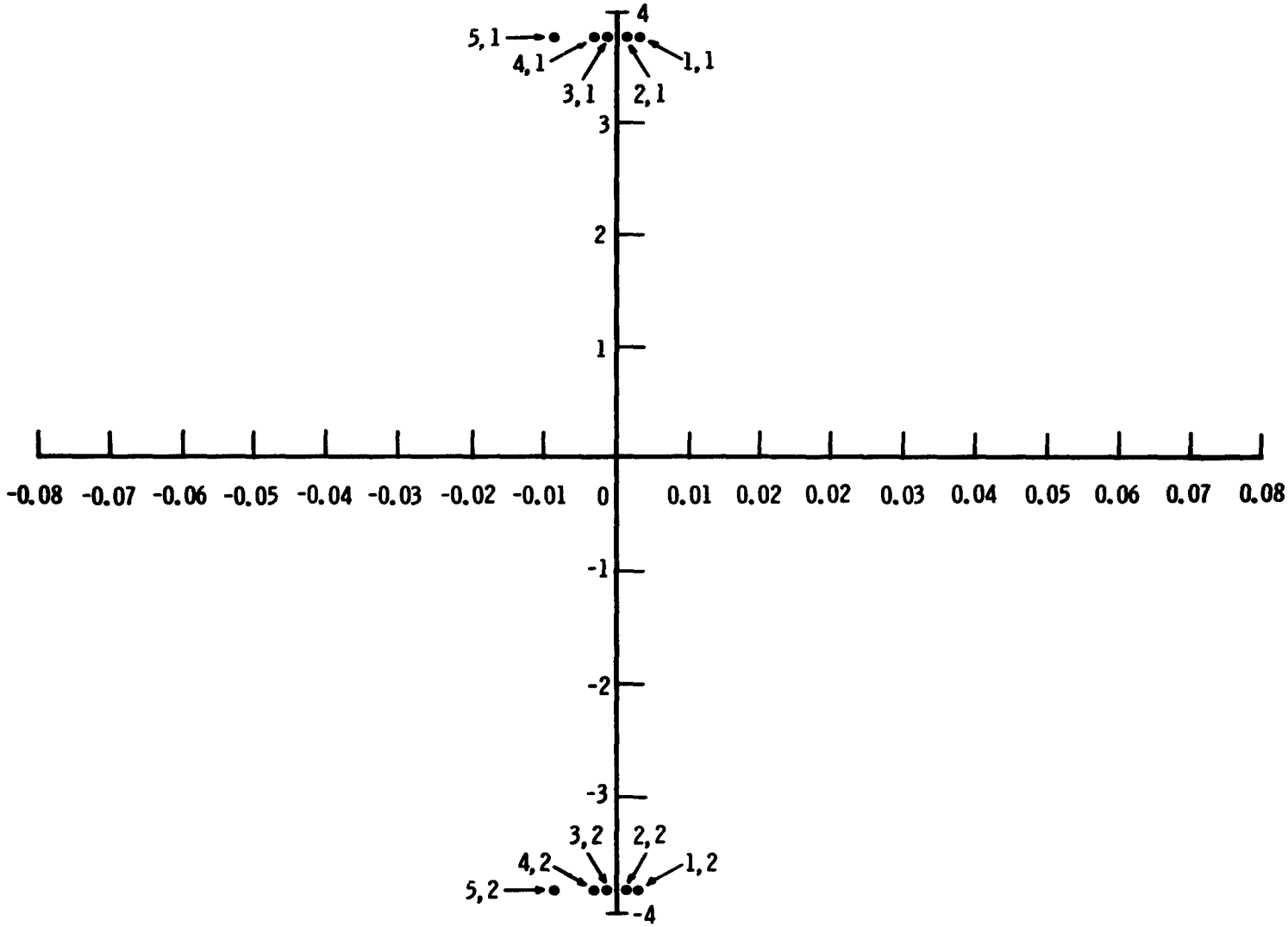

Figure 15. Pole Location vs. Transconductance (Expanded Scale)

2. The number of sign changes in the first column of the array equals the number of roots with positive real parts. If there are no sign changes in the first column, then the system is stable.

3. To produce a sign change in the first column, term C can be set ≤ 0. If $C = 0$ is solved, it yields the value of g_m at which the system becomes unstable. This corresponds to the condition that the roots of the characteristic equation have zero real parts.

In this case:

$$C = (.800 \times 10^{-6} + 3.06 \times 10^{-4} g_m)(.35 \times 10^{-28} + .345 \times 10^{-26} g_m - .62 \times 10^{-24} g_m^2) - (8.46 \times 10^{-2} + 2.8 g_m)(.015 \times 10^{-32} + .0322 \times 10^{-30} g_m + .0172 \times 10^{-28} g_m^2) \quad (45)$$

This can be solved by trying positive realizable values of g_m(.000 to .060) in the expression to find the g_m at which C=0. This yields a value of g_m near .007 or .008.

g_m	C
.004	$.64 \times 10^{-34}$
.006	$.454 \times 10^{-34}$
.007	$.349 \times 10^{-34}$
.008	$-.165 \times 10^{-34}$
.010	$-.44 \times 10^{-34}$

(46)

The value of g_m at which $C = 0$ can be substituted into the characteristic equation and this can be solved for p.

Since we are interested in the roots having zero real parts, $p = 0 + j\omega = 0 + j\,2\pi f$, and the fourth order equation can be reduced to two equations:

$$\text{Re} = 0: \; a\omega^4 - c\omega^2 + e = 0 \quad (47)$$

$$\text{Im} = 0: \; -bj\omega^3 + dj\omega = 0 \quad (48)$$

Both equations should yield the same value for f when the proper g_m is used. The frequency of oscillation is calculated as approximately 60 KC as shown in Table 7 below.

TABLE 7

COMPUTATION OF FREQUENCY OF OSCILLATION

g_m	From Re = 0	From Im = 0
0.007	61.6 KC	59 KC
0.008	61.4 KC	60 KC

A third approach relating to the proceeding results is an explicit determination of the resonant frequency. This procedure is as follows.

Let the denominator of the transfer function be of the form shown in equation (49) where the coefficients are given in terms of g_m and where $p = j\omega$

$$A + bp + cp^2 + dp^3 + p^4 = 0 \tag{49}$$

The technique which follows enables one to solve for g_m and use this result to find the frequency of oscillation. Since we are looking for the complex conjugates, it is possible to write the above equation with these factored out. This gives:

$$(p + ip_0)(p - ip_0)(\alpha + \beta p + p^2) = 0$$

or

$$(p^2 + p_o^2)(\alpha + \beta p + p^2) = 0 \tag{50}$$

Multiplying out and equating like coefficients, one has

$$\alpha p_0^2 + \beta p_0^2 p + (\alpha + p_0^2)p^2 + \beta p^3 + p^4 = a + bp + cp^2 + dp^3 + p^4 \tag{51}$$

$$\alpha p_0^2 = a \qquad \alpha = a/p_0^2 \tag{52}$$

$$\beta p_0^2 = b \qquad p_0^2 = b/\beta \tag{53}$$

$$\alpha + p_0^2 = c \qquad \alpha + b/\beta = \tag{54}$$

$$\beta = d \tag{55}$$

Combining the above, we have the following two equations:

$$\frac{a \cdot d}{b} + \frac{b}{d} = c \tag{56}$$

$$p_0^2 = \frac{b}{d} \tag{57}$$

From these two results the solution for g_m is explicit and the frequency of oscillation is uniquely determined.

CONCLUSIONS:

Of the three methods described above, it appears that the third approach is the most efficient. The results determined analytically, satisfactorily compared with those determined empirically. The above results allow a Monte Carlo simulation to be performed on the oscillator circuit. This will enable the distribution of the performance parameters to be determined for variations in circuit components; both for the initial performance distribution as well as the time-dependent distribution, which may result from a degradation or change in values of components.

3.2.3 Transfer Functions for the High-Level Amplifier

The next circuit to be analyzed is that of the High-Level Video Amplifier shown in Figure 16. This amplifier consists of a two-stage, common emitter feedback pair, driving a common emitter, high voltage mesa type output transistor. Although some compression may occur in the second transistor, the entire chain is designed as a linear amplifier up to the output capabilities of the transistor Q_3. Provision is made for DC restoration at the base of Q_3 to permit operation with long-duty cycle pulses. However, because of the small DC offset inherent in this form of clamp, optimum performance is achieved only if the duty cycle is restricted to 20 percent or less.

This type of amplifier is designed for use mainly to accept positive unipolar signals from low-level sources and deliver a high-level negative control voltage to a radar or some type of cathode ray display device.

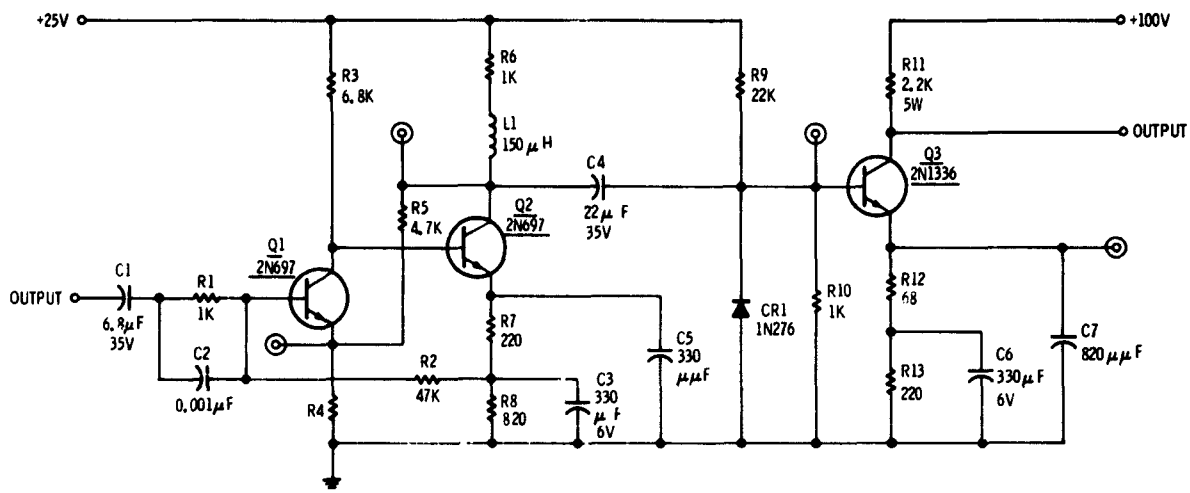

Figure 16. Video High-Level Amplifier Schematic

The analysis of this circuit was performed in two parts; the first being that of the output amplifier or Q_3, and the second that of the common emitter feedback pair.

The DC equivalent circuit of the output amplifier Q_3 is shown in Figure 17. The analysis of this equivalent circuit yields equations (58) through (60).

$$\frac{V_1 - V_{C3}}{R_{11}} = I_{C3} \tag{58}$$

$$\frac{V_2 - V_{E3} - .7}{R_9} = \frac{I_{C3}}{\beta_3} + \frac{V_{E3} + .7}{R_{10}} \tag{59}$$

$$V_{E3} = \frac{\beta_3 + 1}{\beta_3} I_{C3} (R_{12} + R_{13}) \tag{60}$$

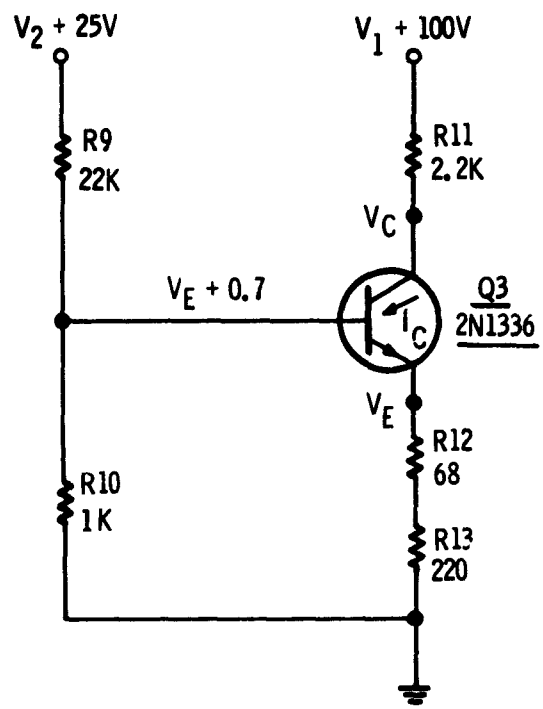

Figure 17. DC Equivalent Circuit of Output State of Video High-Level Amplifier

The equations are then rearranged and put into matrix form for computer solution. When typical values of β are used, the matrix equation (61) may be solved and the computer solution is shown in Table 8.

$$\begin{bmatrix} 1 & 0 & R_{11} \\ 0 & -\beta_3(R_{10}+R_9) & -R_9R_{10} \\ 0 & \beta_3 & -(\beta_3+1)(R_{12}+R_{13}) \end{bmatrix} \begin{bmatrix} V_{C3} \\ V_{E3} \\ I_{C3} \end{bmatrix} = \begin{bmatrix} V_1 \\ -\beta_3R_{10}V_2+0.7\beta_3R_{10}+0.7\beta_3R_9 \\ 0 \end{bmatrix} \quad (61)$$

TABLE 8

COMPUTER SOLUTION OF MATRIX FOR THE OUTPUT STAGE

V_{C3}	V_{E3}	I_{C3}
97.78	0.313	1.008 ma

It is now desirable to solve for the DC operating point for the common emitter feedback pair (Q_1 and Q_2). The equivalent circuit for this problem is shown in Figure 18.

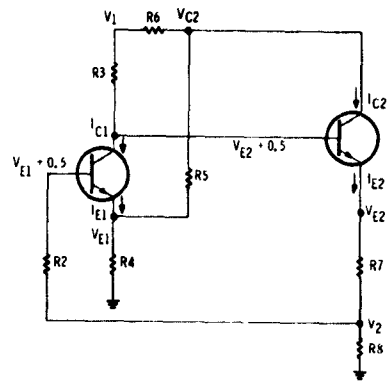

Figure 18. Equivalent Circuit for Common Emitter Pair of High-Level Video Amplifier

The circuit analysis of this equivalent circuit yields equations (62) through (68).

$$\frac{V_1 - V_{C2}}{R_6} + \frac{V_{E1} - V_{C2}}{R_5} - I_{C2} = 0 \tag{62}$$

$$\frac{V_{E2} - V_2}{R_7} = I_{C2} + \frac{I_{C2}}{\beta_2} \tag{63}$$

$$\frac{V_{E2} - V_2}{R_7} - \frac{V_2}{R_8} + \frac{V_{E1} + .5 - V_2}{R_2} = 0 \tag{64}$$

$$\frac{V_1 - V_{C1}}{R_3} - I_{C1} - \frac{I_{C2}}{\beta_2} = 0 \tag{65}$$

$$V_{C1} = V_{E2} + 0.5 \tag{66}$$

$$\frac{V_{E1}}{R_4} - \left(\frac{\beta_1 + 1}{\beta_1}\right) I_{C1} + \frac{V_{E1} - V_{C2}}{R_5} = 0 \tag{67}$$

$$\frac{V_2 - V_{E1} - .5}{R_2} = \frac{I_{C1}}{\beta_1} \tag{68}$$

From the above equations, the matrix equation (69) is formed and the computer solution of the equation is presented in Table 9.

TABLE 9

COMPUTER SOLUTION OF COMMON EMITTER PAIR OF HIGH-LEVEL AMPLIFIER

V_{C1}	V_{C2}	V_{E1}	V_{E2}	V_2	I_{C1}	I_{C2}
5.76	16.78	1.11	5.16	4.05	0.003	0.005

Measurements of the critical circuit parameter were made on a breadboard of the amplifier to validate the transfer functions represented in equations (61) and (69). A comparison of the analytical and empirical results is presented in Table 10.

TABLE 10

COMPARISON OF MEASURED AND COMPUTED VALUES OF VIDEO HIGH-LEVEL AMPLIFIER

VOLTAGE	COMPUTED	MEASURED
V_{C1}	5.756 V	7.0 V
V_{C2}	16.776	14.5
V_{E1}	1.104	0.95
V_{E2}	5.156	6.2
V_2	4.055	5.1
V_{C3}	97.78	98.0
V_{E3}	0.313	0.4

As may be seen from Table 10, the results check rather closely. The agreement between the computed and measured values would improve if the measured values of β_1 and B_2 (35 and 42 respectively) were used in place of the assumed values of 55 and 60. However, the results serve to validate the transfer functions for the DC bias conditions.

$$
\begin{bmatrix}
0 & -\frac{1}{R_5}-\frac{1}{R_6} & \frac{1}{R_5} & 0 & 0 & 0 & -1 \\
0 & 0 & 0 & \frac{1}{R_7} & -\frac{1}{R_7} & 0 & -\frac{(\beta_2+1)}{\beta_2} \\
0 & 0 & \frac{1}{R_2} & \frac{1}{R_7} & -\left(\frac{1}{R_2}+\frac{1}{R_7}+\frac{1}{R_8}\right) & 0 & 0 \\
\frac{1}{R_3} & 0 & 0 & 0 & 0 & 1 & \frac{1}{\beta_2} \\
1 & 0 & 0 & -1 & 0 & 0 & 0 \\
0 & -\frac{1}{R_5} & \frac{1}{R_4}+\frac{1}{R_5} & 0 & 0 & -\frac{(\beta_1+1)}{\beta_1} & 0 \\
0 & c & \frac{1}{R_2} & 0 & -\frac{1}{R_2} & \frac{1}{\beta_1} & 0
\end{bmatrix}
\begin{bmatrix}
V_{C1} \\ V_{C2} \\ V_{E1} \\ V_{E2} \\ V_2 \\ I_{C1} \\ I_{C2}
\end{bmatrix}
=
\begin{bmatrix}
-\frac{V_1}{R_6} \\ 0 \\ -\frac{.5}{R_2} \\ \frac{V_1}{R_3} \\ .5 \\ 0 \\ -\frac{.5}{R_2}
\end{bmatrix}
\qquad (69)
$$

Another important parameter in addition to the DC quiescent point is that of the AC small signal gain. Therefore, an AC equivalent circuit was developed and is shown in Figure 19. Since the frequency AC Equivalent Circuit of Video High-Level Amplifier of interest is 50 KC, the circuit may be simplified to that shown in Figure 20. Utilizing the simplified equivalent circuit, a nodal analysis yields equations (70) through (77). These equations are then formed into matrix equation (78). This matrix is then solved by means of a computer and the results are presented in Table 11.

$$(V_1 - V_2)g_1 + \beta_1 i_{b_1} + (V_4 - V_2)ge_1 = 0 \tag{70}$$

$$\beta_1 i_{b_1} + V_3(g_3 + g_7) - \beta_2 i_{b_2} = 0 \tag{71}$$

$$\beta_2 i_{b_2} + (V_5 - V_4)g_5 + V_5 g_{6,9,10} - \beta_3 i_{b_3} + V_5 \left(\frac{g_{12} ge_3}{g_{12} + ge_3}\right) = 0 \tag{72}$$

$$V_4 g_4 + (V_4 - V_5)g_5 + (V_4 - V_2)ge_1 = 0 \tag{73}$$

$$\beta_3 i_{b_3} + V_6 g_{11} = 0 \tag{74}$$

$$i_{b_1} = (V_1 - V_2)g_1 \tag{75}$$

$$i_{b_2} + \beta_1 i_{b_1} + V_3 g_3 = 0 \tag{76}$$

$$i_{b_3} + \beta_3 i_{b_3} - V_5 \left(\frac{g_{12} ge_3}{g_{12} + ge_3}\right) = 0 \tag{77}$$

Note: $g = \frac{1}{R}$

$g_1 = .001$	$g_{6,9,10} = .00205$	$g_{11} = .000454$
$g_2 = .0000213$	$ge_3 = .077$	$\beta_1 = 55$
$g_3 = .000147$	$ge_1 = .077$	$\beta_2 = 60$
$g_4 = .00555$	$g_7 = .00454$	$\beta_3 = 13$
$g_5 = .000213$	$g_{12} = .0147$	

$$
\begin{bmatrix}
g_1 - ge_1 & 0 & ge_1 & 0 & 0 & \beta_1 & 0 & 0 \\
0 & g_3 + g_7 & 0 & 0 & 0 & \beta_1 & -\beta_2 & 0 \\
0 & 0 & -g_5 & g_5 + g_{6,9,10} + \left(\frac{g_{12}ge_3}{g_{12}+ge_3}\right) & 0 & 0 & \beta_2 & -\beta_3 \\
ge_1 & 0 & g_4 + g_5 + ge_1 & -g_5 & 0 & 0 & 0 & 0 \\
0 & 0 & 0 & 0 & g_{11} & 0 & 0 & \beta_3 \\
g_1 & 0 & 0 & 0 & 0 & 1 & 0 & 0 \\
0 & g_3 & 0 & 0 & 0 & 1 & 1 & 0 \\
0 & 0 & 0 & -\left(\frac{g_{12}ge_3}{g_{12}+ge_3}\right) & 0 & 0 & 0 & 1+\beta_3
\end{bmatrix}
\begin{bmatrix} V_2 \\ V_3 \\ V_4 \\ V_5 \\ V_6 \\ i_{b_1} \\ i_{b_2} \\ i_{b_3} \end{bmatrix}
=
\begin{bmatrix} -g_1 \\ 0 \\ 0 \\ 0 \\ 0 \\ 0 \\ 0 \\ 0 \end{bmatrix}
\tag{78}
$$

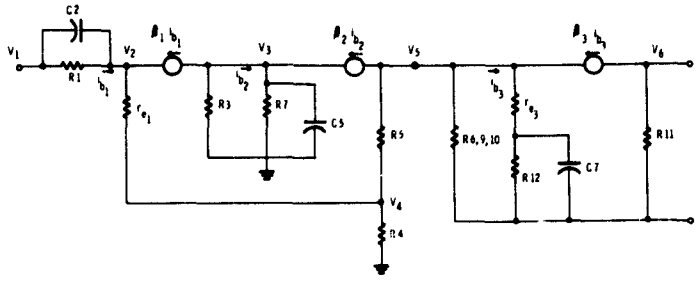

At 50 KC: $-jX_{C2} = j\ 3.14K\ \Omega$ $\quad -jX_{C1} = -j\ 0.47\Omega$

$-jX_{C5} = j\ 9.63K\ \Omega$ $\quad -jX_{C3} = -j\ 0.00962\Omega$

$-jX_{C7} = j\ 3.88\ K\Omega$ $\quad jX_{L_1} = j\ 47.2\ \Omega$

$r_{b_i} \hat{\wedge} r_{b_2} \hat{\wedge} 50\Omega$

Figure 19. AC Equivalent Circuit of High-Level Video Amplifier

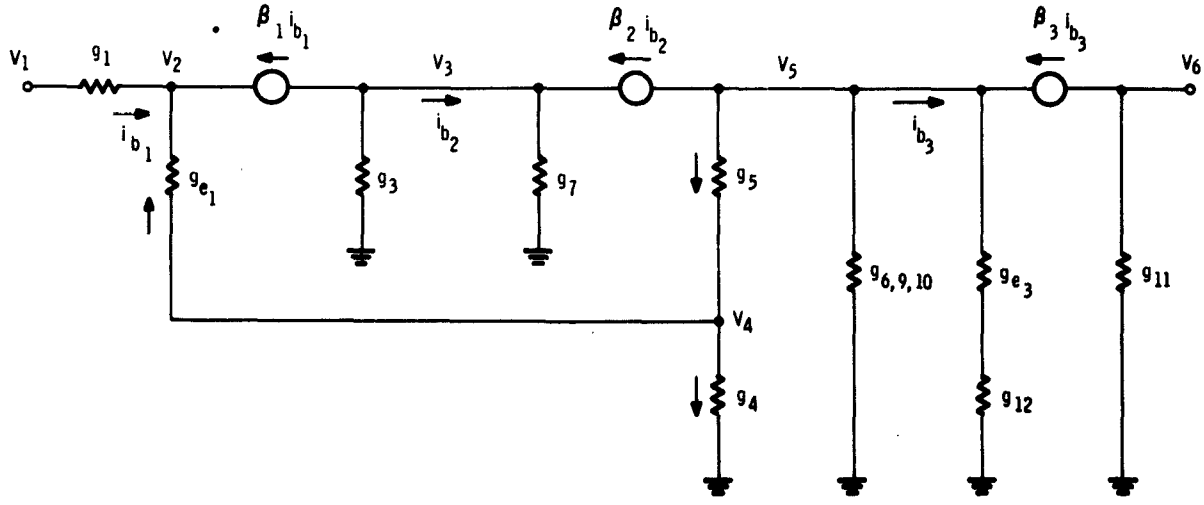

Figure 20. Simplified AC Equivalent Circuit of Video High-Level Amplifier

TABLE 11

COMPUTER SOLUTION OF AC CIRCUIT ANALYSIS OF VIDEO HIGH-LEVEL AMPLIFIER

V_2	V_3	V_4	V_5	V_6	i_{b1}	i_{b2}	i_{b3}
0.96	-9.4 .	0.93	14.6	-379.8	0.00004	-0.0008	0.008

The above analysis is based on small signal equivalent circuits and assumes that the transistors are linear devices. In practice the predicted performance will only be valid for low-level signals. Specifically, the output stage Q_3 will be extremely non-linear to large input voltages.

Table 12 presents the computed and measured values of small signal voltage gain, input impedance and output impedance in the 50 KC frequency range.

TABLE 12

COMPARISON OF COMPUTED AND MEASURED SMALL SIGNAL GAIN OF VIDEO HIGH-LEVEL AMPLIFIER

Transfer Function or Impedance	Computed	Measured
Voltage Gain	$\frac{V_6}{V_1} = -380$	-330 + 25%
Input Impedance	$Z_{in}\ R_1 + \frac{V_6}{Ib_1} = 22.5K$	18K
Output Impedance	$Z_{out}\ R_{11} = 2.2K$	2.2K

The pulse voltage gain of the amplifier was also measured using a 10% duty cycle. This transfer function is plotted in Figure 21 and illustrates that the gain is quite linear for V_{in} less than 100 MV and approximates the computed small signal value in this region. In fact from Figure 21, the low-level pulse voltage gain = V_{C3}/V_{in} = 38V/0.1V = 380. This indicates that the small signal

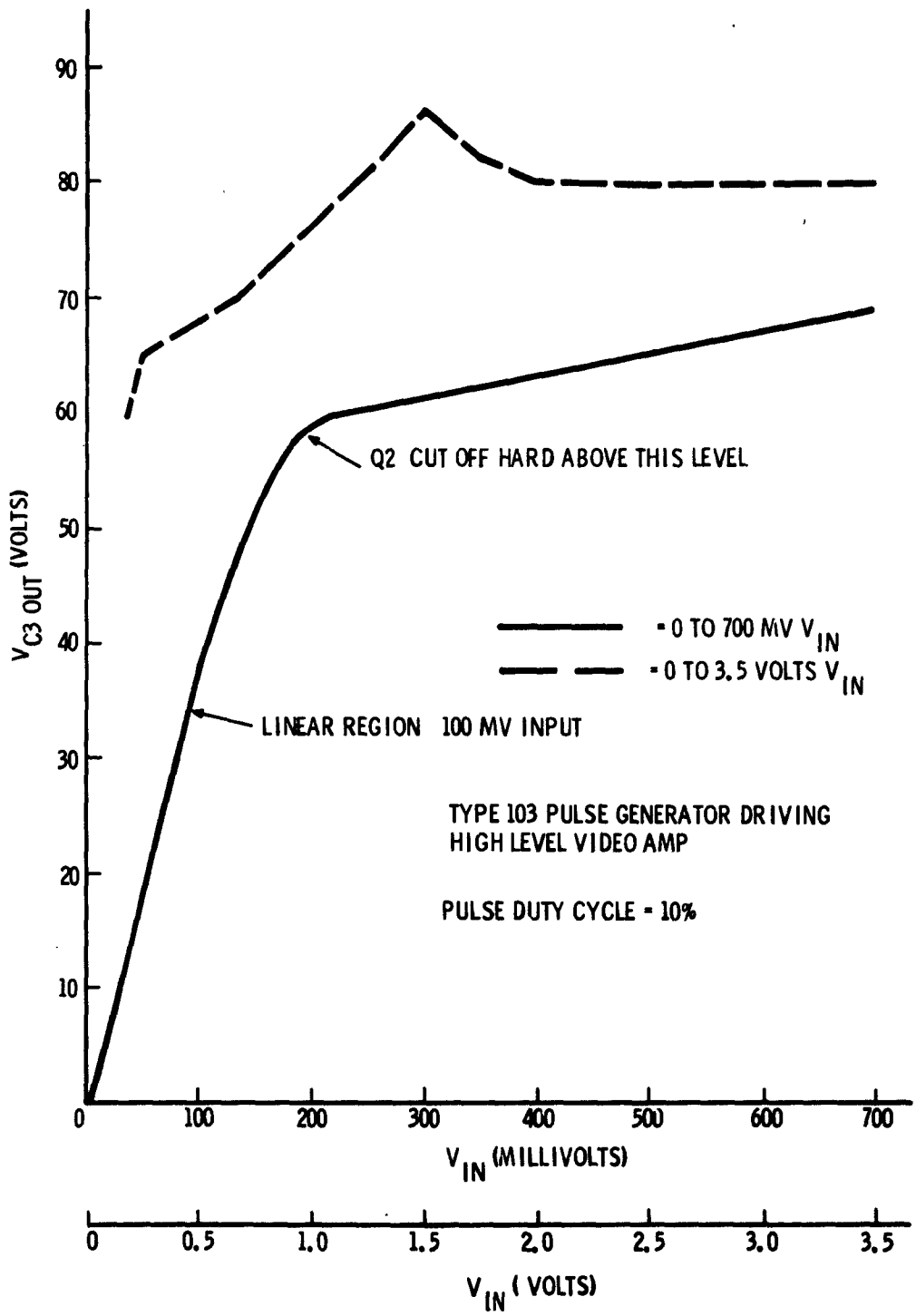

Figure 21. Voltage Gain of High-Level Video Amplifier

voltage gain transfer function is also valid for the low-level pulse voltage gain for duty cycles under 50%. Transistor Q_2 begins to compress the signal for inputs above 100 MV because its gain drops as it is driven to cutoff.

Table 13 presents the performance criteria of the amplifier.

NOTE: The current gain and the base emitter voltage of the three transistors used in this amplifier were taken from manufacturer's documents: [13] and [14].

3.2.4 Transfer Function of the Video Low-Level Limiting Amplifier

This subsection will develop the transfer function for the DC bias conditions of the Video Low-Level Limiting Amplifier presented on page 3 of the RADC Technical Report RADC-TR-59-243.

The circuit accepts short duty cycle positive pulses from a radar detector or some other source and provides a nominal voltage gain of 12 up to the limiting level. Input signals in excess of 5 volts are delivered to the output terminals at a 5 volt level. The maximum signal swing capability and limiting action is achieved by biasing the first stage near cutoff, the second stage near saturation and the output stage at cutoff. A biasing scheme of this type admits unipolar positive pulses at the input and provides for minimum standby power dissipation in the amplifier. Thus, power dissipation capabilities of the output stage are used most advantageously for efficient signal power transfer to succeeding stages. By properly controlling the gain of the first two stages, the output stage may be driven to saturation and limiting action occurs at the desired input signal level. The performance criteria of the amplifier is presented in Table 14.

The amplifier schematic is shown in Figure 22. Critical performance criteria that are considered in the following analysis are the DC quiescent currents and voltages for the condition of no input signal.

The DC equivalent circuit of the amplifier is presented in Figure 23. Note that all AC dependent parameters are removed from the circuit and the diode CR1 is removed because of reversed biasing. The analysis of this circuit yields equations (79) through (87).

TABLE 13

PERFORMANCE CRITERIA OF VIDEO HIGH-LEVEL LINEAR AMPLIFIER

REQUIREMENTS	MAXIMUM	DESIGN CENTER	MINIMUM
INPUT (ONE, UNBALANCED)	— — —	— — —	— — —
INPUT VOLTAGE, POSITIVE PEAK	5V	1V	.01V
INPUT IMPEDANCE	— — —	10,000 Ω	— — —
BANDWIDTH	5 MC	— — —	50 CPS
RISE TIME	— — —	.05 μ SEC	— — —
REPETITION RATE	100 KC	— — —	50 PPS
DUTY CYCLE	0.5	0.2	— — —
OUTPUT IMPEDANCE	— — —	2,200 Ω	— — —
LOAD IMPEDANCE	— — —	— — —	10,000 Ω
DISTORTION DROOP (500- SEC PULSE)	— — —	5%	— — —
OVERSHOOT	10%	5%	— — —
LINEARITY	10%	5%	— — —
VOLTAGE GAIN	— — —	60	— — —
OUTPUT VOLTAGE, NEGATIVE PEAK	100 V	60V	— — —
D-C SUPPLY VOLTAGES	— — —	+25V	— — —
	— — —	+100V	— — —
OPERATING TEMPERATURE	85°C	— — —	-55°C

TABLE 14

PERFORMANCE CRITERIA OF VIDEO LOW-LEVEL LIMITING AMPLIFIER

REQUIREMENTS	MAXIMUM	DESIGN CENTER	MINIMUM
INPUT LEVEL, PEAK POSITIVE	5V	— — —	0.001V
INPUT IMPEDANCE	— — —	— — —	1000 Ω
OUTPUT LEVEL (75-OHM LEAD)	5V	— — —	0.012V
VOLTAGE GAIN (0.001 V TO 0.1 V)	15	12	8
RISE TIME	0.05μSEC	0.035μSEC	— — —
DROOP (500- SEC PULSE)	10%	— — —	— — —
OVERSHOOT	5%	— — —	— — —
LINEARITY (0.001V TO 0.05V)	5%	— — —	— — —
D-C SUPPLY VOLTAGE	— — —	+25V	— — —
OPERATING TEMPERATURE	85°C	+12V	-55°C

$$\frac{V_{E1}}{R_3} = I_{C1} + \frac{I_{C1}}{\beta_1} + \frac{0.6}{r_{b1}} + \frac{V_{C2} - V_{E1}}{R_4} \tag{79}$$

$$\frac{25 - V_{C1}}{R_2} = I_{C1} + \frac{I_{C2}}{\beta} + \frac{0.6}{r_{b2}} \tag{80}$$

$$\frac{V_{E2}}{R_6} + \frac{V_{E2} - V_{E1} - 0.6}{R_{11}} = I_{C2} + \frac{I_{C2}}{\beta_2} + \frac{0.6}{r_{b2}} \tag{81}$$

$$\frac{25 - V_{C2}}{R_5} = I_{C2} + \frac{V_{C2} - V_{E1}}{R_4} \tag{82}$$

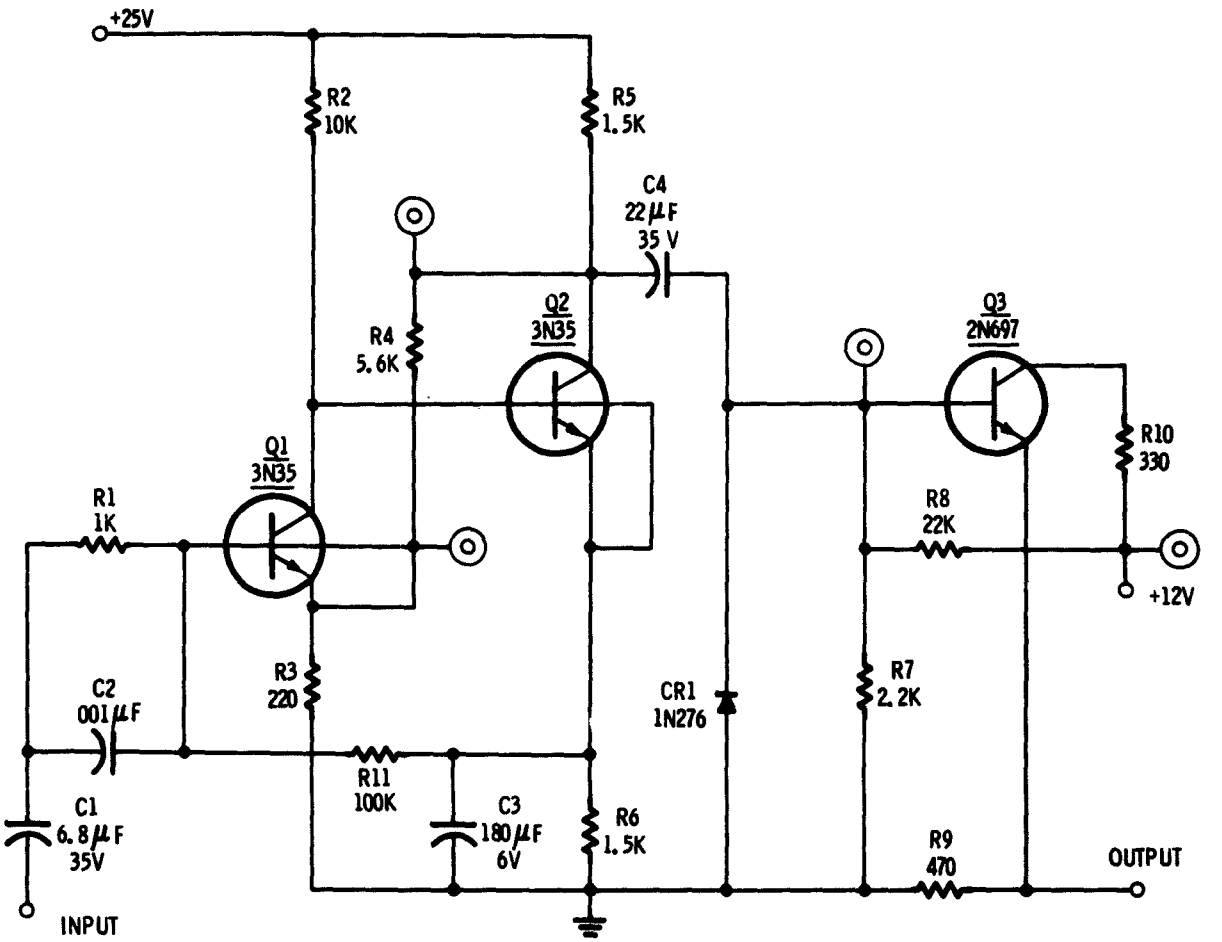

Figure 22. Schematic of Video Low-Level Limiting Amplifier

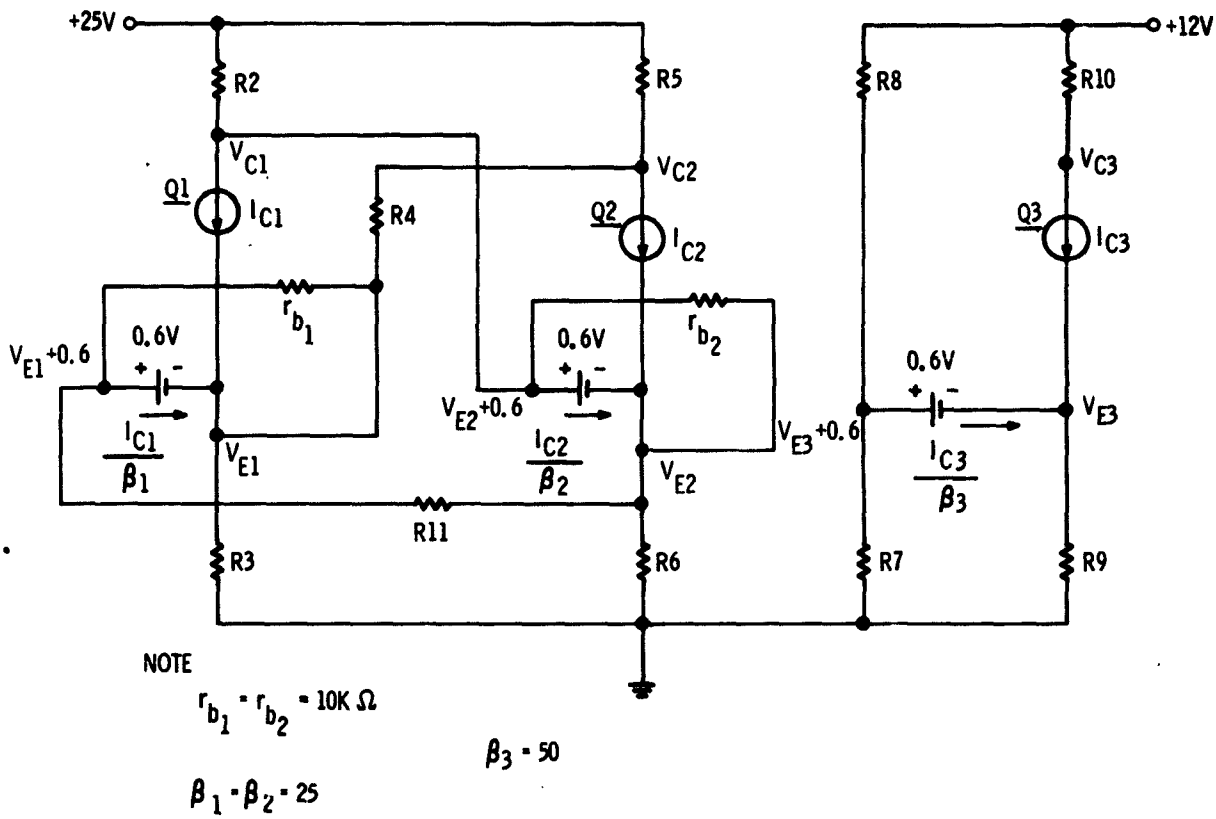

Figure 23. DC Equivalent Circuit of Video Low-Level Limiting Amplifier

$$V_{E2} + 0.6 = V_{C1} \tag{83}$$

$$\frac{I_{C1}}{\beta_1} + \frac{0.6}{r_{b1}} = \frac{V_{E2} - V_{E1} - 0.6}{R_{11}} \tag{84}$$

$$\frac{V_{E3}}{R_9} = I_{C3} + \frac{I_{C3}}{\beta_3} \tag{85}$$

$$\frac{I_{C3}}{\beta_3} = \frac{12 - V_{E3} - 0.6}{R_8} - \frac{V_{E3} + 0.6}{R_7} \tag{86}$$

$$I_{C3} = \frac{12 - V_{C3}}{R_{10}} \tag{87}$$

These equations are used to form the matrix equation (88).

The matrix equation is then solved using a computer and Table 15 presents a comparison of the measured and calculated values of the critical circuit parameters. Thus, an examination of the results validates the developed transfer function.

TABLE 15

COMPARISON OF MEASURED AND CALCULATED VALUES OF THE LOW-LEVEL LIMITING AMPLIFIER

COMPUTED:								
V_{C1}	V_{C2}	V_{C3}	V_{E1}	V_{E2}	V_{E3}	I_{C1}	I_{C2}	I_{C3}
11.76	11.34	11.68	0.5656	11.16	0.453	0.000976	0.000719	0.00945
MEASURED:								
V_{C1}	V_{C2}	V_{C3}	V_{E1}	V_{E2}	V_{E3}			
11.0V	12.0	11.7	0.55	10.0	0.50			

$$
\begin{bmatrix}
\frac{1}{R_2} & 0 & 0 & 0 & 0 & 0 & 1 & \frac{1}{\beta_2} & 0 \\
0 & -\frac{1}{R_4} & 0 & \frac{1}{R_3}+\frac{1}{R_4} & 0 & 0 & -1-\frac{1}{\beta_1} & 0 & 0 \\
0 & 0 & \frac{1}{R_{10}} & 0 & 0 & 0 & 0 & 0 & 1 \\
0 & \frac{1}{R_4}+\frac{1}{R_5} & 0 & -\frac{1}{R_4} & 0 & 0 & 0 & 1 & 0 \\
1 & 0 & 0 & 0 & -1 & 0 & 0 & 0 & 0 \\
0 & 0 & 0 & 0 & 0 & -\frac{1}{R_9} & 0 & 0 & 1+\frac{1}{\beta_3} \\
0 & 0 & 0 & -\frac{1}{R_{11}} & -\frac{1}{R_{11}} & 0 & \frac{1}{\beta_1} & 0 & 0 \\
0 & 0 & 0 & -\frac{1}{R_{11}} & \frac{1}{R_6}+\frac{1}{R_{11}} & 0 & 0 & -1-\frac{1}{\beta_2} & 0 \\
0 & 0 & 0 & 0 & 0 & \frac{1}{R_8}+\frac{1}{R_7} & 0 & 0 & \frac{1}{\beta_3}
\end{bmatrix}
\begin{bmatrix}
V_{C1} \\ V_{C2} \\ V_{C3} \\ V_{E1} \\ V_{E2} \\ V_{E3} \\ I_{C1} \\ I_{C2} \\ I_{C3}
\end{bmatrix}
=
\begin{bmatrix}
\frac{25}{R_2}-\frac{0.6}{r_{b_2}} \\
\frac{0.6}{r_{b_1}} \\
\frac{12}{r_{10}} \\
\frac{25}{R_5} \\
0.6 \\
0 \\
-\frac{0.6}{r_{b_1}}-\frac{0.6}{R_{11}} \\
\frac{0.6}{R_{11}}+\frac{0.6}{r_{b_2}} \\
\frac{11.4}{R_8}-\frac{0.6}{R_7}
\end{bmatrix}
\qquad (88)
$$

3.2.4.1 Low-Level Amplifier Mathematical Simulation

As was described in detail in Section 2, the performance of the Low-Level Limiting Amplifier was evaluated by simulating the assembling of 1000 amplifiers utilizing the 9400 Sylvania computer. The necessary computer routine to accomplish this evaluation is represented by the flow diagram shown in Figure 24.

Table 16 describes the underlying frequency distribution of the various components in the circuits. The μ represents the nominal value, the σ represents the standard deviation, (σ^2 = variance), the upper and lower limits represent the truncation points of the distribution, i.e., the tolerance limits for each component.

These underlying frequency distributions which define the parameters in a statistical manner are utilized in the repeated computation of the transfer function. The results of 1000 iterations are shown in Figures 25 through 28. Having determined acceptable boundary conditions for each of the critical performance criteria required for acceptable operation of the circuit, it is possible to determine from Figures 25 through 28 the over-all reliability of the circuit. Moreover, the sensitivity of the individual performance criteria as a function of the variability of the individual circuit components is also established. This process can be repeated for any number of hours of simulated use. This is accomplished by simulating the aging of component parts using degradation rates as shown in Table 16. These rates must be determined by analyzing the physics of failure of various elements of a circuit. [20]

Referring to Table 16, the means and variances (μ s and σ s) for the various components (at t = 1000 hours) are given. With this information that describes the underlying frequency distribution of the parts, it is possible to determine the cumulative distribution functions of the circuit parameters at t = 1000 hours by repeating the technique outlined above. The cumulative distribution functions are plotted in Figures 29 through 34. As a check on the randomness of the number generator, two of the circuit input cumulative distribution functions were plotted. At t = 0, the cumulative distribution function of R_1 was plotted and is presented in Figure 35. At t = 1000 hours, the cumulative distribution function of β_1 was plotted and is shown in Figure 36. The general shape of these curves i.e., the straight line indicating uniform distribution and the S shape curve indicating normal distribution, validate the correct operation of the random number generator.

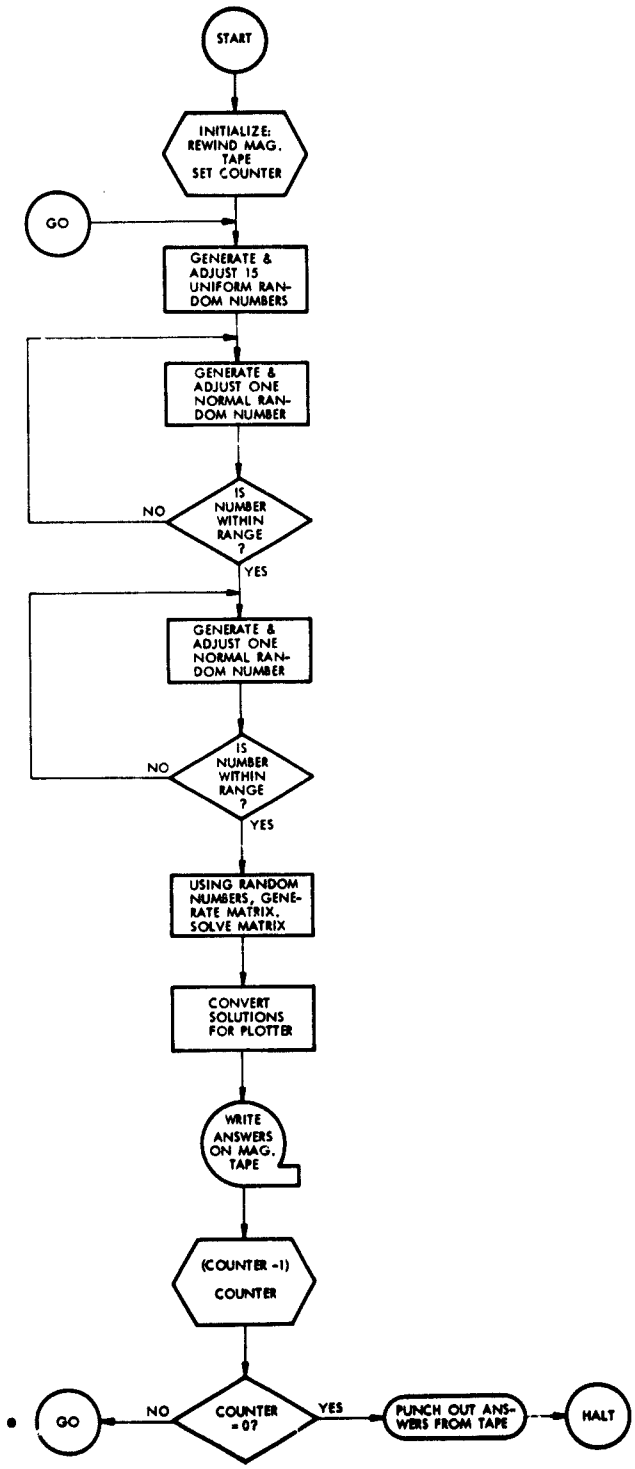

ure 24. Flow Chart of Monte Carlo Techniques Using Matrix of Order Nine for Low-Level Video Amplifier

TABLE 16

UNDERLYING A FREQUENCY DISTRIBUTION OF PARAMETERS USED IN LOW-LEVEL LIMITING AMPLIFIER

	t = 0 HRS				t = 1000 HRS			
	MEAN μ	STANDARD DEVIATION σ	LOWER LIMIT	UPPER LIMIT	MEAN μ	STANDARD DEVIATION σ	LOWER LIMIT	UPPER LIMIT
R1	1,000	29	950	1,050	1,000	58	900	1,100
R2	10,000	290	9,500	10,500	10,000	578	9,000	11,000
R3	220	6	209	231	220	13	198	242
R4	5,600	162	5,320	5,880	5,600	324	5,040	6,160
R5	1,500	43	1,425	1,575	1,500	87	1,350	1,650
R6	1,500	43	1,425	1,575	1,500	87	1,350	1,650
R7	2,200	64	2,090	2,310	2,200	127	1,980	2,420
R8	22,000	640	20,900	23,100	22,000	1270	19,800	24,200
R9	470	14	446	493	470	27	423	517
R10	330	10	313	346	330	19	297	363
R11	100,000	2890	95,000	105,000	100,000	5780	90,000	110,000
*β1	20	4	10	38	27	7	10	50
*β2	20	4	10	38	27	7	10	50
rb1	10,000	2890	5,000	15,000	10,000	2890	5,000	15,000
rb2	10,000	2890	5,000	15,000	10,000	2890	5,000	15,000
*β3	75	26	30	120	75	36	25	150

NOTE: ALL DISTRIBUTIONS UNIFORM EXCEPT β1 & β2 WHICH ARE TRUNCATED NORMAL

*TEXAS INSTRUMENT TRANSISTOR RELIABILITY DATA 3RD QUARTER 1961

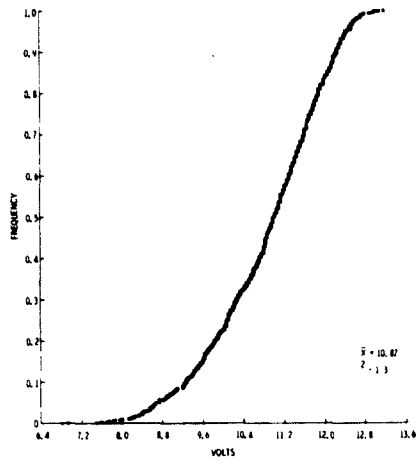

Figure 25. Cumulative Distribution Function of V_{C2} (Zero Time)

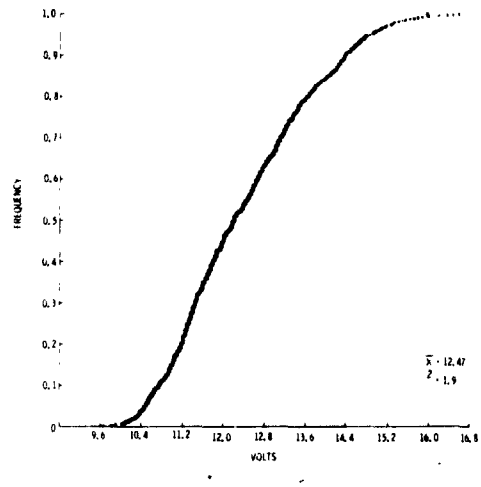

Figure 26. Cumulative Distribution Function of V_{C1} (Zero Time)

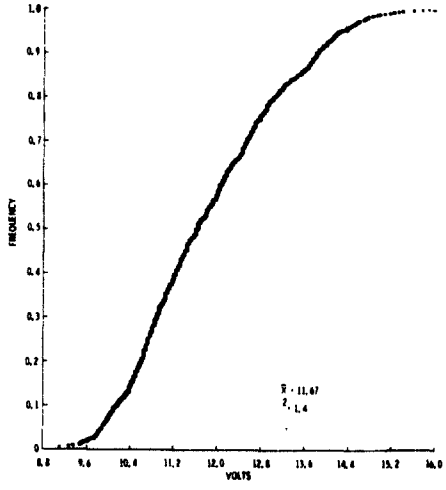

Figure 27. Cumulative Distribution Function of V_{C3} (Zero Time)

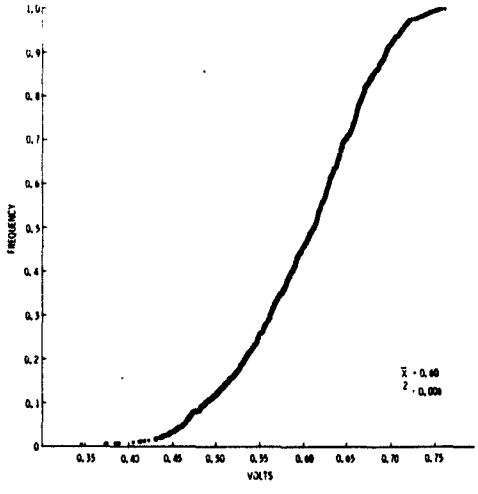

Figure 28. Cumulative Distribution Function of V_{E1} (Zero Time)

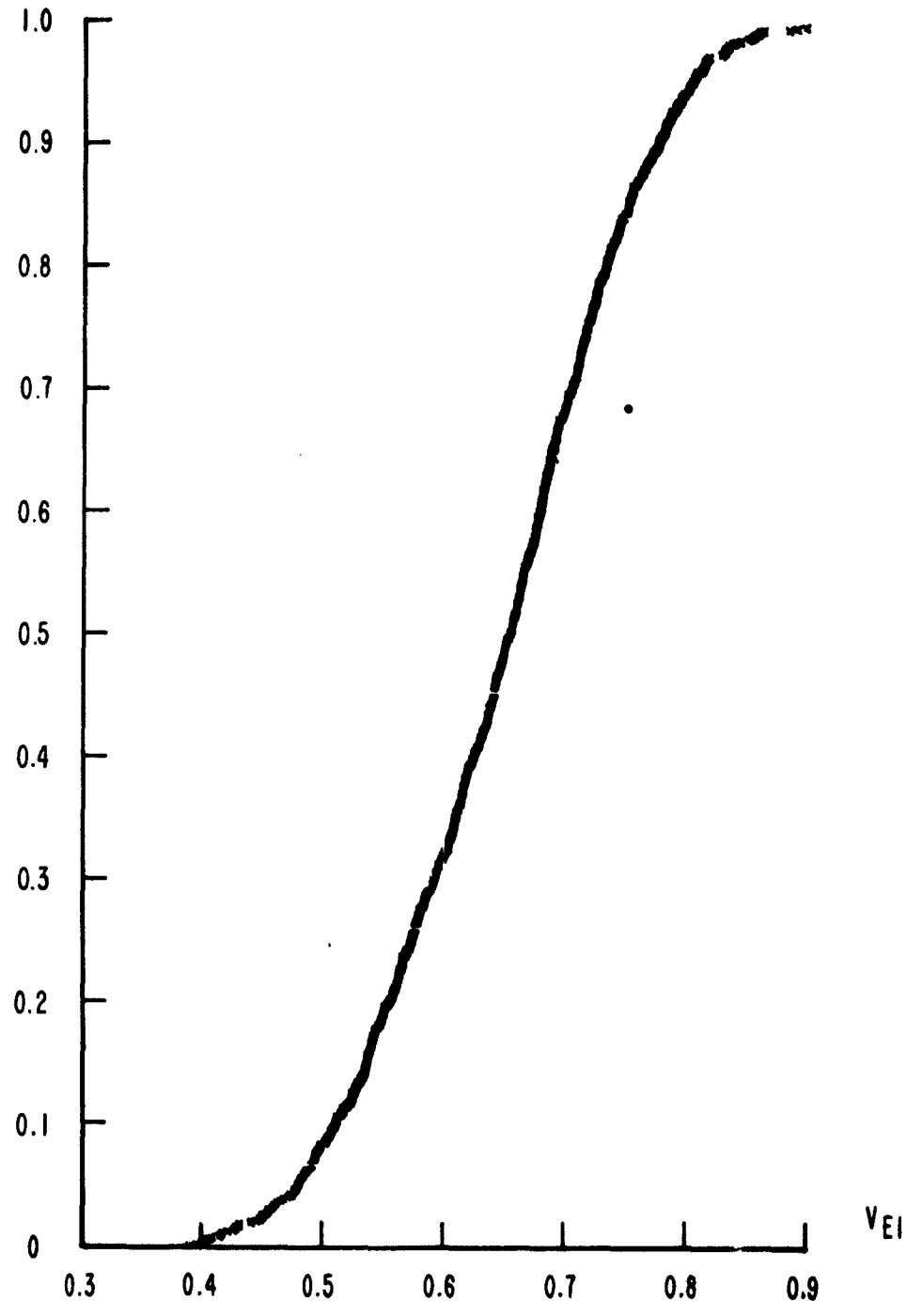

Figure 29. Cumulative Distribution Function of V_{E1} (t = 1000 Hrs.)

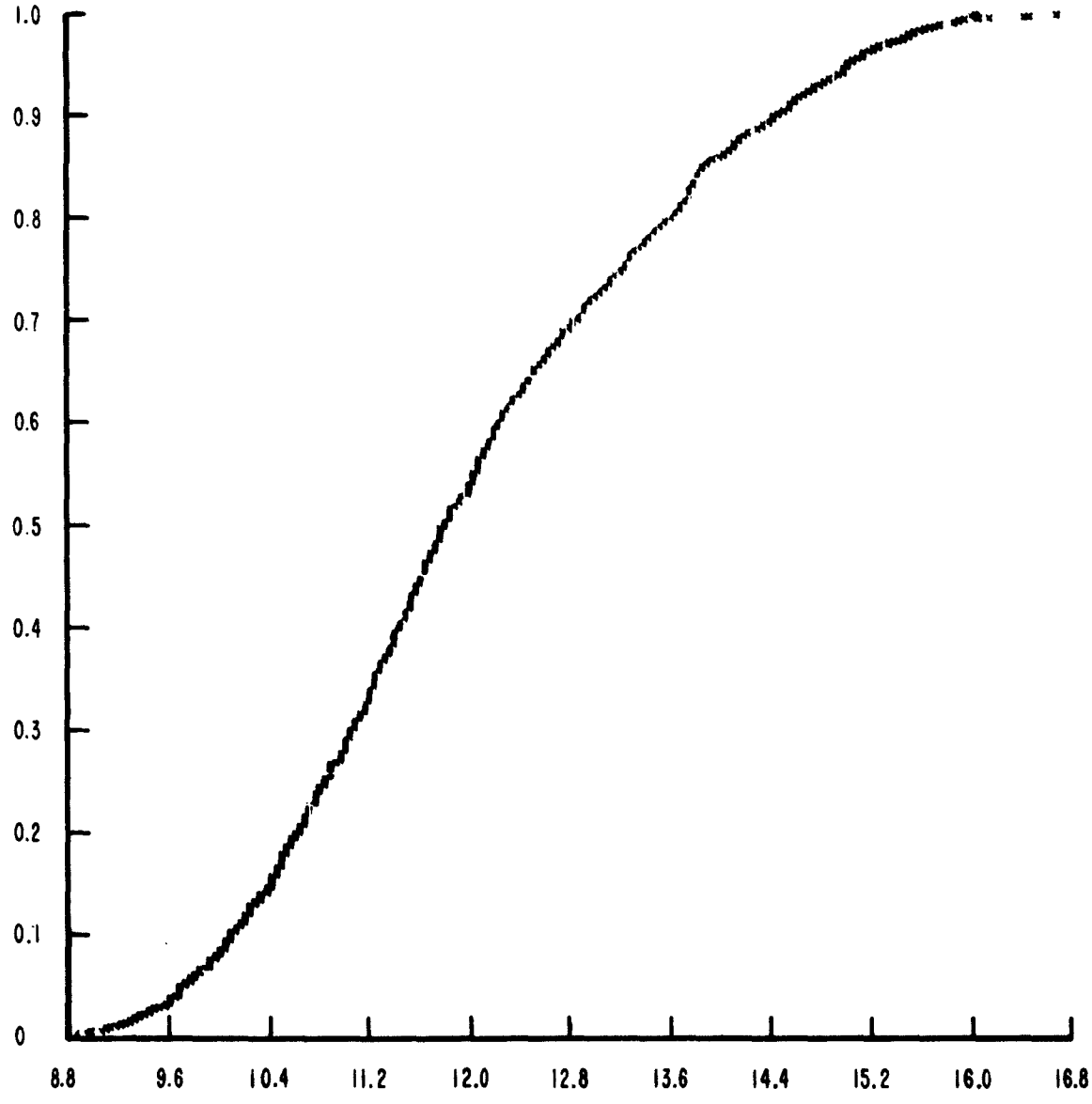

Figure 30. Cumulative Distribution Function of V_{Cl} (t = 1000 Hrs.)

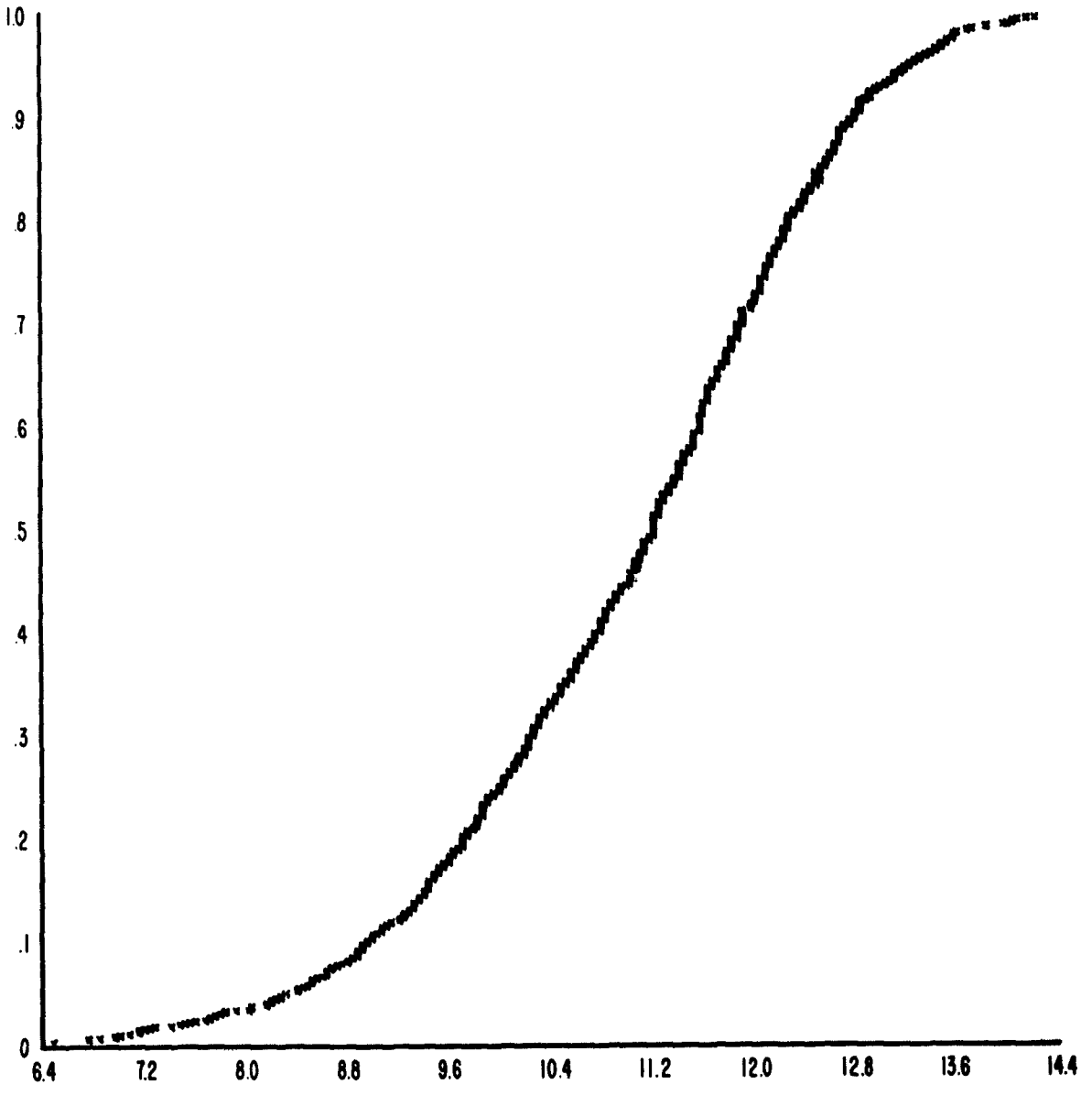

Figure 31. Cumulative Distribution Function of V_{C2} (t = 1000 Hrs.)

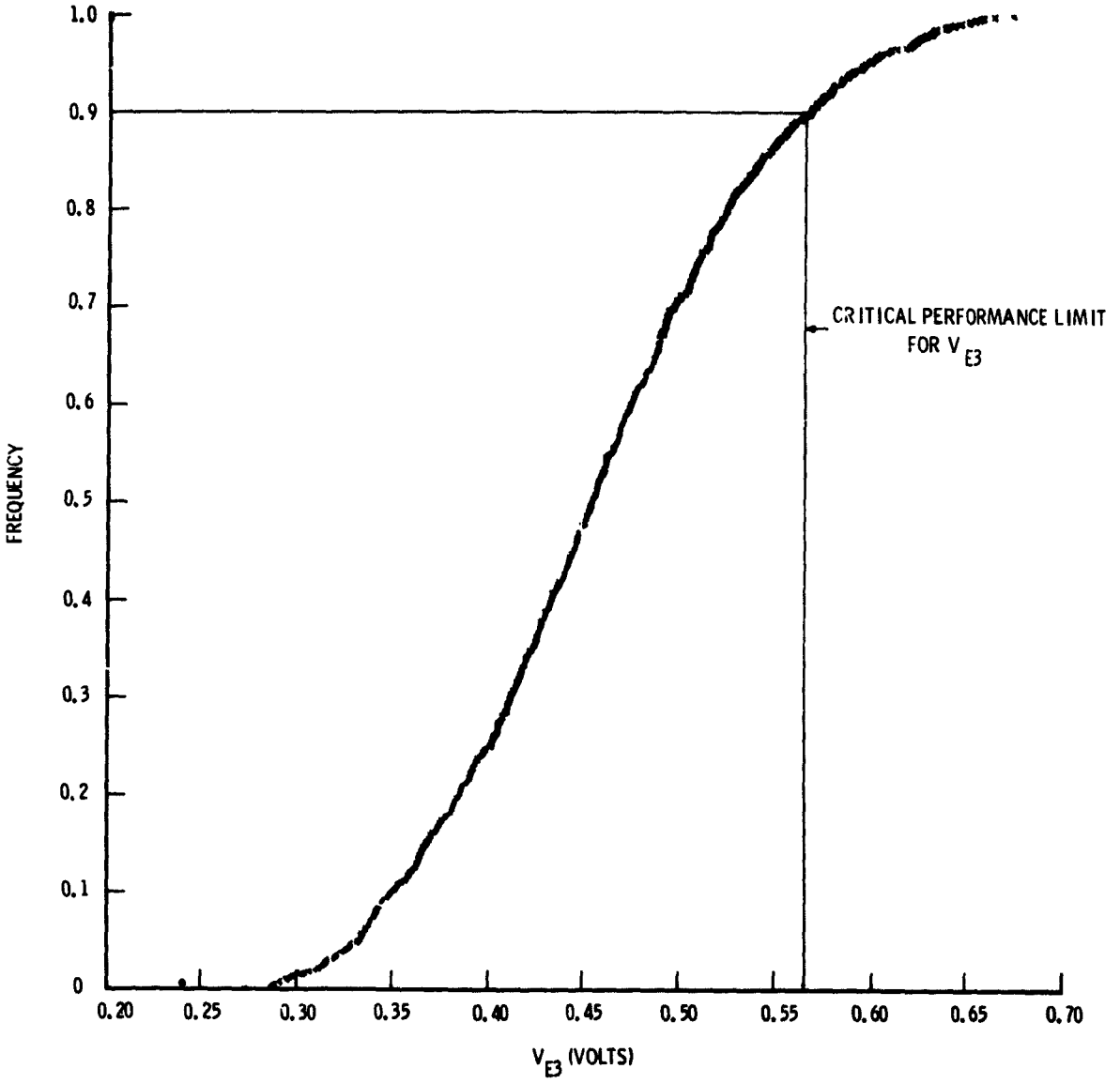

Figure 32. Cumulative Distribution Function of V_{E3} (t = 1000 Hrs.)

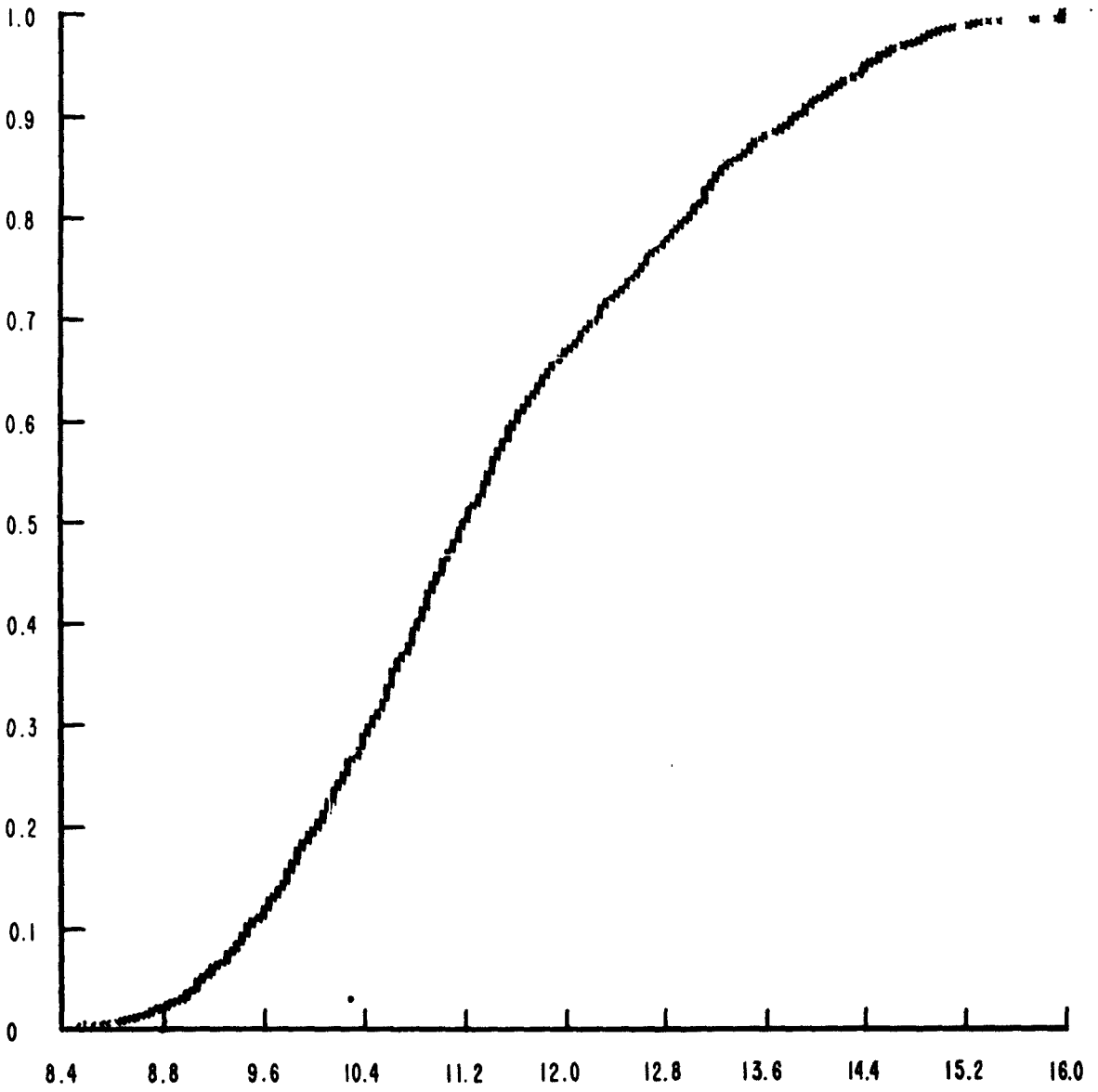

Figure 33. Cumulative Distribution Function of V_{E2} (t = 1000 Hrs.)

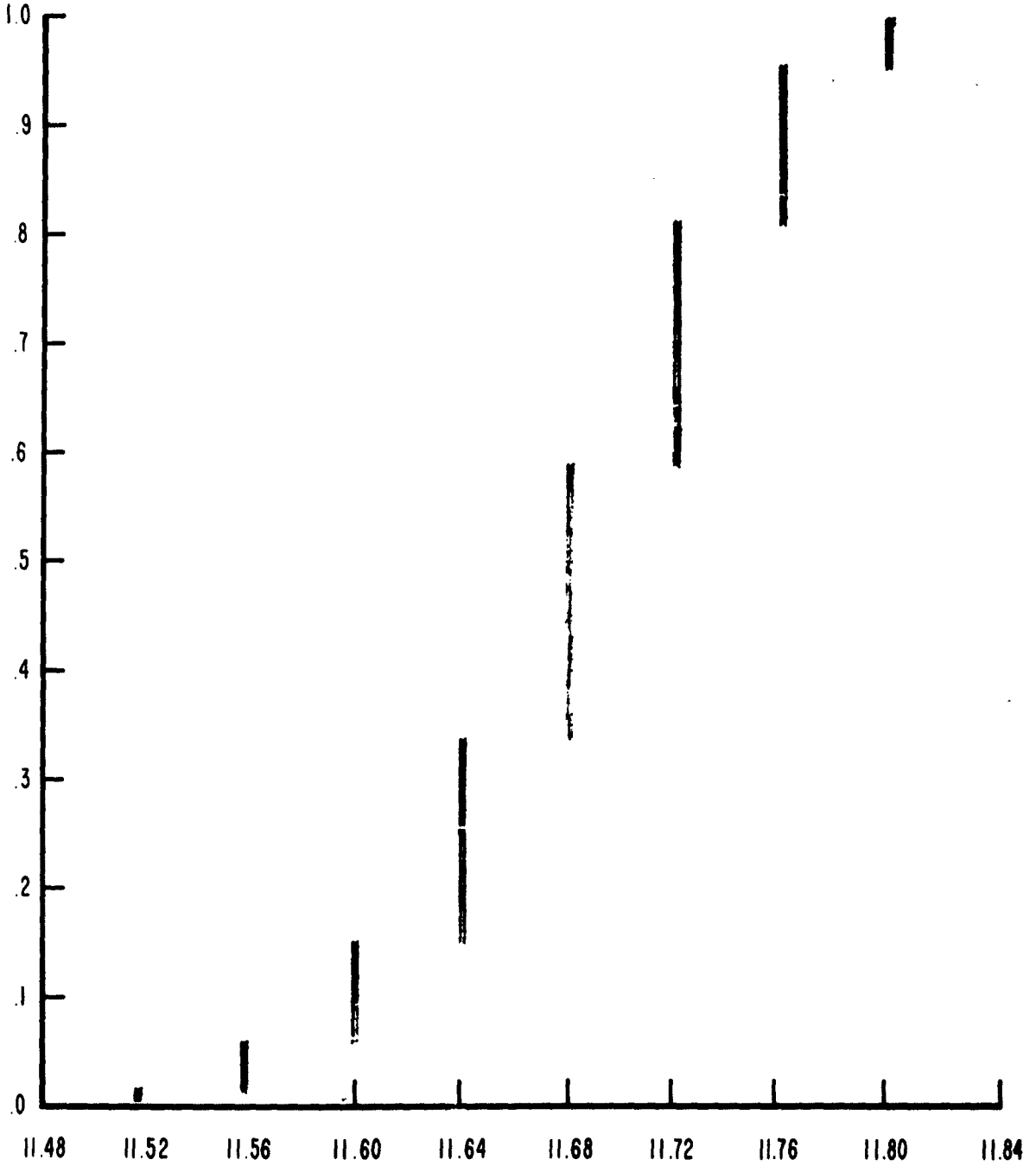

Figure 34. Cumulative Distribution Function of V_{C3} (t = 1000 Hrs.)

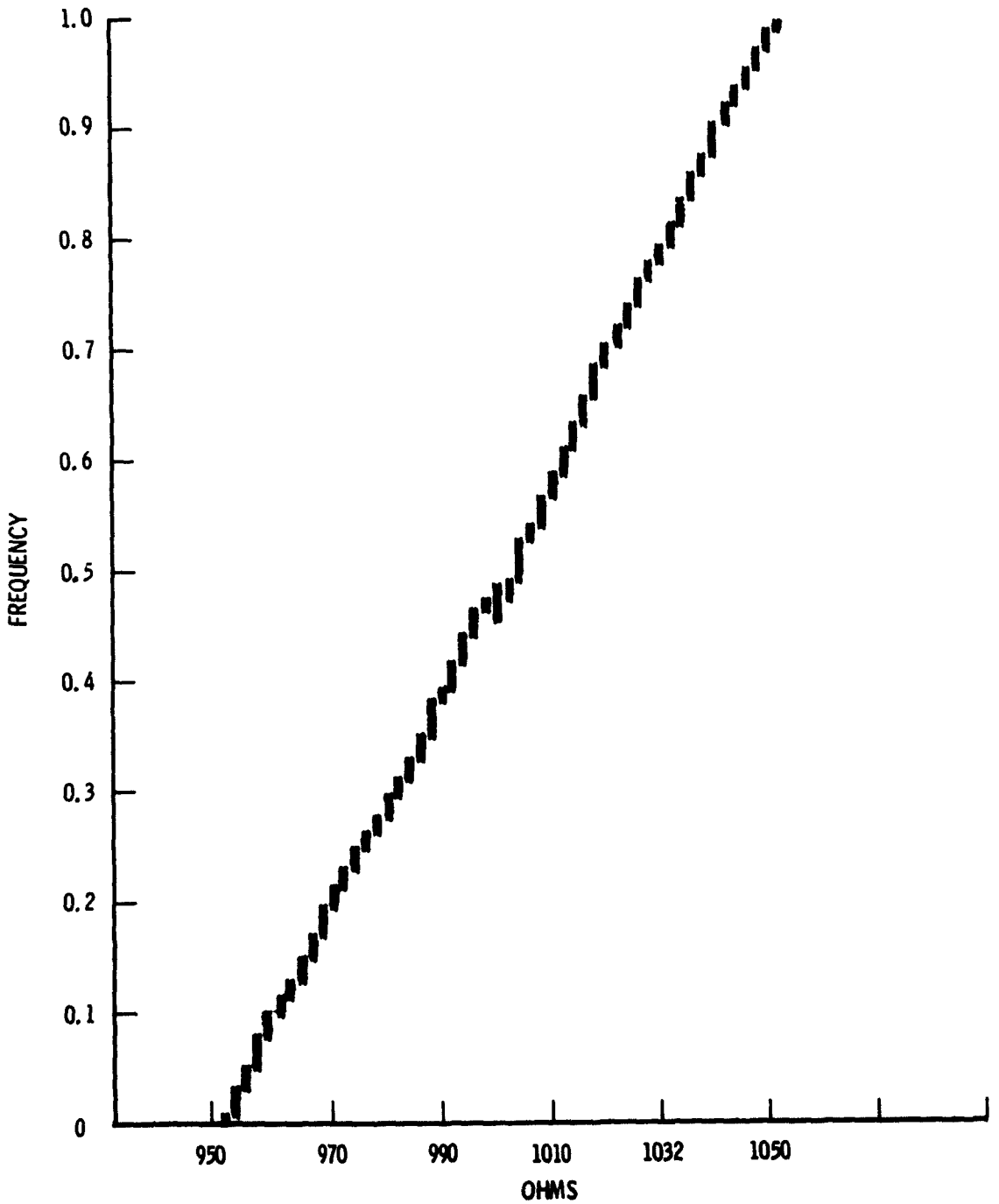

Figure 35. Cumulative Distribution Function of R_1 (Zero Time)

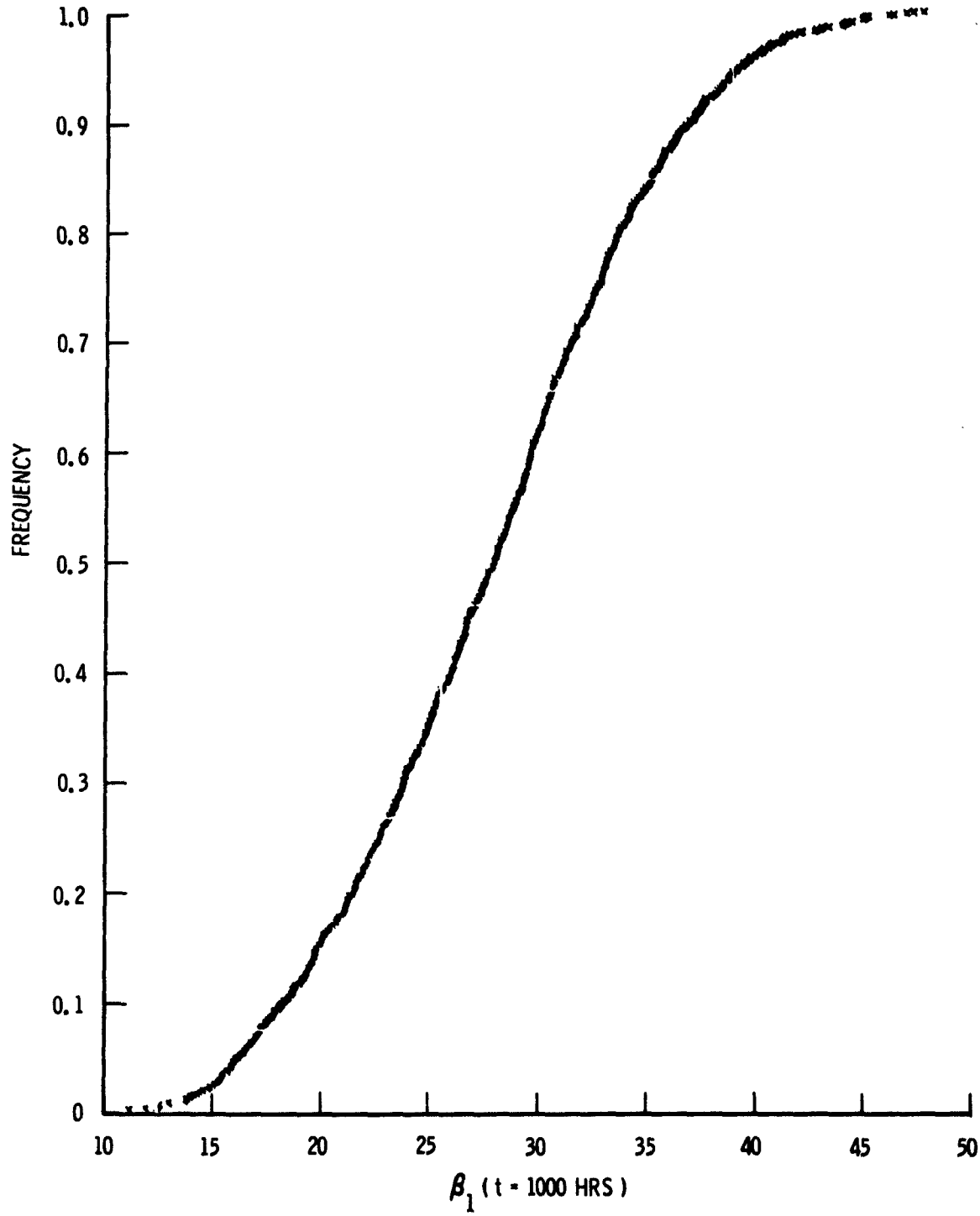

Figure 36. Cumulative Distribution Function of β_1 (t = 1000 Hrs.)

As an example of the usefulness of this technique, consider the critical performance limit of V_{E3} to be 0.6 volts. Referring to Figure 37, the cumulative distribution function of V_{E3} at $t = 0$, it may be seen that a 0.6 critical performance limit produces no failures. However, making use of the Monte Carlo technique, referring to Figure 32 it may be seen that at $t = 1000$ hours that 4 percent of the units would fail. Thus, the example above briefly highlights the usefulness of this technique in predicting the future reliability of a circuit or system.

3.2.5 Transfer Functions of the Monostable Multivibrator

The monostable multivibrator circuit appearing on page 55 of the RADC Technical Report RADC-TR-59-243 has been analyzed and the following transfer functions as a function of individual circuit parameters as well as the supply voltages have been developed:

(a) Quiescent current and voltage

(b) Output amplitude

(c) Output pulse width

The schematic of the monostable multivibrator is shown in Figure 38 and the performance criteria of this circuit is presented in Figure 39.

The monostable multivibrator has two states, one permanently stable and one quasi-stable state. This type of multivibrator requires a triggering signal to change from the stable to the quasi-stable state. It is possible for the multivibrator to remain in its quasi-stable state for a long period of time in comparison to the time required for transition between states. However, no external signal is required to reverse this transition, i.e., eventually the multivibrator will return from the quasi-stable state to its stable state unaided. [24]

When a single negative input trigger is fed to the monostable multivibrator represented in Figure 38, an output gate with a controlled width and a fixed amplitude is delivered to its output terminal. Transistors Q_1 and Q_2 form a regenerative feedback pair while transistors Q_3 and Q_4 operate as emitter followers providing a low output impedance as well as isolating the timing and trigger functions from external disturbances. Transistor Q_2 is normally operating in the non-saturated condition while Q_1 is cut off. When a trigger is fed to the multivibrator, Q_2 is cut off and regenerative action drives Q_1 into saturation. During

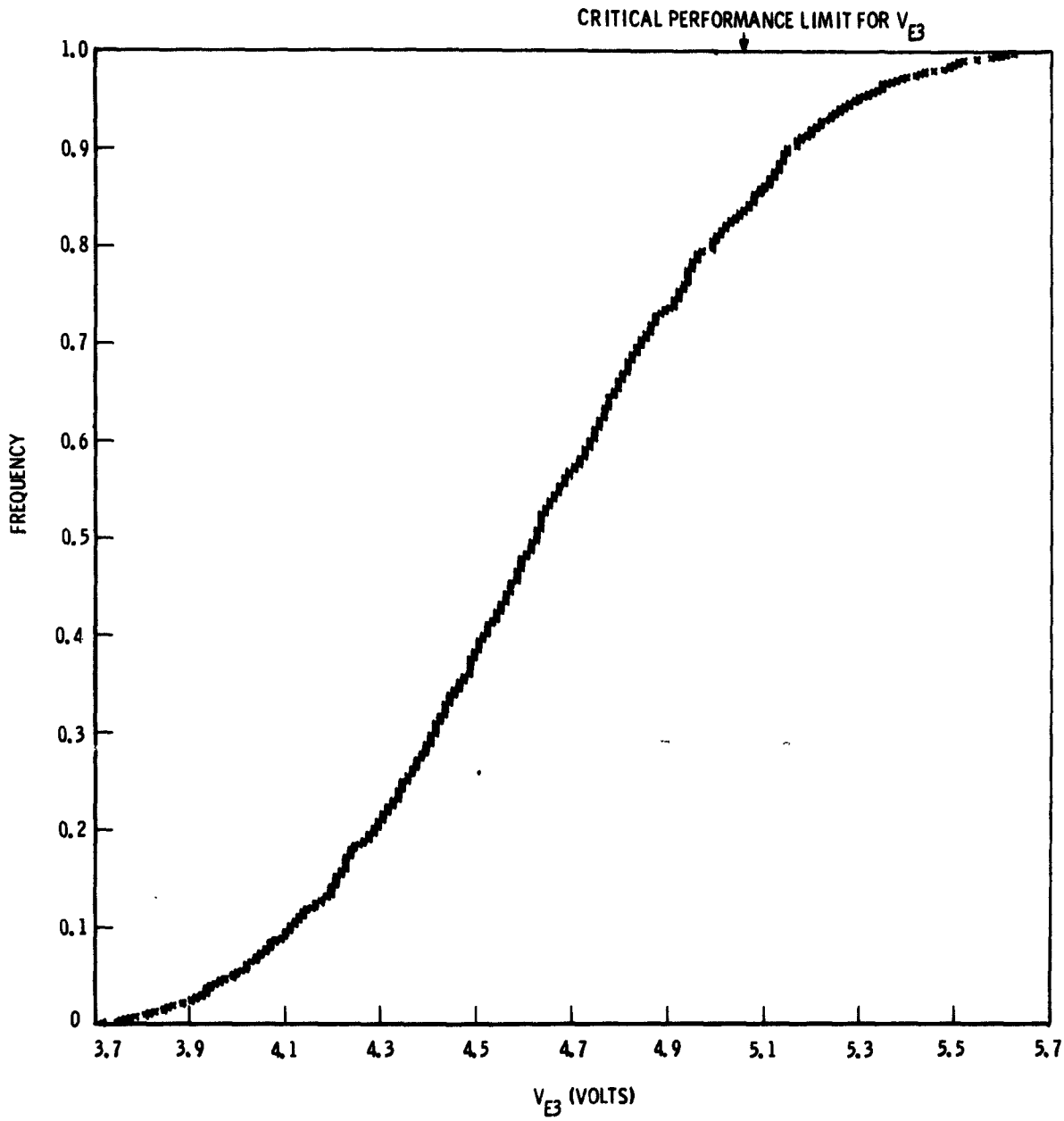

Figure 37. Cumulative Distribution Function of V_{E3} at Time Zero

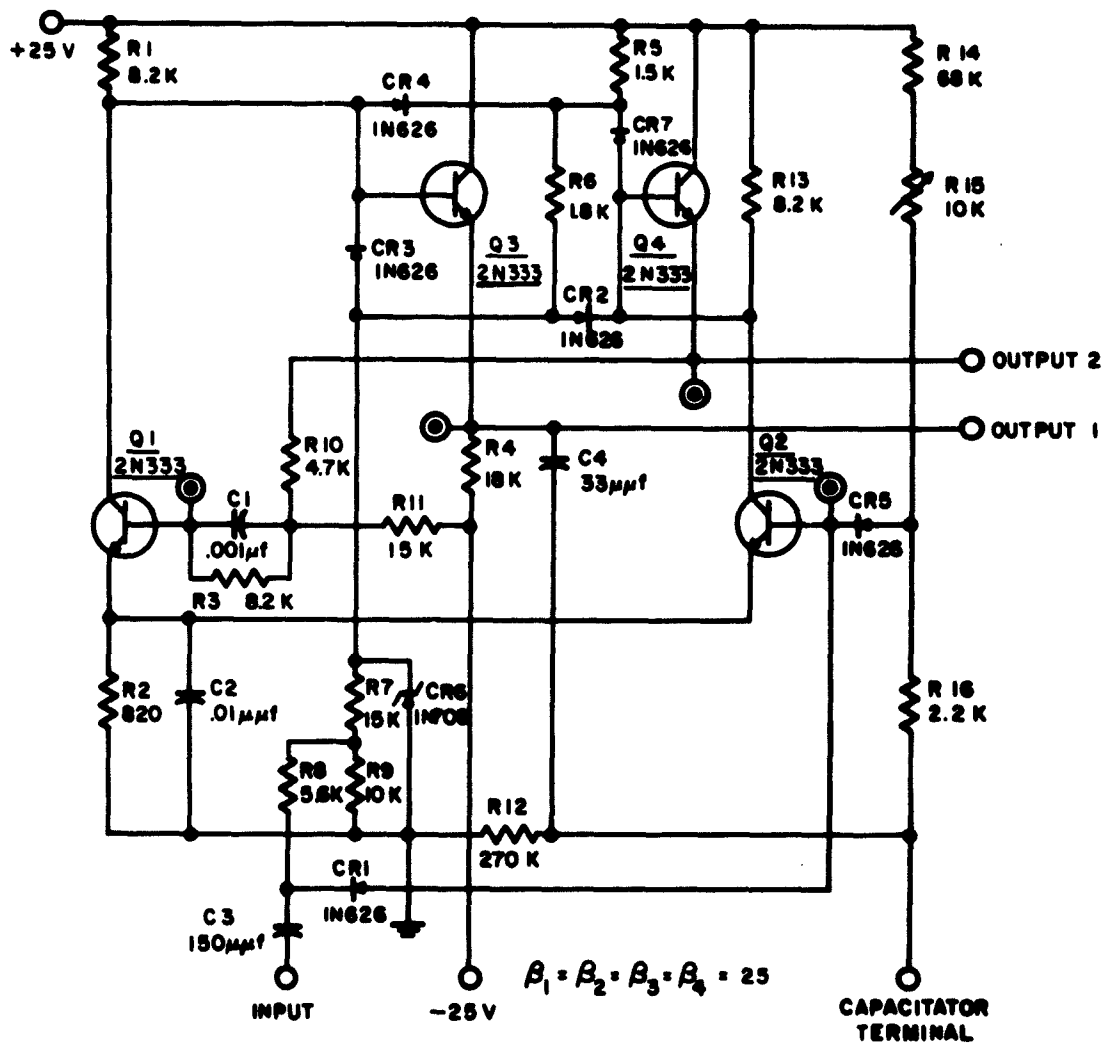

Note: All Resistors ± 5% Tolerance, 1/2 watt Rating.

Figure 38. Schematic of Monostable Multivibrator

Requirements	Maximum	Design Center	Minimum
Trigger Amplitude	-10 v	-5.0 v	-4.0 v
Trigger Risetime	1 μsec	---	0.1 μsec
Input Impedance	---	---	9,000 Ω
Output Amplitude	18 v	15 v	10 v
Output Polarity, Both AC Coupled	---	---	---
Output Risetime	1 μsec	0.6 μsec	---
Output Decay Time	1 μsec	0.6 μsec	---
Repetition Rate (Limited to 50% Duty Cycle)	250 kc	---	---
Pulse Width, Minimum (Adjustable ± 10%)	---	2.0 μsec	---
Pulse Width, Maximum (C_x = 0.5 μfd, adjustable ±10%)	---	20 μsec	---
Output Loading	---	---	2,500
Distortion, Droop	10%	---	---
Distortion, Overshoot	10%	---	---
DC Supply Voltages	---	+25 v	---
	---	-25 v	---
Operating Temperature	85°C	---	-55°C

Figure 39. Performance Criteria of Monostable Multivibrator

the transition, a charge is stored on the parallel combination of capacitor C_4 and the external timing capacitor. The charge on these capacitors dissipates in a finite time period corresponding to the gate length.

The basic application, that of a gating or timing circuit, of this type of multivibrator results from the fact that it may be used to establish a fixed time interval, the beginning and end of which are marked by an abrupt discontinuity in the voltage waveform.

Quiescent Current and Voltage for Q_1 Off During Stable State

The DC quiescent currents and voltages are derived when the monostable multivibrator is in its stable state with no input signal applied. When the circuit is in this condition, Q_1, CR_3, and CR_7 can be removed because they are reverse biased. Then, Figure 40 is the DC equivalent circuit for the state in which Q_1 is nonconducting and Q_2 is conducting. Transistors Q_3 and Q_4 are emitter followers and, therefore, are conducting but are not saturated nor cut off. A 0.6 V drop was assumed across each transistor input and also across CR_1, CR_2, CR_4 and CR_5 since they are forward biased. The cathode of zener diode CR_6 was assumed to be at or less than 6.2V because of the zener diode equivalent circuit in Figure 41. A complete circuit analysis of the multivibrator for this state yields equations (89) through (99).

$$\frac{25 - V_{E3} - 0.6}{R_1} = \frac{-(25 - V_{E3})}{R_5} + \frac{V_{E3} - V_{E4} - 1.2}{R_6} + \frac{I_{C3}}{\beta_3} \qquad (89)$$

$$I_{C3} + \frac{I_{C3}}{\beta_3} = \frac{V_{E3}}{R_{L1}} + \frac{V_{E3} + 25}{R_4} \qquad (90)$$

$$\frac{V_{E3} - V_{E4} - 1.2}{R_6} = \frac{I_{C4}}{\beta} + \frac{V_{E4} + 1.2 - V_1}{R_7} - \frac{25 - V_{E4} - 0.6}{R_{13}} + I_{C2} \qquad (91)$$

$$\frac{25 - V_{E2} - 1.2}{R_{14} + R_{15}} = \frac{V_{E2} + 1.2}{R_{16} + R_{12}} + \frac{I_{C2}}{\beta_2} + \frac{V_{E2} - V_1}{R_8} \qquad (92)$$

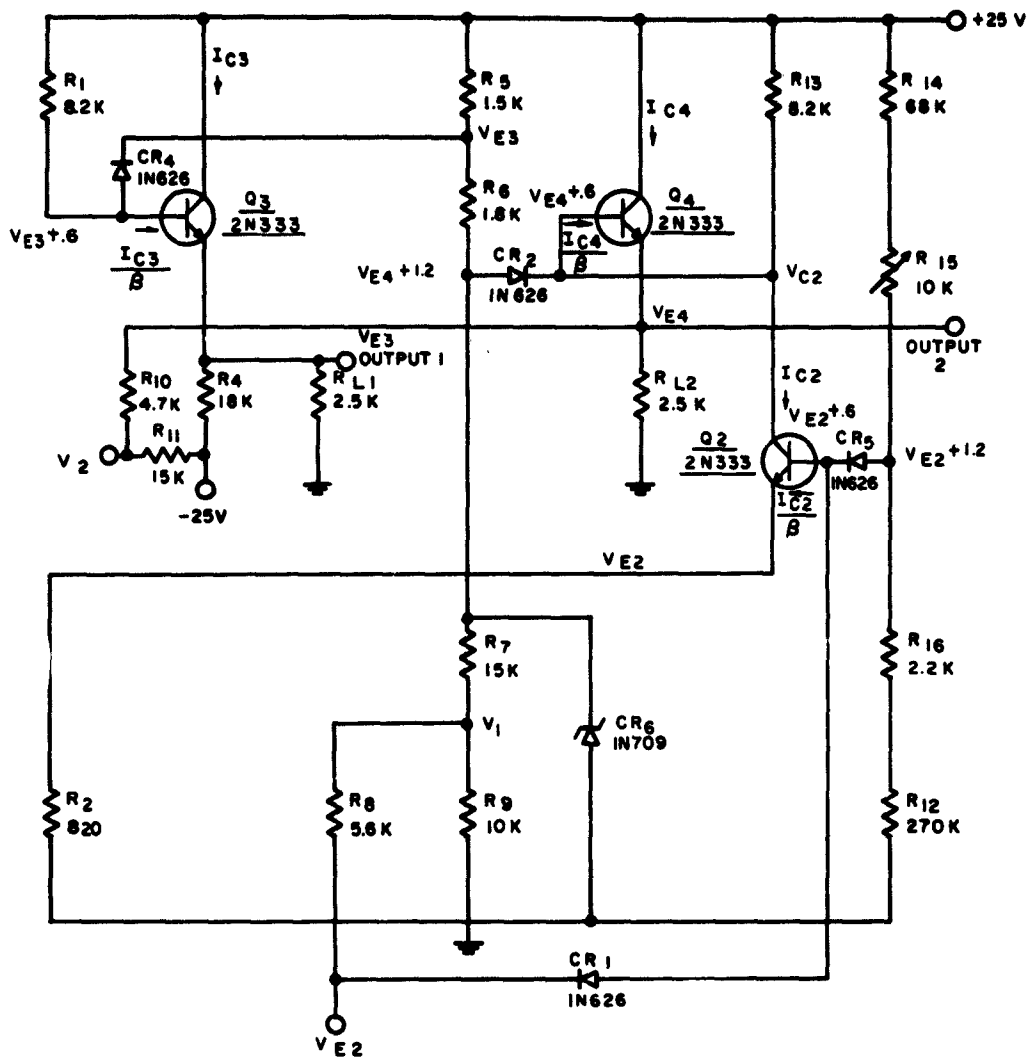

Figure 40. DC Equivalent Circuit for the Monostable during the Stable State, with Q_1 Off and Q_2 Conducting.

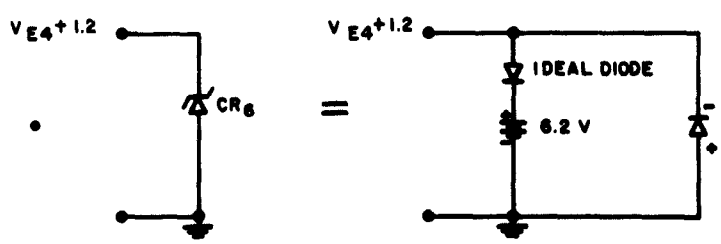

Figure 41. DC Equivalent Circuit for Zener Diode CR6

$$\frac{V_{E2} - V_1}{R_8} + \frac{V_{E4} + 1.2 - V_1}{R_7} = \frac{V_1}{R_9} \tag{93}$$

$$I_{C2} + \frac{I_{C2}}{\beta_2} = \frac{V_{E2}}{R_2} \tag{94}$$

$$I_{C4} + \frac{I_{C4}}{\beta_4} = \frac{V_{E4}}{R_{L2}} + \frac{V_{E4} - V_2}{R_{10}} \tag{95}$$

$$\frac{V_{E4} - V_2}{R_{10}} = \frac{V_2 + 25}{R_{11}} \tag{96}$$

$$V_{C2} = V_{E4} + 0.6 \tag{97}$$

$$V_{E4} + 1.2 \leqq 6.2 \quad \text{Due to CR6} \tag{98}$$

$$V_{C2} > V_{E2} + 0.2 \quad \text{For } Q_2 \text{ Non-Saturated} \tag{99}$$

These equations completely describe the quiescent currents and voltages of the monostable multivibrator. It must be noted that in order for the transistor Q_2 to be saturated the inequalities (98) and (99) must be satisfied. Therefore, it is possible to obtain four different solutions when Equations (89) through (97) are solved. The following procedure will indicate which of the solutions is correct.

(a) If the solution is such that $V_{E4} \leqq 5V$ and $V_{C2} > V_{E2} + 0.2$ then equations (89) through (97) are valid.

(b) If the solution is such that $V_{E4} \leqq 5V$ and $V_{C2} \leqq V_{E2} + 0.2$, then Q_2 is saturated and equations (89) through (97) must be revised as follows: In equations (92) and (94) set $I_{C2}/\beta = I_{B2}$ and add equation (100)

$$V_{C2} = V_{E2} + 0.2 \tag{100}$$

(c) If the solution is such that $V_{E4} > 5V$ and $V_{C2} > V_{E2} + 0.2$, then CR_6 is in zener breakdown, Q_2 is not saturated and equations (89) through (97) must be revised as follows:

In equations (89), (91), (93), (95), (96) and (97) set $V_{E4} = 5V$.

(d) If the solution is such that $V_{E4} \leqq 5\,V$ and $V_{C2} \leqq V_{E2} + 0.2$, then CR_6 is in zener breakdown, Q_2 is saturated and the equations must be revised as in (b) and (c).

Equations (89) through (97) are now used to form the matrix equation (101). It now must be determined which of the four conditions listed above is appropriate. Table 17 presents the computer solution of the matrix equation (101). As may be seen from the solution, the inequality of equation (98) is not satisfied. Therefore, matrix equation (101) is not appropriate and condition(c) must be used.

TABLE 17

COMPUTER SOLUTION OF MONOSTABLE MULTIVIBRATOR FOR Q_1 OFF

V_{E2}	V_{E3}	V_{E4}	V_{C2}	V_1	V_2	I_{C2}	I_{C3}	I_{C4}
4.67	18.89	9.85	10.45	4.55	1.54	.0055	.0096	.0055

Table 18 presents the computer solution of the multivibrator utilizing condition (c) and the actual measurements made on a breadboard circuit in the laboratory. As may be seen from Table 18, all equalities are satisfied and the close comparison of calculated and measured values validate the accuracy of the transfer function.

TABLE 18

COMPARISON OF COMPUTED AND MEASURED VALUES OF MONOSTABLE MULTIVIBRATOR FOR Q_1 OFF AND CONDITION C

	V_{E2}	V_{E3}	V_{E4}	V_{C2}	V_1	V_2	I_{C2}	I_{C3}	I_{C4}
COMPUTED	3.55	16.91	5.0	5.6	3.04	-2.16	0.00417	0.0087	0.0013
MEASURED	3.9	15.7	4.5	5.2	3.2	-2.37	---	---	---

$$
\begin{bmatrix}
0 & \left(\frac{1}{R_1}+\frac{1}{R_5}+\frac{1}{R_6}\right) & -\frac{1}{R_6} & 0 & 0 & 0 & 0 & \frac{1}{\beta_3} & 0 \\
0 & \left(\frac{1}{R_{L1}}+\frac{1}{R_4}\right) & 0 & 0 & 0 & 0 & 0 & -1-\frac{1}{\beta_3} & 0 \\
0 & -\frac{1}{R_6} & \frac{1}{R_6}+\frac{1}{R_7}+\frac{1}{R_{13}} & 0 & -\frac{1}{R_7} & 0 & 1 & 0 & \frac{1}{\beta_4} \\
\frac{1}{R_{12}+R_{15}}+\frac{1}{R_{16}+R_{12}}+\frac{1}{R_{18}} & 0 & 0 & 0 & -\frac{1}{R_8} & 0 & \frac{1}{\beta_2} & 0 & 0 \\
-\frac{1}{R_8} & 0 & -\frac{1}{R_7} & 0 & \frac{1}{R_8}+\frac{1}{R_7}+\frac{1}{R_9} & 0 & 0 & 0 & 0 \\
\frac{1}{R_2} & 0 & 0 & 0 & 0 & 0 & -1-\frac{1}{\beta_2} & 0 & 0 \\
0 & 0 & \frac{1}{R_{L2}}+\frac{1}{R_{10}} & 0 & 0 & -\frac{1}{R_{10}} & 0 & 0 & -1-\frac{1}{\beta_4} \\
0 & 0 & -\frac{1}{R_{10}} & 0 & 0 & \frac{1}{R_{10}}+\frac{1}{R_{11}} & 0 & 0 & 0 \\
0 & 0 & 1 & -1 & 0 & 0 & 0 & 0 & 0
\end{bmatrix}
\begin{bmatrix} V_{E2} \\ V_{E3} \\ V_{E4} \\ V_{C2} \\ V_1 \\ V_2 \\ I_{C2} \\ I_{C3} \\ I_{C4} \end{bmatrix}
=
\begin{bmatrix}
\frac{24.4}{R_1}+\frac{25}{R_5}+\frac{1.2}{R_6} \\
-\frac{25}{R_4} \\
-\frac{1.2}{R_6}-\frac{1.2}{R_7}+\frac{24.4}{R_{13}} \\
\frac{23.8}{R_{14}+R_{15}}-\frac{1.2}{R_{16}+R_{12}} \\
\frac{1.2}{R_7} \\
0 \\
0 \\
-\frac{25}{R_{11}} \\
-.6
\end{bmatrix}
\qquad (101)
$$

Quiescent Current and Voltage for Q_2 Off

When the monostable multivibrator receives a negative trigger of sufficient amplitude to change its state, the equivalent circuit of Figure 42 with Q_2 off applies at the beginning of this quasi-stable interval. In this state, Q_2, CR_4 and CR_2 are out of the circuit because they are reverse biased. Transistors Q_3 and Q_4 are conducting in the active region. The drop across the base emitter junctions of Q_1, Q_3 and Q_4 and across CR_1, CR_3, CR_5 and CR_7 was assumed to be 0.6V because they are forward biased. The cathode of zener diode CR_6 is at or below 6.2V.

$$\frac{25 - VE_3 - 0.6}{R_1} = I_{C1} + \frac{I_{C3}}{\beta_3} + \frac{V_{E3} + 1.2 - V_1}{R_7} - \frac{V_{E4} - V_{E3} - 1.2}{R_6} \tag{102}$$

$$\frac{V_{E1}}{R_2} = I_{C1} + \frac{I_{C1}}{\beta_1} \tag{103}$$

$$\frac{V_{E3}}{R_{L1}} + \frac{V_{E3} + 25}{R_4} = I_{C3} + \frac{I_{C3}}{\beta_3} \tag{104}$$

$$\frac{V_{E3} + 1.2 - V_1}{R_7} + \frac{V_3 - V_1}{R_8} = \frac{V_1}{R_9} \tag{105}$$

$$\frac{V_{E4}}{R_{L2}} + \frac{V_{E4} - V_2}{R_{10}} = I_{C4} + \frac{I_{C4}}{\beta_4} \tag{106}$$

$$\frac{V_{E4} - V_{E3} - 1.2}{R_6} = \frac{25 - V_{E4}}{R5} + \frac{25 - V_{E4} - 0.6}{R_{13}} - \frac{I_{C4}}{\beta_4} \tag{107}$$

$$\frac{25 - V_3 - 1.2}{R_{14} + R_{15}} = \frac{V_3 + 1.2}{R_{16} + R_{12}} + \frac{V_3 - V_1}{R_8} \tag{108}$$

$$\frac{V_{E4} - V_2}{R_{10}} = \frac{V_2 - V_{E1} - 0.6}{R_3} + \frac{V_2 + 25}{R_{11}} \tag{109}$$

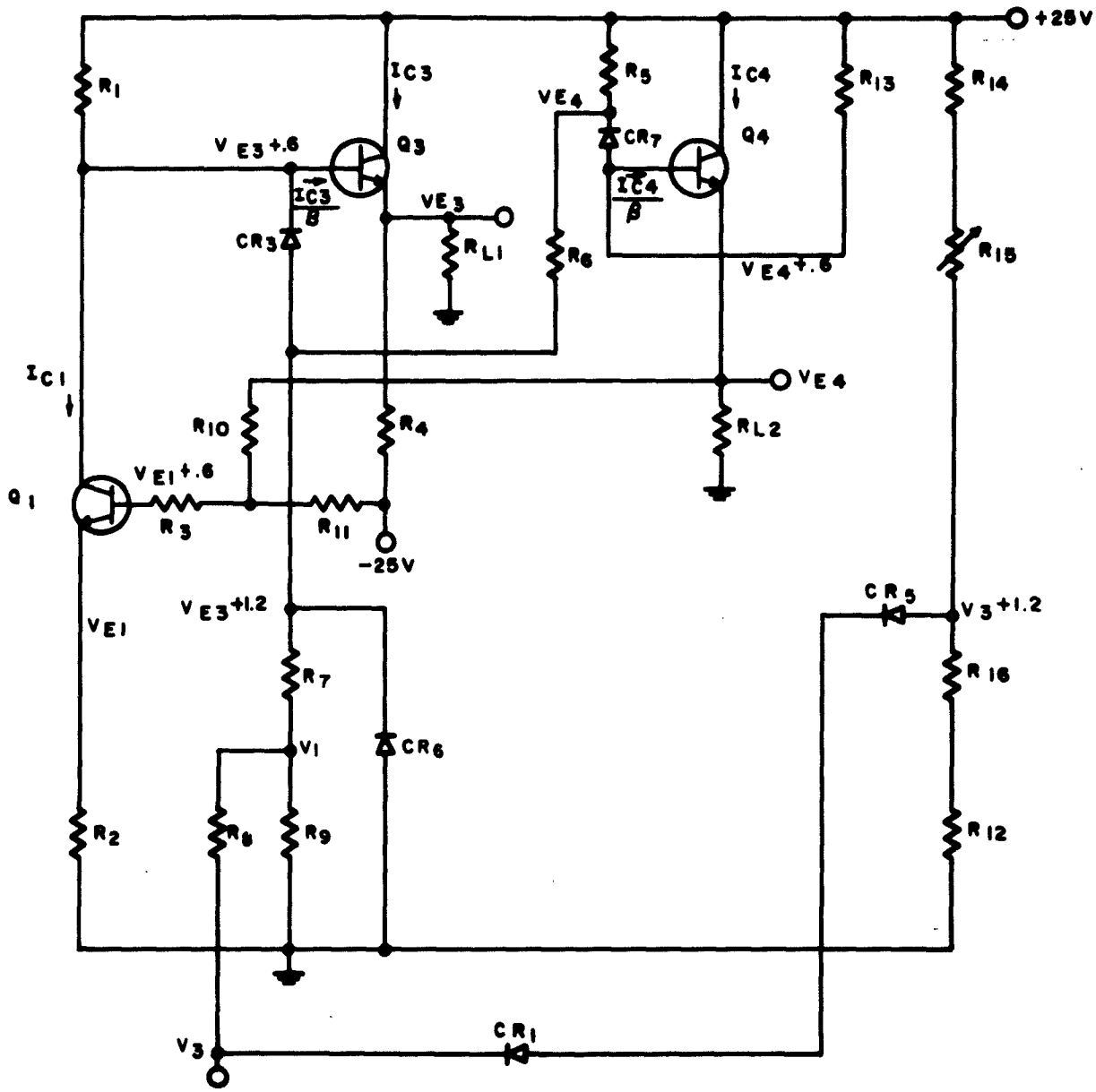

Figure 42. DC Equivalent Circuit of Monostable Multivibrator at the Start of the Quasi-Stable State with Q_2 off and Q_1 Conducting

$$\frac{V_2 - V_{E1} - 0.6}{R_3} = \frac{I_{C1}}{\beta_1} \tag{110}$$

$$V_{E3} + 1.2 \leqq 6.2 \tag{111}$$

$$V_{C1} > V_{E1} + 0.2 \tag{112}$$

Equations (103) through (110) define the bias voltages and currents assuming Q_1 is not saturated at the start of the quasi-stable period. Inequalities (111) and (112) must also be satisfied or a procedure similar to that previously outlined must be followed.

Equations (103) through (110) are used to form matrix equation (113). The matrix is then solved by a computer and Table 19 presents this solution. As may be seen from Table 19 the inequalities of equations (111) and (112) are not satisfied; therefore, the matrix equation (113) is not appropriate and again condition (c) must be used.

TABLE 19

COMPUTER SOLUTION OF MONOSTABLE MULTIVIBRATOR FOR Q_2 OFF

V_{E1}	V_{E3}	V_{E4}	V_1	V_2	V_3	V_{C1}	I_{C3}	I_{C4}
7.099	20.13	23.09	9.40	10.43	10.21	.00833	.01015	.01147

Table 20 presents the computer solution utilizing condition (c) and the laboratory measurements made on a breadboard of the circuit. Thus, the accuracy of the transfer function is determined.

Output Amplitude

The output amplitude is the difference between the outputs (V_{E3} or V_{E4}) computed from Figure 40 and from Figure 42. The measured amplitudes were ΔV_{E3} = 16V and ΔV_{E4} = 16V for C_x = 1000 micro-farad and pulse width = 30 microseconds.

$$
\begin{bmatrix}
0 & \frac{1}{R_1}+\frac{1}{R_7}+\frac{1}{R_6} & -\frac{1}{R_6} & -\frac{1}{R_7} & 0 & 0 & 1 & \frac{1}{\beta_3} & 0 \\
\frac{1}{R_2} & 0 & 0 & 0 & 0 & 0 & 1+\frac{1}{\beta_1} & 0 & 0 \\
0 & -\frac{1}{R_{L1}}-\frac{1}{R_4} & 0 & 0 & 0 & 0 & 0 & 1+\frac{1}{\beta_3} & 0 \\
0 & -\frac{1}{R_7} & 0 & \frac{1}{R_7}+\frac{1}{R_8}+\frac{1}{R_9} & 0 & -\frac{1}{R_8} & 0 & 0 & 0 \\
0 & 0 & -\frac{1}{R_{10}}-\frac{1}{R_{L2}} & 0 & \frac{1}{R_{10}} & 0 & 0 & 0 & 1+\frac{1}{\beta_4} \\
0 & \frac{1}{R_L} & -\frac{1}{R_6}-\frac{1}{R_5}-\frac{1}{R_{13}} & 0 & 0 & 0 & 0 & 0 & -\frac{1}{\beta_4} \\
0 & 0 & 0 & -\frac{1}{R_8} & 0 & \frac{1}{R_{14}+R_{15}}+\frac{1}{R_8}+\frac{1}{R_{16}+R_{12}} & 0 & 0 & 0 \\
\frac{1}{R_3} & 0 & -\frac{1}{R_{10}} & 0 & \frac{1}{R_3}+\frac{1}{R_{11}}+\frac{1}{R_{10}} & 0 & 0 & 0 & 0 \\
-\frac{1}{R_3} & 0 & 0 & 0 & -\frac{1}{R_3} & 0 & \frac{1}{\beta_1} & 0 & 0
\end{bmatrix}
\begin{bmatrix} V_{E1} \\ V_{E3} \\ V_{E4} \\ V_1 \\ V_2 \\ V_3 \\ I_{C1} \\ I_{C3} \\ I_{C4} \end{bmatrix}
=
\begin{bmatrix}
\frac{24.4}{R_1}-\frac{1.2}{R_7}-\frac{1.2}{R_6} \\
0 \\
\frac{25}{R_4} \\
\frac{1.2}{R_7} \\
0 \\
-\frac{1.2}{R_6}-\frac{25}{R_5}-\frac{24.4}{R_{13}} \\
\frac{23.8}{R_{14}+R_{15}}-\frac{1.2}{R_{16}+R_{12}} \\
\frac{0.6}{R_3}-\frac{25}{R_{11}} \\
-\frac{0.6}{R_3}
\end{bmatrix}
\qquad (113)
$$

TABLE 20

COMPARISON OF COMPUTER AND MEASURED VALUES OF MONOSTABLE MULTIVIBRATOR FOR Q_2 OFF AND CONDITION C

	V_{E1}	V_{E3}	V_{E4}	V_1	V_2	V_3	I_{C1}	I_{C3}	I_{C4}
COMPUTED	6.8	5.0	17.0	3.8	7.1	5.2	0.008	0.004	0.008
MEASURED	6.5	4.0	15.0	---	---	---	---	---	---

Monostable Pulse Width

The time that the monostable will remain in its quasi-stable state is a function of the circuit parameters and supply voltages. Figure 43 shows the complete circuit and its similarity to a simple monostable with the addition of emitter followers and clamp diodes. The voltage at the junction of C_4 and R_{16} can be determined by the same techniques used on similar circuits. [21] The collector voltage of Q_1 and the base voltage of Q_3 are constrained to two voltage levels by means of diodes CR_4 and CR_3. These voltages have been computed previously and they appear at V_{E3} shifted by approximately 0.6V at a relatively low impedance. An equivalent circuit is shown in Figure 44 for Q_2 and CR_5 conducting.

The voltage across R_{12} in the steady state is:

$$R_{12} = (V_{E2} + 1.2) \frac{R_{12}}{R_{12} + R_{16}} \tag{114}$$

However, during the quasi-stable state, Q_2 and CR_5 will be cut off and the equivalent circuit will appear as shown in Figure 45. Applying Thévenin's Theorem, the circuit in Figure 45a can be transformed to that shown in Figure 45b, where:

$$R = \frac{(R'_{14} + R_{16})\, R_{12}}{R_{12} + R'_{14} + R_{16}} \tag{115}$$

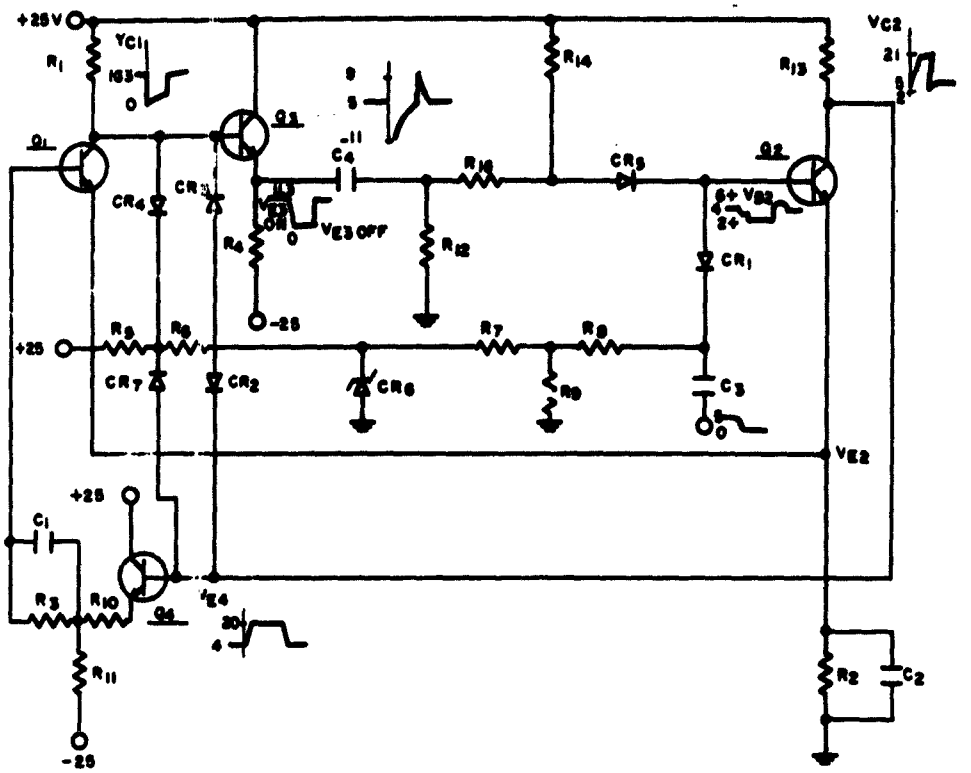

Figure 43. Monostable Circuit Used to Solve for Pulse Width

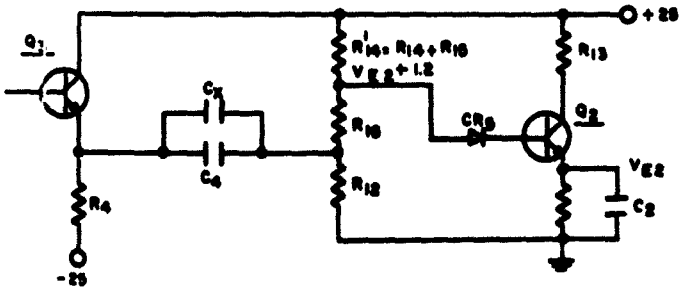

Figure 44. Equivalent Circuit for Monostable Pulse Width for Q_2 Conducting

$$C = C_4 + C_x \tag{116}$$

$$V = \left(\frac{R_{12}}{R_{12} + R'_{14} + R_{16}}\right) 25 \tag{117}$$

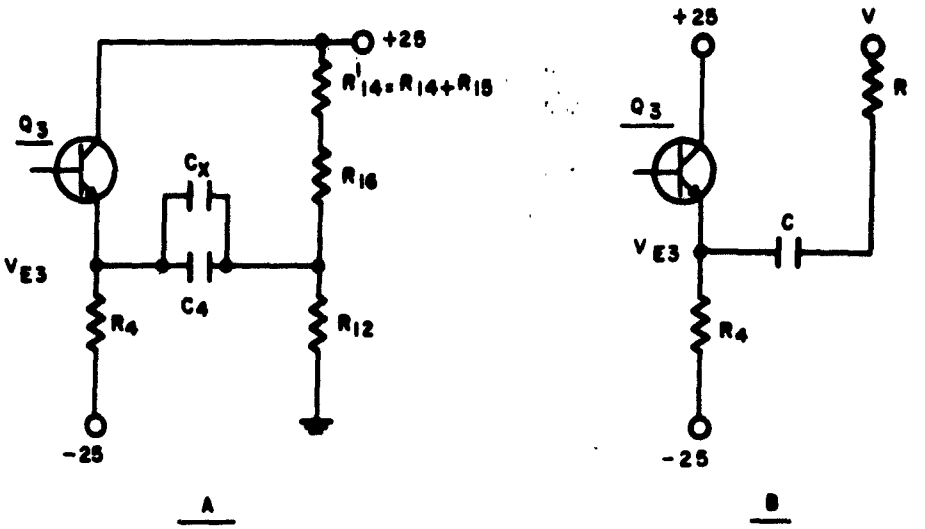

Figure 45. Thevenin Equivalent Circuit for Monostable Pulse Width

The voltage at the junction of C and R will appear as shown in Figure 46.

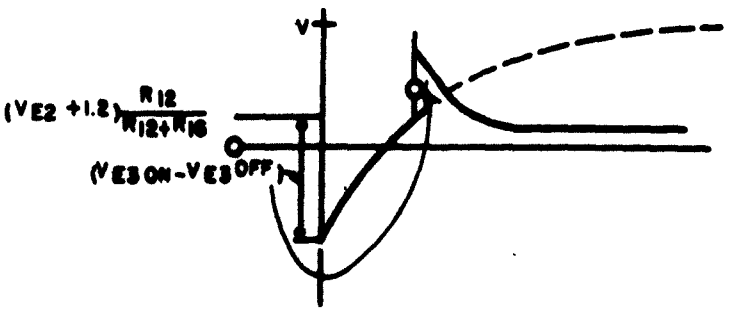

Figure 46. Output Voltage Waveform

where:

$$E = V - \left[(V_{E2} + 1.2) \frac{R_{12}}{R_{12} + R_{16}} - (V_{E3}\ \text{On} - V_{E3}\ \text{Off}) \right] \qquad (118)$$

and the capacitor C discharges toward V so that the voltage at the junction of R and C during the quasi-stable state is:

$$V - E \quad \exp\left(\frac{-t}{RC}\right) \qquad (119)$$

The quasi-stable state will terminate when $e = (V_{E2} + 1.2) \frac{R_{12}}{R_{12} + R_{16}}$. Therefore, the width of the pulse t_{1p} can be obtained by solving the following equation for t_p.

$$(V_{E2} + 1.2) \frac{R_{12}}{R_{12} + R_{16}} = V - E \quad \exp\left(\frac{-t_p}{RC}\right)$$

$$E \quad \exp\left(\frac{-t_p}{RC}\right) = V - (V_{E2} + 1.2) \frac{R_{12}}{R_{12} + R_{16}}$$

$$\exp\left(\frac{-t_p}{RC}\right) = \frac{V - (V_{E2} + 1.2) \frac{R_{12}}{R_{12} + R_{16}}}{E} \qquad (120)$$

Solving for t_p

$$\exp \frac{t_p}{RC} = \frac{E}{V - (V_{E2} + 1.2)\left(\frac{R_{12}}{R_{12} + R_{16}}\right)}$$

therefore,

$$t_p = RC \ln \frac{E}{V - (V_{E2} + 1.2)\left(\frac{R_{12}}{R_{12} + R_{16}}\right)} \qquad (121)$$

where:

$$E = V - [(V_{E2} + 1.2) - (V_{E3} \text{ On} - V_{E3} \text{ Off})] \quad (122)$$

and

$$V = \frac{R_{12}}{R_{12} + R'_{14} + R_{16}} \quad (25) \quad (123)$$

For nominal values of circuit parameters:

$$V = 19.5V$$

$$E = 19.5 - [(3.56 + 1.2) - (16.91 - 5.0)] = 25.65V$$

$$t_p = RC \ln \frac{25.65}{19.5 - 4.76 \frac{270K}{272.2K}} = (55.7K)\, C \ln 1.74$$

$$t_p = (31.0 \times 10^3)\, C \quad (124)$$

Therefore, it may be seen from equation (124) that the pulse width is directly proportional to the value of the external capacitor C_x and C_4. Table 21 presents a comparison of the computed and measured values of the pulse width. It may be seen by referring to the table that the values check closely, thus indicating the accuracy of the transfer function.

TABLE 21

COMPARISON OF COMPUTED AND MEASURED VALUES OF PULSE WIDTH

C_x	$C_x+C_4+C_{stray}$	Computed t_p	Measured t_p	PRF
0	50 pf	1.56 microsec.	2 microsec.	50 KC
160 pf	210 pf	6.5 microsec.	7 microsec.	50 KC
100 pf	1050 pf	32.5 microsec.	30 microsec.	5 KC
.1 μf	.1 μf	3.1 millisec.	2.6 millisec.	50 cps
.5 μf	.5 μf	15.5 millisec.	12.5 millisec.	20 cps

3.2.6 Transfer Functions of the Bistable Multivibrator

The bistable multivibrator circuit shown in Figure 47 has been studied and the following transfer functions have been developed:

a. Quiescent current and voltage as a function of individual circuit parameters as well as the DC supply voltage.

b. Output amplitude as a function of individual circuit parameters as well as the DC supply voltage.

c. Minimum trigger amplitude as a function of individual circuit parameter.

Table 22 lists the performance criteria for this circuit.

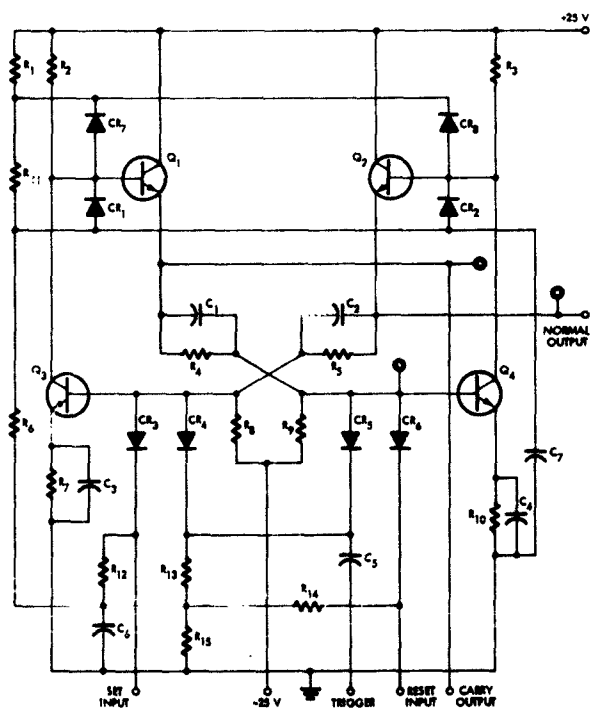

Note: This circuit is contained in RADC TR 59-243, dated December 15, 1959, Titled Reliable Preferred Solid State Functional Divisions. Contract AF 30(602)-1906.

Figure 47. Bistable Multivibrator Schematic

TABLE 22

PERFORMANCE CRITERIA OF THE BISTABLE MULTIVIBRATOR

Requirements	Maximum	Design Center	Minimum
Trigger (Flip-Flop) Input	-	-	-
AC Coupled	-	-	-
Trigger Amplitude	-8 v	-5 v	-4 v
Trigger Risetime	1 μsec	-	0.1 μsec
Trigger Frequency	250 kc	-	-
Input Impedance	-	-	9,000Ω
Set-Reset (Bistable) Input	-	-	-
DC Coupled	-	-	-
Voltage Level	+6 v	+2 v	0 v
Risetime	-	-	0.1 μsec
Pulse Frequency	250 kc	-	-
Input Impedance	-	-	9,000Ω
Output Amplitude, Peak-to-Peak	18 v	15 v	10 v
Output Polarity, Both DC Coupled	-	-	-
Output Risetime	1 μsec	-	0.1 μsec
Output Decay Time	1 μsec	-	0.1 μsec
Output Loading	-	-	2,500Ω
DC Supply Voltages	-	+25 v	-
	-	-25 v	-
Operating Temperature	85°C	-	-55°C

NOTE:

This is contained in RADC TR 59-243, dated December 15, 1959, Titled, Reliable Preferred Solid State Functional Divisions, Contract AF 30 (602-1906)

Quiescent Currents and Voltages

Since this circuit is symmetrical, the DC bias conditions will be computed for the bistable multivibrator circuit in one state (Q_4 non-conducting, Q_3 conducting). Thus, the bias will be known for the opposite stable state.

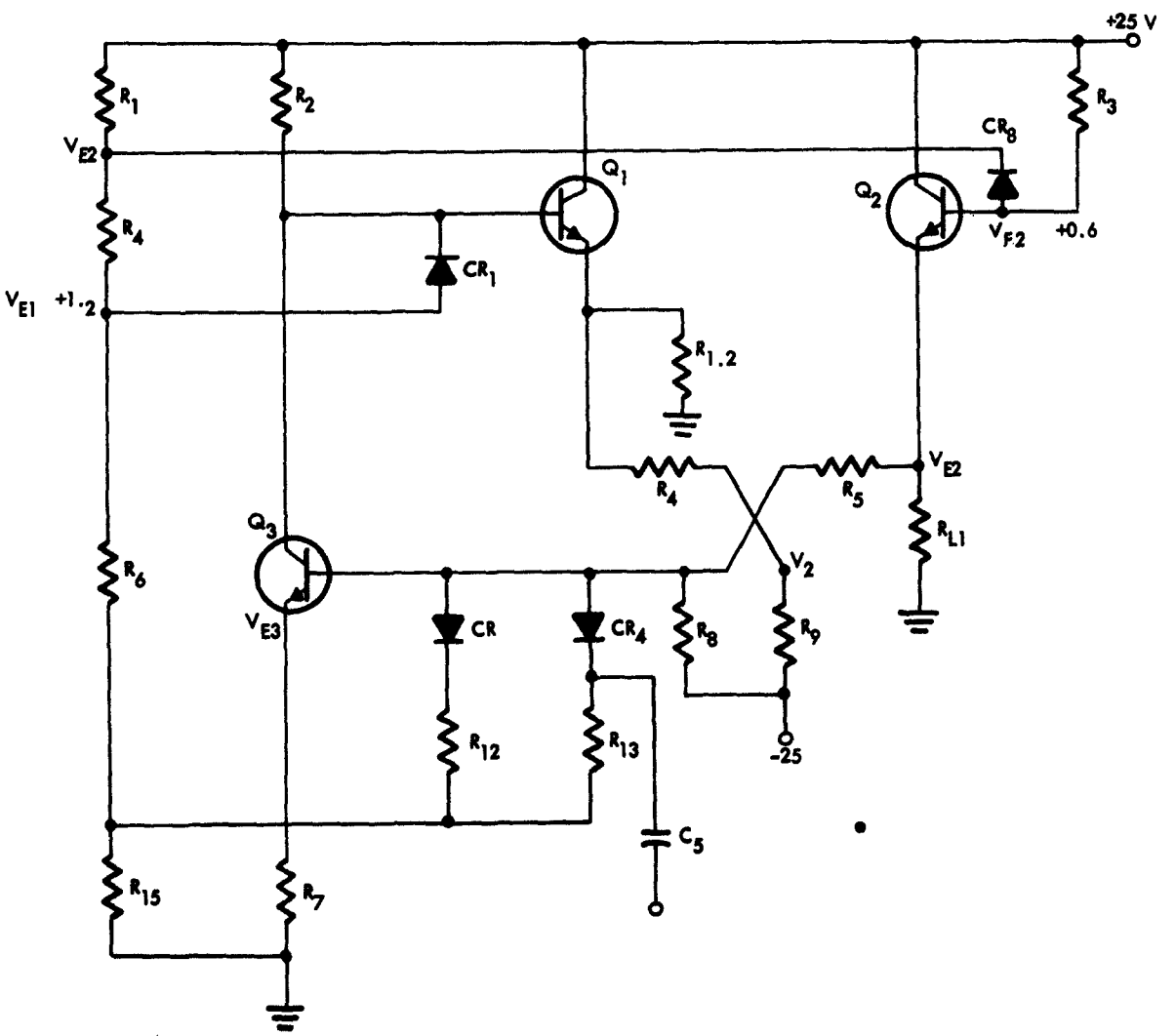

Figure 48. DC Equivalent Circuit of Bistable with Q_4 off

Figure 48 is the DC equivalent circuit for the state in which Q_4 is non-conducting and Q_3 is conducting. Q_4, CR_7, CR_2, CR_5, and CR_6 are removed from the circuit because they are reverse biased. Figure 9 is the DC equivalent circuit for a conducting, non-saturated transistor. Diodes CR_1, CR_3, CR_4 and CR_8 were assumed to have a 0.6 volt drop between anode to cathode because they are forward biased. Figure 10 represents the DC equivalent circuit of a transistor in saturation. The equivalent circuits presented in Figures 9 and 10 were utilized in solving the transfer functions for the condition of Q_3 non-saturated and saturated respectively.

An analysis of the circuit yields equations (124) through (132). These equations are then simplified:

$$\frac{V_{E3}+0.6-V_{E2}}{R_5}+\frac{V_{E3}+0.6+25}{R_8}+I_{B3}+\frac{V_{E3}-V_1}{R_{12}}+\frac{V_{E3}-V_1}{R_{13}}=0 \tag{124}$$

$$\frac{25-V_{E2}}{R_1}+\frac{25-V_{E2}-0.6}{R_3}-\frac{I_{C2}}{\beta}=\frac{V_{E2}-V_{E1}-1.2}{R_{11}} \tag{125}$$

$$\frac{V_{E2}-V_{E1}-1.2}{R_{11}}=\frac{V_{E1}+1.2-V_1}{R_6}+\frac{I_{C1}}{\beta}+\frac{V_{E1}+0.6-25}{R_2}+I_{C3} \tag{126}$$

$$\frac{V_{E1}+1.2-V_1}{R_6}+\frac{V_{E3}-V_1}{R_{12}}+\frac{V_{E3}-V_1}{R_{13}}=\frac{V_1}{R_{15}} \tag{127}$$

$$I_{C1}+\frac{I_{C1}}{\beta}=\frac{V_{E1}}{R_{L2}}+\frac{V_{E1}-V_2}{R_4} \tag{128}$$

$$\frac{V_{E1}-V_2}{R_4}=\frac{V_2+B5}{R_9} \tag{129}$$

$$I_{C2}+\frac{I_{C2}}{\beta}=\frac{V_{E2}}{R_{L1}}+\frac{V_{E2}-V_{E3}-0.6}{R_5} \tag{130}$$

$$V_{E1} + 0.6 = V_{E3} + 0.2 \tag{131}$$

$$I_{B3} + I_{C3} = \frac{V_{E3}}{R_7} \tag{132}$$

The matrix equation (133) is then solved using a computer and the results are presented in Table 23.

TABLE 23

COMPUTER SOLUTION FOR BISTABLE MULTIVIBRATOR WITH Q_4 OFF, Q_3 SATURATED, $R_{L1} = R_{L2} = 2500, \beta = 25$

V_1	0.9039
V_2	- 2.624
V_{E1}	4.3868
V_{E2}	16.68
V_{E3}	4.7868
I_{C1}	0.00312
I_{C2}	0.008727
I_{C3}	0.0051859
I_{B3}	- 0.000399

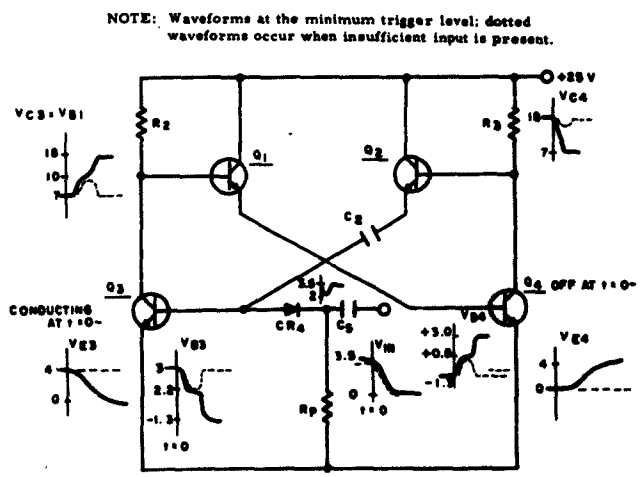

Figure 49. Bistable Equivalent Circuit at the Leading Edge of the Trigger Pulse

The solution for Q_3 in saturation appears satisfactory. However, a negative answer for base current I_{B3} is not physically possible. The negative answer indicates that the circuit does not allow sufficient base current to saturate Q_3 as it would if the solution for base current were positive. This means that the assumed condition (Q_3 saturated) cannot be physically realized.

Therefore, the analysis must be repeated using Figure 9 to represent Q_3 which is apparently conducting but is not saturated. This change results in the following changes in the equations (124) to (132).

(This page intentionally left blank)

I_{C3}/β is substituted for I_{B3} in equations (124) and (132); and equation (131) is eliminated.

The revised matrix equation (134) is then solved and the results together with the measured results are presented in Table 24.

TABLE 24

BISTABLE MULTIVIBRATOR Q_4 OFF Q_3 NONSATURATED

$\beta = 25$, $R_{L1} = R_{L2} = 2500$

	V_1	V_2	V_{E1}	V_{E2}	V_{E3}	I_{C1}	I_{C2}	I_{C3}
Computed:	1.058 V	-1.244 V	6.199 V	17.40 V	4.016 V	3.907 MA	9.31 MA	3.86 MA
Measured: with $R_{L1} = R_{L2} =$	1.07 V	-1.33 V	6.1 V	17.0 V	4.2 V	---	---	---

Computed: $V_{c3} = V_{E1} + 0.6 = 6.80$ V

Measured: $V_{c3} = 6.8$ V

Table 25 shows the solutions for the 8 variables for transistor β's of 10, 20, . . . 60. This data shows the changes in bias due to changes in transistor current gain and indicates that the output amplitude ($V_{E2} - V_{E1}$) increased by 11.4 percent for a change in β from 10 to 60.

TABLE 25

BISTABLE MULTIVIBRATOR Q_4 OFF Q_3 NONSATURATED

$R_{L1} = R_{L2} = 2500$, $= 10, 20, \ldots, 60$

V_1	V_2	V_{E1}	V_{E2}	V_{E3}	I_{C1}	I_{C2}	I_{C3}	
1.063	-1.010	6.506	17.07	3.528	0.003819	0.008715	0.003207	= 10
1.060	-1.193	6.265	17.35	3.926	0.003890	0.009208	0.003675	= 20
1.056	-1.280	6.151	17.45	4.079	0.003916	0.009377	0.003847	= 30
1.054	-1.329	6.087	17.47	4.159	0.003929	0.009466	0.003933	= 40
1.052	-1.361	6.045	17.50	4.209	0.003915	0.009512	0.003986	= 50
1.051	-1.383	6.016	17.52	4.243	0.003915	0.009546	0.004018	= 60

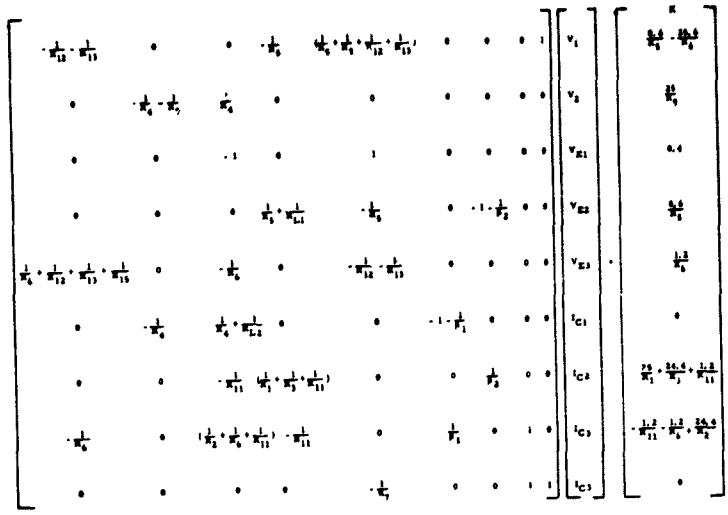

(133)

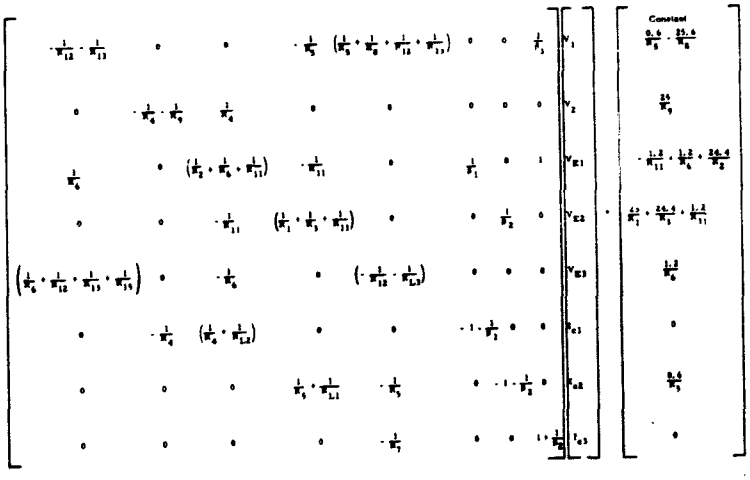

(134)

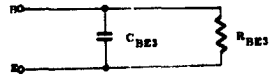

$R_{BE3} = (\beta + 1)r_e = (\beta + 1)\frac{0.026}{I_E} = (20)\frac{0.026}{0.002} = 169\Omega$

Since:

$f_\alpha = \frac{1}{2\pi R_{BE} C_{BE}} = 5\ MC$, from transistor data sheet

$C_{BE3} = \frac{1}{2\pi R_{BE} f_\alpha} = \frac{1}{2\pi(169)5 \times 10^6} \simeq 200\ pf$

In terms of transistor data sheet parameters and DC emitter current:

$C_{BE3} = \frac{1}{2\pi(\beta + 1)\frac{0.026}{I_E} f_\alpha}$

Figure 50. Equivalent Circuit for the Input of Q_3 Prior to Turn Off

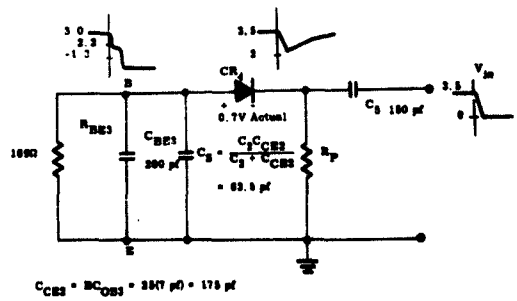

$C_{CB2} = BC_{OB3} = 2047\ pf) = 175\ pf$

$C_2 = 100\ pf$

Figure 51. Equivalent Circuit for Q_3 and the Input Circuit Prior to Turn Off with Observed Waveforms

Table 26 is the computed solution of the bias equations assuming no output loading, i.e., $R_{L1} = R_{L2} = \infty$. The major difference between this case and that of Table 24 is that the collector currents of Q_1 and Q_2 are reduced by 300 percent. The other bias conditions changed less than 10 percent.

TABLE 26

COMPUTER SOLUTION FOR BISTABLE MULTIVIBRATOR WITH Q_4 OFF Q_3 NONSATURATED

$R_{L1} = R_{L2} = \infty$

	V_1	V_2	V_{E1}	V_{E2}	V_{E3}	I_{C1}	I_{C2}	I_{C3}
Computed:	1.08 V	-1.15	6.32	17.7	4.14	0.00152	0.00264	0.00398
Measured:	1.07 V	-1.33	6.1	17.0	4.2	---	---	---

Solution for Output Amplitude

The output amplitude of the bistable multivibrator providing sufficient trigger voltage is present to change its state, equals the difference in quiescent values of the emitter voltages Q_1 and Q_2, i.e., the output amplitude = $(V_{E2} - V_{E1})$. The value computed from Figure 12 using nominal values for all components is 17.7 - 6.3 = 11.4V. The measured value obtained from the breadboard circuit was 11V. The measured and calculated values compare favorably, therefore, confirming the accuracy of the solution.

Minimum Trigger Amplitude

To find the minimum required trigger amplitude, the equivalent circuits of Figures 49, 50, and 51 must be used. From Figure 49, it can be seen that V_B must be changed negatively by at least 0.6V to nullify its 0.6V "on" bias. Then V_{C3} will rise enough to propagate through Q_1 and turn Q_4 on. Figure 50 shows the calculations for obtaining the input capacitance C_{BE3} and resistance R_{BE3} of Q_3. Figure 51 is used to compute the V_{in} required to turn Q_3 off. At the leading edge of the V_{in} pulse, from the circuit of Figure 51:

$$V_{BE3} = V_{in} \frac{\frac{1}{s(C_{BE3}+C_s)}}{\frac{1}{sC_5} + \frac{1}{s(C_{BE3}+C_s)}} - V_{CR4} = V_{in}\left(\frac{C_5}{C_5 + C_{BE3}+C_s}\right) - V_{CR4} \tag{135}$$

The required $V_{in} = (V_{BE3} + V_{CR4})\left(\frac{C_5 + C_{BE3} + C_s}{C_5}\right)$ or in terms of the circuit parameters and specified transistor parameters,

$$V_{in} = \frac{(V_{BE3}+V_{CR4})}{C_5}\left[C_5 + \frac{1}{2\pi(\beta+1)(0.26/I_E)f\alpha} + \frac{C_2\beta C_{oB2}}{C_2+\beta C_{oB2}}\right] \tag{136}$$

Substituting nominal values into the above equation yields

$$V_{in} = \frac{(0.6+0.6)}{150}\ [150 + 200 + 63.5] = 3.3V \tag{137}$$

The measured minimum required trigger amplitude was 3.5V peak to peak at the "trigger" input. This input becomes differentiated by C_5 and R_{13} so that a negative spike of 1.5V amplitude occurs at the junction of C_5 and R_{13} when the input is going negative. This appears as a negative step of 0.8V amplitude at V_{B3}. This step instantaneously raises the collector of Q_3 by 3V and is propagated through the emitter follower Q_1 to the base of Q_4. It appears as a positive step of 2.1V at V_{B4} thus raising the base of Q_4 to +0.8V thereby, causing Q_4 to conduct. The negative voltage V_{C4} is fed back through Q_2 to the base of Q_3, turning Q_3 off.

Thus, the procedure described above details the steps used in the development of three transfer functions for the bistable multivibrator circuit.

3.2.7 Transfer Functions of the Pulse Adder

The pulse adder analyzed is basically a form of a wide band video amplifier. The basic amplifier schematic is shown in Figure 52. This amplifier can be used to perform the function on an OR circuit, which is basically a mixer or buffer that permits a number of pulses to be connected to a common load. It also minimizes the interaction of the pulse sources on each other. If a positive pulse with a maximum amplitude of 5 volts is applied to either of the input terminals, a pulse

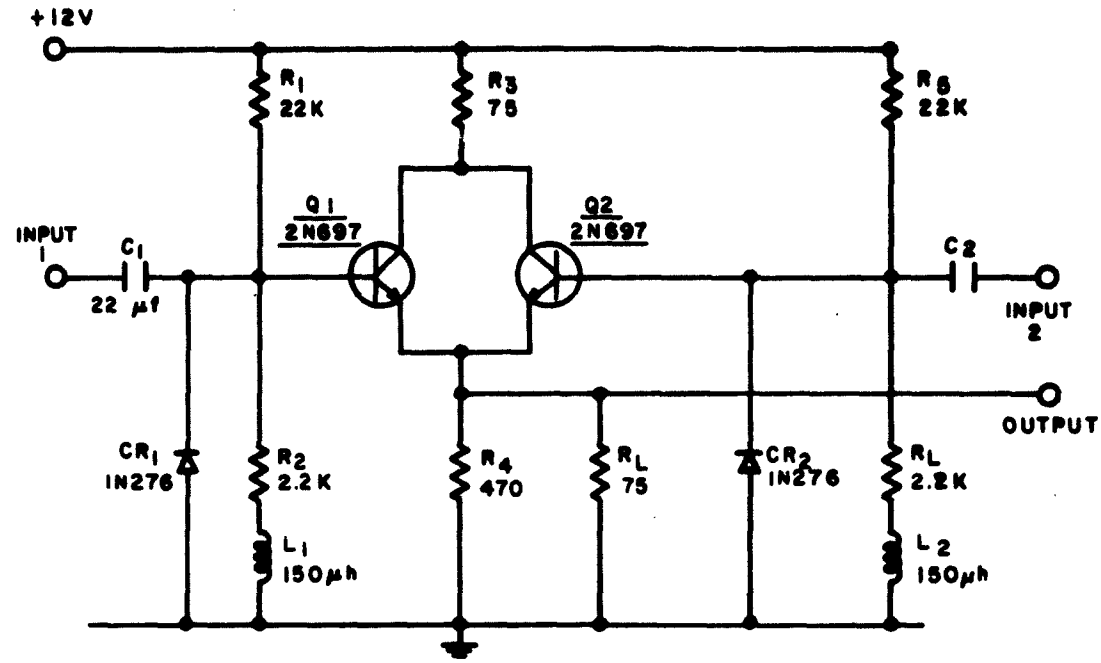

Figure 52. Pulse Adder Schematic

of similar amplitude and form will be available at the output. However, if a pulse is applied at both terminals simultaneously, the output consists of the sum of the two. If the pulses are of sufficient amplitude to saturate the stage, then only the wider of the two is transmitted, i. e., a pulse of sufficient width and amplitude inhibits and prevents the transmission of a smaller or narrower pulse through the circuit. The performance criteria of this circuit is presented in Table 27.

Quiescent Currents and Voltages

The DC equivalent circuit presented in Figure 53 was used to perform the analysis of the pulse adder. From this circuit, equations (138) through (144) relating the individual circuit components and their corresponding parameters were derived.

$$\frac{12 - V_{B2}}{R_5} - \frac{V_{B2}}{R_6} = \frac{I_{C2}}{\beta_2} \tag{138}$$

$$V_{B1} = V_E + 0.6 \tag{139}$$

$$V_{B2} = V_E + 0.6 \tag{140}$$

TABLE 27

PERFORMANCE CRITERIA OF PULSE ADDER

Requirements	Maximum	Design Center	Minimum
Inputs (Two Unbalanced to Ground)			
Input Impedance	--	--	800 Ω
Input, Positive Peak	5 v	3.5 v	--
Source Impedance	--	75 Ω	--
Voltage Gain, Either Input	1	0.75	0.6
Output Impedance	--	75 Ω	--
Bandwidth	4 mc	--	10 cps
Rise Time	0.15 μsec	0.1 μsec	--
Output (One Unbalanced)	--	--	--
Output Level	5 v	3.5 v	--
Output Polarity Positive			
Repetition Rate	5000 pps	--	20 pps
Pulse Duty Cycle	0.20	--	--
Additive-Factor	0.25	--	--
Load Impedance	--	75 Ω	--
DC Supply Voltage	--	+12 v	--
Operating Temperature	85°C	--	-55°C

$$I_{C1} + I_{C2} + \frac{12 - V_{B1}}{R_1} + \frac{12 - V_{B2}}{R_5} - \frac{V_{B1}}{R_2} - \frac{V_{B2}}{R_6} = \frac{V_E}{R_4 \parallel R_L} \tag{141}$$

$$\frac{12 - V_C}{R_3} = I_{C1} + I_{C2} \tag{142}$$

$$\frac{12 - V_{B1}}{R_1} - \frac{V_{B1}}{R_2} = \frac{I_{C1}}{\beta_1} \tag{143}$$

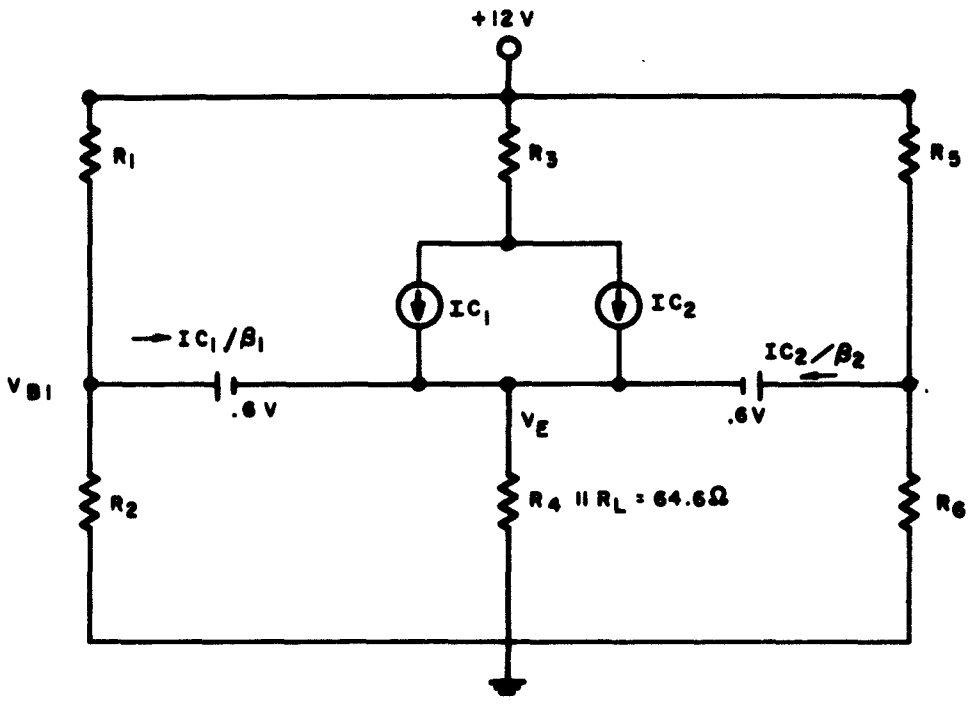

Figure 53. DC Equivalent Circuit of Pulse Adder

The equations are then simplified and are used to form matrix equation (144). Then, assuming all components to be at their nominal value, $\beta_1 = \beta_2 = 50$ and $R_L = 75$ ohms, the matrix equation is then solved using a computer. Also, a breadboard circuit of this pulse adder was constructed and tested in the laboratory. Table 28 presents a comparison of the measured and calculated values of the circuit parameters. As may be seen from Table 28, the calculated and measured values compare quite favorably, thus validating the accuracy of the transfer function.

$$\begin{bmatrix} \frac{1}{\beta_1} & 0 & \frac{1}{R_1}+\frac{1}{R_2} & 0 & 0 & 0 \\ 0 & \frac{1}{\beta_2} & 0 & \frac{1}{R_5}+\frac{1}{R_6} & 0 & 0 \\ 0 & 0 & 1 & 0 & -1 & 0 \\ 0 & 0 & 0 & 1 & -1 & 0 \\ 1 & 1 & -\frac{1}{R_1}-\frac{1}{R_2} & -\frac{1}{R_5}-\frac{1}{R_6} & -\frac{1}{R_4 \| R_L} & 0 \\ 1 & 1 & 0 & 0 & 0 & \frac{1}{R_3} \end{bmatrix} \begin{bmatrix} I_{C1} \\ I_{C2} \\ V_{B1} \\ V_{B2} \\ V_E \\ V_C \end{bmatrix} = \begin{bmatrix} \frac{12}{R_1} \\ \frac{12}{R_5} \\ .6 \\ .6 \\ -\frac{12}{R_1}-\frac{12}{R_5} \\ \frac{12}{R_3} \end{bmatrix} \quad (144)$$

TABLE 28

COMPARISON OF CALCULATED AND MEASURED VALUES OF THE PULSE ADDER

	V_{B1}	V_{B2}	V_{E2}	V_C	I_{C1}	I_{C2}
Calculated	0.98	0.98	0.38	11.57	0.003	0.003
Measured	0.93	0.94	0.30	11.20	-----	-----

Maximum Output Amplitude

The maximum peak to peak output amplitude is the difference between the output (V_{E1}) with Q_1 and/or Q_2 saturated, and the output (V_{E2}) under quiescent conditions. The voltage V_{E2} has been previously calculated and found to be 0.38 volts. In order to find the voltage V_{E1} with Q_1 and/or Q_2 saturated, the equivalent circuit of Figure 54 must be used. The analysis of this circuit yields equations (145) through (147). These equations, when rearranged, form the matrix equation (148).

$$\frac{12 - V_E - 0.6}{R_1} + \frac{-V_E - 0.6}{R_2} + I_C = \frac{V_E}{R_4 \,||\, R_L} \qquad (145)$$

$$V_C = V_E + 0.2 \qquad (146)$$

$$\frac{12 - V_C}{R_3} = I_C \qquad (147)$$

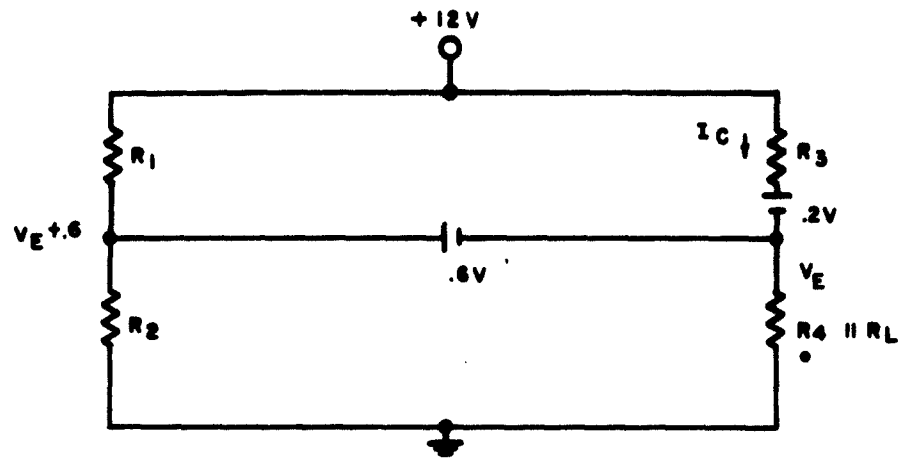

Figure 54. Equivalent Circuit of Pulse Adder with Q_1 and/or Q_2 Saturated

$$\begin{bmatrix} \frac{1}{R_1} + \frac{1}{R_2} + \frac{1}{R_4} & 0 & -1 \\ -1 & 1 & 0 \\ 0 & \frac{1}{R_3} & 1 \end{bmatrix} \begin{bmatrix} V_E \\ V_C \\ I_C \end{bmatrix} = \begin{bmatrix} \frac{11.4}{R_1} - \frac{0.6}{R_2} \\ 0.2 \\ \frac{12}{R_3} \end{bmatrix} \quad (148)$$

This matrix is solved using a computer, and the results, along with those made on a breadboard circuit are presented in Table 29.

TABLE 29

COMPARISON OF CALCULATED AND MEASURED VALUES OF THE PULSE ADDER WITH Q_1 and/or Q_2 SATURATED

	V_{E1}	V_C	I_C
Calculated:	5.38	5.57	0.086
Measured:	4.8	5.0	———

Since the maximum output amplitude is defined as $V_{E1} - V_{E2}$, it is possible to determine the desired results:

$$\text{Maximum Amplitude} = V_{E1} - V_{E2} = 5.38 - 0.38 = 5 \text{ volts}$$

The above analysis allows the transfer function relating input and output voltages to be graphed as shown in Figure 55.

3.2.7.1 Determining Incremental AC Gain Utilizing the Signal Flow Graph Technique

In order to determine the incremental AC gain, the AC equivalent circuit of the pulse adder (Figure 56) must be constructed. An analysis of this circuit yields equations (149) through (151). The signal flow graph is then constructed from the equivalent circuit and the equations and is presented in Figure 57.

$$e_o = R_4^1 \left(I_{e2} + \frac{I_{e2}}{\beta_2} + I_{e1} + \frac{I_{e1}}{\beta_1}\right) \tag{149}$$

$$\frac{I_{c1}}{\beta_1} = \frac{E_{i1}}{r_{b1}} - \frac{e_o}{r_{b1}} - \frac{0.6}{r_{b1}} = \frac{e_{i1} - 0.6}{r_{b1}} - \frac{e_o}{r_{b1}} \tag{150}$$

$$\frac{I_{c2}}{\beta_2} = \frac{e_{i2}}{r_{b2}} - \frac{e_o}{r_{b2}} - \frac{0.6}{r_{b2}} = \frac{e_{i2} - 0.6}{r_{b2}} - \frac{e_o}{r_{b2}} \tag{151}$$

It is now possible to determine the incremental voltage gain $\frac{e_o}{e_{in}}$ from the flow graph and in equation (152).

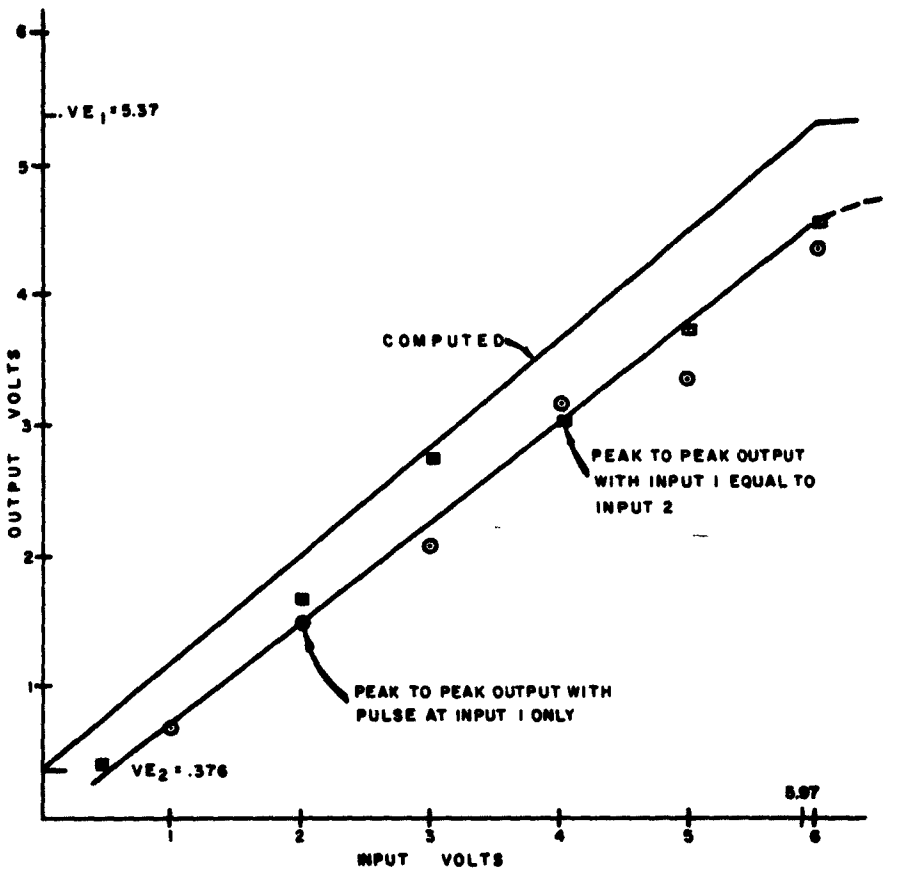

Figure 55. Graph of Computed and Measured Input Versus Output Voltage for Pulse Adder

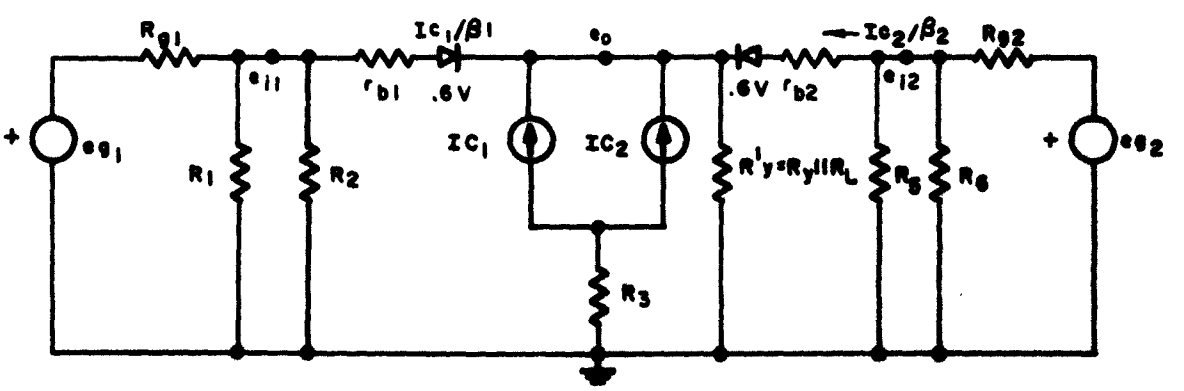

Figure 56. AC Equivalent Circuit of Pulse Adder

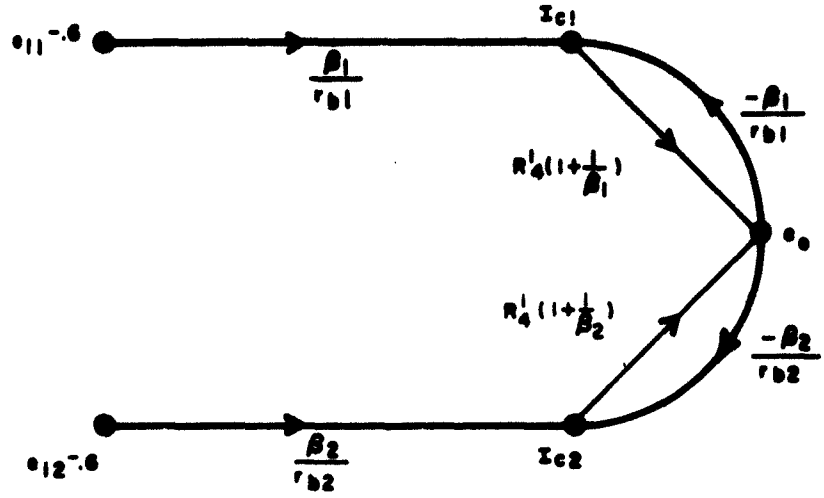

Figure 57. Flow Graph for Pulse Adder Voltage Gain

$$\frac{e_o}{e_{i1} - 0.6} = \frac{\frac{\beta_1}{r_{b1}}\left(1+\frac{1}{\beta_1}\right) R_4^{\,1}}{1+\frac{B_1}{r_{b1}}\left(1+\frac{1}{\beta_1}\right)R_4^{\,1}} = \frac{(\beta_1+1)R_4^{\,1}}{r_{b1}+(\beta_1+1)R_4^{\,1}} \qquad (152)$$

For $\beta_1 = 50$, $R_4^{\,1} = 64.6\Omega$ and $r_{b1} = 50\Omega$:

$$\frac{e_o}{e_{i1} - 0.6} \doteq \frac{(51)64.6}{50+(51)64.6} = \frac{3300}{3350} = 0.985$$

3.2.8 Transfer Functions of the Distribution Amplifier

The distribution amplifier (emitter follower) functions as a general purpose amplifier in a similar manner to a chathode follower. It is designed to accept short duty cycle pulses and to provide power gain with a voltage gain of unity. The input impedance of this amplifier is normally higher than the load resistance of the source. Thus, the parallel connection of several amplifiers to a common source can be effected without loading the input. Isolation is provided between input and output signals.

The schematic of the amplifier is shown in Figure 58 and its performance criteria is shown in Table 30. The input impedance of this transistor amplifier is frequency sensitive and appears reactive above the β cutoff. frequency. Compensating for this is the network $L_1 R_1 R_2$ shown in Figure 58. R_1 and R_2 provide circuit stability by determining the quiescent operating points of the transistor. Diode CR_1 acts as a direct current restorer permitting operation with duty cycles up to 50 percent. Optimum performance is achieved by restricting duty cycles to 20 percent.

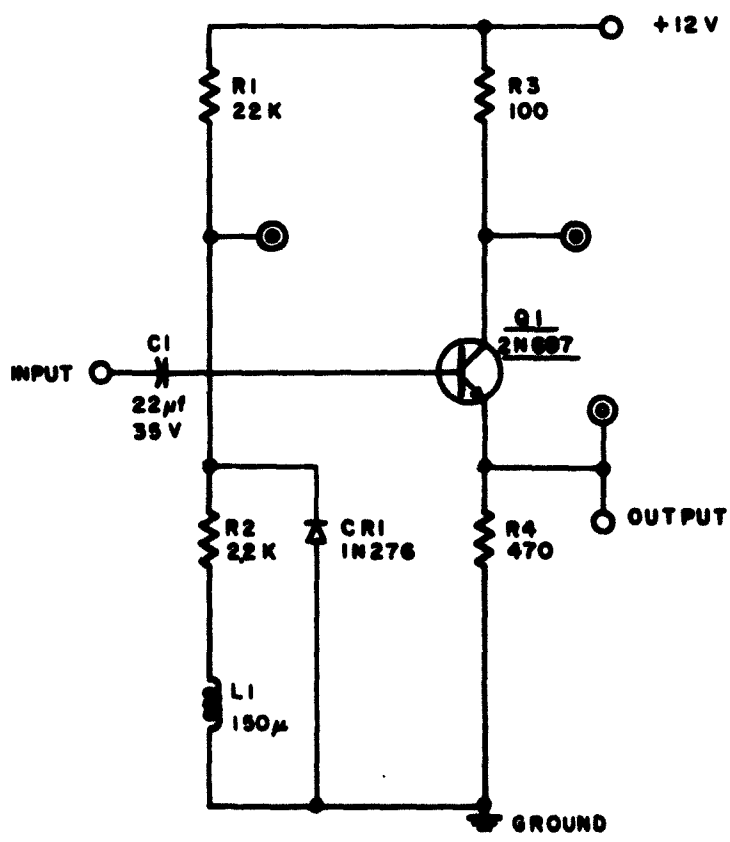

Figure 58. Schematic of the Distribution Amplifier

TABLE 30

PERFORMANCE CRITERIA OF DISTRIBUTION AMPLIFIER

Requirements	Maximum	Design Center	Minimum
Input (One, Unbalanced to Ground)	---	---	---
Input Impedance	---	---	800 Ω
Input Level, Positive Peak	5	3.5 v	---
Source Impedance	---	75Ω	---
Voltage Gain	1	0.75	0.6
Bandwidth (3db Down Frequencies)	4 mc	---	10 cps
Rise Time	0.15 μsec	0.1 μsec	---
Output (One, Unbalanced)	---	---	---
Output Polarity Positive			
Load Impedance	---	75Ω	50Ω
DC Supply Voltage	---	+12 v	---
Operating Temperature	85°C	---	-55°C

The direct current, quiescent current and voltages were determined by utilizing the equivalent circuit shown in Figure 59.

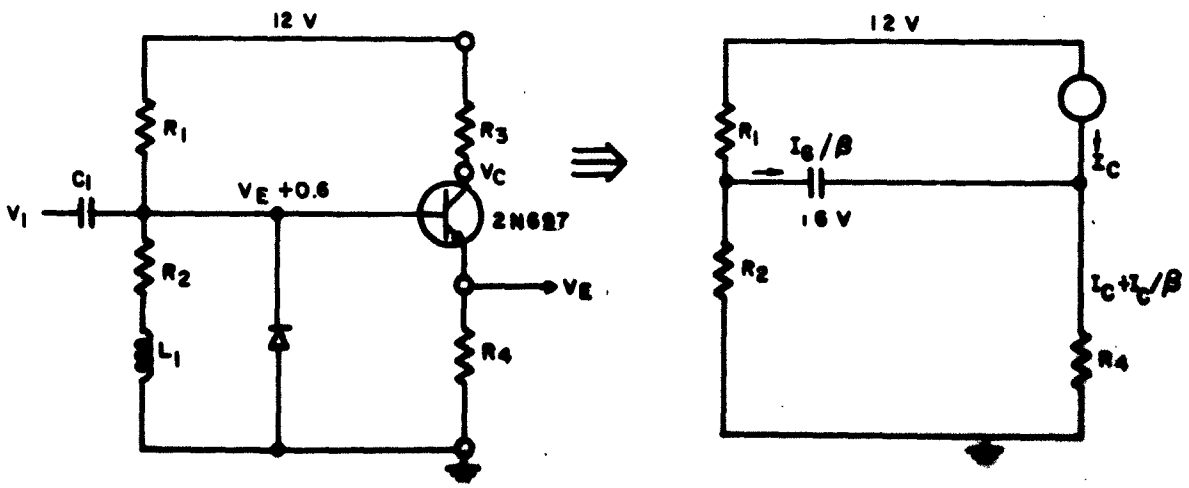

Figure 59. Equivalent Circuit of Distribution Amplifier

A nodal analysis of this equivalent circuit results in equations (153) and (155).

$$\frac{12 - V_E - 0.6}{R_1} = \frac{I_c}{\beta} + \frac{V_E + 0.6}{R_2} \tag{153}$$

$$\frac{V_E}{R_4} = I_c + \frac{I_c}{\beta} \tag{154}$$

$$I_c = \frac{12 - V_c}{R_3} \tag{155}$$

These equations when rearranged form the matrix equation (156).

$$\begin{bmatrix} \frac{1}{R_1} + \frac{1}{R_2} & 0 & \frac{1}{\beta} \\ 0 & \frac{1}{R_3} & 1 \\ \frac{1}{R_4} & 0 & -1\frac{1}{\beta} \end{bmatrix} \begin{bmatrix} V_E \\ V_c \\ I_c \end{bmatrix} = \begin{bmatrix} \frac{11.4}{R_1} - \frac{0.6}{R_2} \\ \frac{12}{R_2} \\ 0 \end{bmatrix} \tag{156}$$

The matrix shown in equation (156) was programmed on the Burroughs 205 computer and the solution is shown in Table 31.

TABLE 31

COMPUTER SOLUTION OF DISTRIBUTION AMPLIFIER

V_E	V_c	I_c
.453	11.9	.0094

The input voltage required to saturate the transistor Q_1 can be obtained by analyzing the equivalent circuit shown in Figure 60.

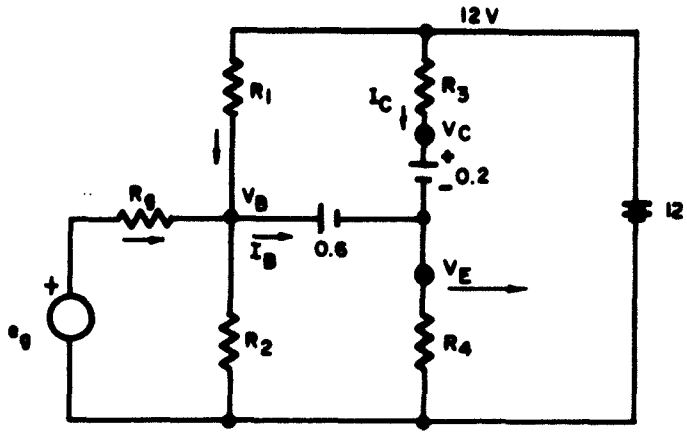

Figure 60. Equivalent Circuit of Distribution Amplifier with Q_1 Saturated

A circuit analysis results in equations (157) to (161).

$$I_c + I_B = \frac{V_E}{R_4} \tag{157}$$

$$I_c = \frac{12 - V_c}{R_3} \tag{158}$$

$$\frac{e_g - V_B}{R_g} + \frac{12 - V_B}{R_1} = I_B + \frac{V_B}{R_2} \tag{159}$$

$$V_B = V_E + 0.6 \tag{160}$$

$$V_C = V_E + 0.2 \tag{161}$$

These equations when rearranged form the matrix equation (162).

$$\begin{bmatrix} -1 & 0 & 1 & 0 & 0 \\ 0 & \frac{1}{R_1}+\frac{1}{R_2}+\frac{1}{R_g} & 0 & 1 & 0 \\ -1 & 0 & 1 & 0 & 0 \\ -\frac{1}{R_4} & 0 & 0 & 1 & 1 \\ 0 & 0 & \frac{1}{R_3} & 0 & 1 \end{bmatrix} \begin{bmatrix} V_E \\ V_B \\ V_C \\ I_B \\ I_C \end{bmatrix} = \begin{bmatrix} 0.6 \\ \frac{e_g^*}{R_g} + \frac{12}{R_1} \\ 0.2 \\ 0 \\ \frac{12}{R_3} \end{bmatrix} \qquad (162)$$

$^* e_g$ = (1.5, 3.5, 5.0, 7.0, 8.0, 9.0, 10.0, 10.2, 10.4, 10.6, 10.8, 11, 12)

To determine the minimum input voltage required to saturate Q_1, the computer was programmed to search for the value of e_g which results in a negative base current which would indicate that the amplifier is in saturation. The results of this computer program is shown in Table 32. This shows a transition of positive to negative base current occurring at an input voltage of 10.677 volts.

3.2.8.1 Small Signal Gain of Distribution Amplifier

To find the small signal gain the equivalent circuit shown in Figure 61 is utilized.

A circuit analysis is performed and equations (163) to (167) are formulated.

$$\frac{e_{in} - V_b}{R_{in}} - \frac{V_b}{R_A} = i_b \qquad (163)$$

$$i_b - \frac{e_o}{R_4} + \beta i_b = 0 \qquad (164)$$

TABLE 32

DISTRIBUTION AMPLIFIER WITH Q_1 SATURATED

V_E	V_B	V_C	I_B	I_C	e_g
5.02	5.62	5.22	-0.0572	0.0678	1.5
6.04	6.64	6.24	-0.0447	0.0576	3.5
6.81	7.41	7.01	-0.0354	0.0499	5.0
7.84	8.44	8.04	-0.0229	0.0396	7.0
8.36	8.96	8.56	-0.0167	0.0344	8.0
8.87	9.47	9.07	-0.0104	0.0293	9.0
9.38	9.98	9.58	-0.00421	0.0242	10.0
9.49	10.1	9.69	-0.00297	0.0231	10.2
9.59	10.2	9.79	-0.00172	0.0221	10.4
9.69	10.3	9.89	-0.00048	0.0211	10.6
9.72	10.3	9.92	-0.00016	0.0208	10.65
9.72	10.3	9.92	-0.00010	0.0208	10.66
9.72	10.3	9.92	-0.00010	0.0197	10.67
9.73	10.3	9.93	-0.00002	0.0207	10.673
9.73	10.3	9.93	-0.00001	0.0207	10.674
9.73	10.3	9.93	0	0.0207	10.675
9.73	10.3	9.93	0	0.0207	10.676
9.73	10.3	9.93	0	0.0207	10.677
9.73	10.3	9.93	0.00001	0.0207	10.678
9.73	10.3	9.93	0.00002	0.0207	10.679
9.73	10.3	9.93	0.00002	0.0207	10.68
9.74	10.3	9.94	0.00008	0.0206	10.69
9.74	10.3	9.94	0.00015	0.0206	10.7
9.77	10.4	9.97	0.00046	0.0203	10.75
9.79	10.4	9.99	0.00077	0.0201	10.8
9.90	10.5	10.1	0.0020	0.0190	11.0
10.4	11.0	10.6	0.0082	0.0139	12.0

$$\beta\, i_b = -\frac{V_c}{R_3} \tag{165}$$

$$i_b = \frac{V_b - e_o}{r_b} = \frac{V_b}{r_b} - \frac{e_o}{r_b} \tag{166}$$

Using equation (164) to solve for e_o

$$e_o = i_b R_4 (1 + \beta) \tag{167}$$

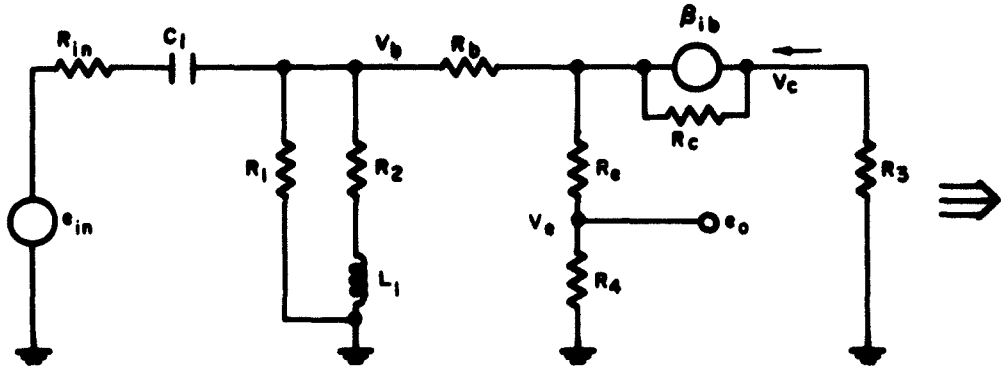

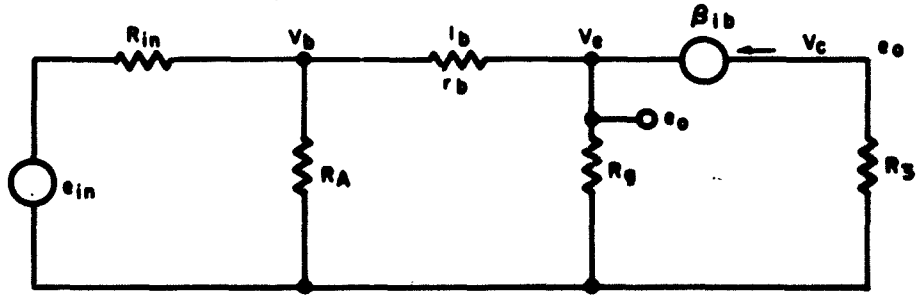

Where $R_A = \dfrac{R_1 R_2}{R_1 + R_2}$

and $C_1 + L_1$ are low impedances at frequency of interest.

Figure 61. Small Signal Equivalent Circuit

Using equation (163) to solve for V_b

$$V_b = \frac{R_{in} R_A}{R_A + R_{in}} - i_b \frac{R_A R_{in}}{R_A + R_{in}} \tag{168}$$

Using equations (165), (166), (167), and (168) the signal flow graph shown in Figure 62 can be obtained and the gain determined. [22]

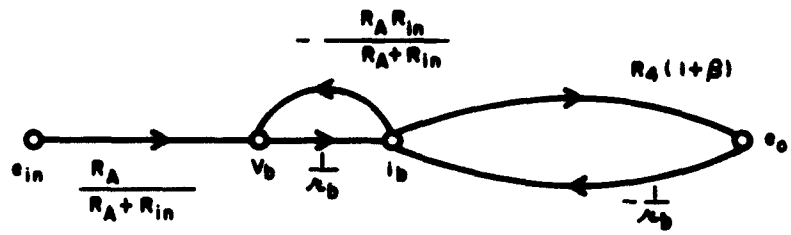

Figure 62. Signal Flow Graph of Distribution Amplifier

$$\frac{e_o}{e_{in}} = \frac{\frac{R_A R_4(1+\beta)}{(R_A + R_{in}) r_b}}{1 + \frac{R_A R_{in}}{(R_A + R_{in}) r_b} + \frac{R_4}{r_b}(1+\beta)} \tag{169}$$

$$\frac{e_o}{e_{in}} = \frac{R_A R_4(1+\beta)}{(R_A + R_{in}) r_b + R_A R_{in} + R_4(1+\beta)(R_A + R_{in})} \tag{170}$$

$$\frac{e_o}{e_{in}} = \frac{R_A R_4(1+\beta)}{R_A r_b + R_{in} r_b + R_A R_{in} + R_4 R_A + R_4 R_{in} + \beta R_4 R_A + \beta R_4 R_{in}} \tag{171}$$

Where

$$R_A = \frac{2200\,(22,000)}{24,200} \qquad r_b = 50$$

$$R_4 = 470 \qquad R_{in} = 75$$

$$\beta = 60,\ 50,\ 40,\ 30,\ 20 \qquad \left.\frac{e_o}{e_{in}}\right|_{\beta=50} = 9.589 \times 10^{-1}$$

A conventional analysis using nodal equations gives the same results. Equations (172), (173) and (174) are the nodal equations for the equivalent circuit shown in Figure 61. This is shown in matrix form in equation (175).

$$V_b\left(\frac{1}{R_{in}} + \frac{1}{R_A}\right) + i_b = \frac{e_{in}}{R_{in}} \tag{172}$$

$$i_b(1+\beta) - \frac{e_o}{R_4} = 0 \tag{173}$$

$$-\frac{V_b}{r_b} + i_b + \frac{e_o}{r_b} = 0 \tag{174}$$

$$\begin{bmatrix} \frac{1}{R_{in}} + \frac{1}{R_A} & 1 & 0 \\ 0 & (1+\beta) & -\frac{1}{R_4} \\ -\frac{1}{r_b} & 1 & \frac{1}{r_b} \end{bmatrix} \begin{bmatrix} V_b \\ i_b \\ e_o \end{bmatrix} = \begin{bmatrix} \frac{e_{in}}{R_{in}} \\ 0 \\ 0 \end{bmatrix} \tag{175}$$

Equation (176) shows the matrix with nominal circuit parameters, and Table 33 is the solution to the matrix obtained by using the Burroughs 205 computer.

$$\begin{bmatrix} 0.013833\ldots & 1 & 0 \\ 0 & 51 & -0.002127 \\ -0.02 & 1 & 0.02 \end{bmatrix} \begin{bmatrix} V_b \\ i_b \\ e_o \end{bmatrix} = \begin{bmatrix} 0.0133 \\ 0 \\ 0 \end{bmatrix} \quad (176)$$

TABLE 33

COMPUTER SOLUTION OF DISTRIBUTION AMPLIFIER SMALL SIGNAL GAIN

V_b	i_b	e_o
.96147v	40	.95947v

3.3 TRANSFER FUNCTIONS OF MICROMINIATURE CIRCUITS

This section presents the transfer functions of the microminiature circuits developed by the Sylvania Microelectronics Laboratory.

The circuits presented in this section of the report were, in some instances, analyzed not simply as individual circuits with their supply voltages, but also with respect to their use in the system represented in Figure 6. An example of this is the steering circuit which was analyzed with consideration for the loading of the previous stage. Also, the active circuits (the Flip-Flop and NOR circuit) were analyzed with their respective transistors operating in both the saturated and non-saturated states. The accuracy of the transfer functions was verified by measuring the voltages on actual circuits in the laboratory. Since the flip-flop is of a symmetrical nature, the transformation matrix solved for Q_2 conducting and Q_1 off also represents the condition when Q_1 is conducting and Q_2 is off.

3.3.1 Transfer Function of the 5 mc Flip-Flop

The flip-flop or bistable multivibrator circuit utilized for analysis is shown in Figure 63.

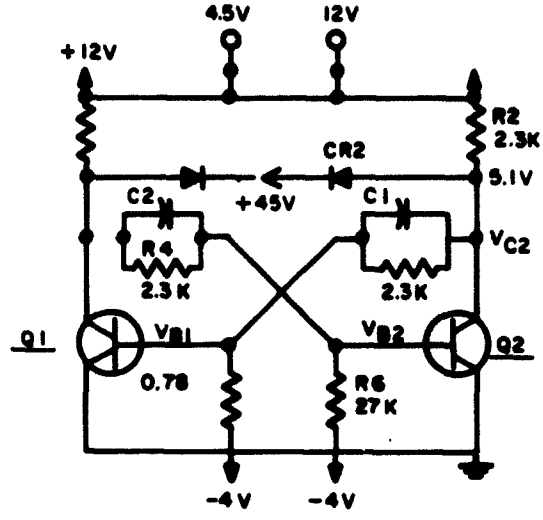

Figure 63. Five Mc. Flip-Flop Circuit

This general purpose type circuit is specifically designed to operate in the saturated mode at a maximum repetition rate of 5 mc. This type of circuit finds extensive application in pulse circuitry being used not only for the generation of square waves from pulses but also for the performance of certain digital operations such as counting. The actual operation of the circuit is similar to the one previously discussed in Section 3.2.6.

Quiescent Currents and Voltages

When the condition exists that Q_1 is off and Q_2 is in either the saturated or the non-saturated state, Q_1 and CR_2 and the associated circuitry are removed from the circuit. Figure 64 is the equivalent circuit used for the analysis.

TABLE 34

PERFORMANCE CRITERIA OF MICROMINIATURE FLIP FLOP

Maximum operating frequency = 5 mc

INPUT REQUIREMENTS:

Input pulse derived from pulse level gate
Maximum "Fan in" (pulse level gates) - 3 per input

OUTPUT REQUIREMENTS:

R_L min (max load to ground) = 6K (0.8 ma)

R_S min (max load to V_{CC}) = 2K (6 ma)

Maximum DC "Fan out" = 2 logic inputs or
2 level inputs (pulse level gate)
Maximum AC "Fan out" = 4 pulse inputs (pulse level gate)
Maximum capacitive load = 50 pf

Typical output characteristics for operation with pulse level gate output at 25°C unloaded

turn on time = 30 ns
turn off time = 50 ns
turn on delay = 25 ns
turn off delay = 20 ns

Logic levels: "false" = +5 volts
"true" = +0.3 volts

Supply Voltages

V_{cc} = +12 volts $\pm$5 percent

V_{bb} = -4 volts $\pm$5 percent

V_H = +4.5 volts $\pm$5 percent

V_{EE} = ground

Storage temperature = -55°C to + 125°C

Operating temperature = -55°C to + 125°C

Power dissipation = 90 mw

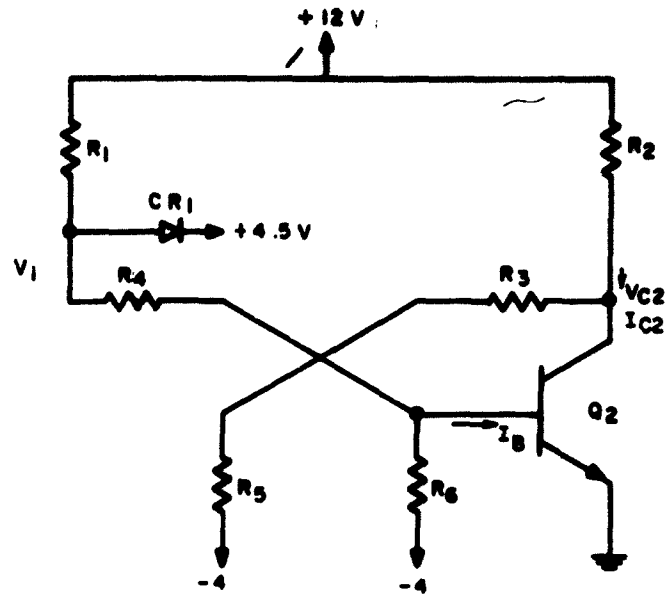

Figure 64. DC Equivalent Circuit of Flip-Flop with Q_1 off and Q_2 Conducting

The equivalent circuits used for the transistors are presented in Figures 9 and 10. Utilizing the above set of equivalent circuits, the analysis yields equations (177) through (182); these equations are then rearranged and form matrix equation (183).

$$V_{C2} = 0.2 \tag{177}$$

$$V_1 = 5.1 \tag{178}$$

$$V_{B2} = 0.78 \tag{179}$$

$$V_{C2}(1/R_3) + V(-1/R_3 - 1/R_5) - 4/R_5 \tag{180}$$

$$V_{B2}(1/R_6 + 1/R_4) + V_1(-1/R_4) + I_B = -4/R_6 \tag{181}$$

$$V_{C2}(-1/R_2 - 1/R_3) + V(1/R_3) - I_C = -12/R_2 \tag{182}$$

$$\begin{bmatrix} 1 & 0 & 0 & 0 & 0 & 0 \\ 0 & 0 & 1 & 0 & 0 & 0 \\ \frac{1}{R_3} & 0 & 0 & -\frac{1}{R_3} - \frac{1}{R_5} & 0 & 0 \\ 0 & \frac{1}{R_6} + \frac{1}{R_4} & -\frac{1}{R_4} & 0 & 1 & 0 \\ -\frac{1}{R_2} - \frac{1}{R_3} & 0 & 0 & \frac{1}{R_3} & 0 & -1 \\ 0 & 1 & 0 & 0 & 0 & 0 \end{bmatrix} \begin{bmatrix} V_{C2} \\ V_{B2} \\ V_1 \\ V \\ I_B \\ I_C \end{bmatrix} = \begin{bmatrix} 0.2 \\ 5.1 \\ \frac{4}{R_5} \\ -\frac{4}{R_6} \\ -\frac{12}{R_2} \\ 0.78 \end{bmatrix} \quad (183)$$

This matrix equation is then solved using a computer. The results of this computer solution along with the results received from laboratory measurements on this circuit are presented in Table 35.

TABLE 35

COMPARISON OF CALCULATED AND MEASURED VALUES OF FLIP-FLOP WITH Q_1 OFF AND Q_2 SATURATED

	V_{C2}	V_{B2}	V_{C1}	V_{B1}	I_B	I_C
CALCULATED	0.2	0.78	5.1	-0.61	0.00138	0.0078
MEASURED	0.2	0.85	5.0	-0.60	0.0013	0.0087

As may be seen from Table 35, the calculated and measured values compared very closely, and therefore, confirm the accuracy of the transfer function.

Let us now consider the case when Q_1 is off and Q_2 is non-saturated. This condition is represented by the DC equivalent circuit presented in Figure 65. The analysis of this circuit is quite simple since most of the nodal voltages are known, i.e., the voltages V_{C1}, V_{B1}, V_{C2} are known and are shown on the

diagram. Also, I_B is approximately equal to I_C and since it is of the order of 10^{-9} amps, it is neglected. Therefore, the analysis yields only equation (184).

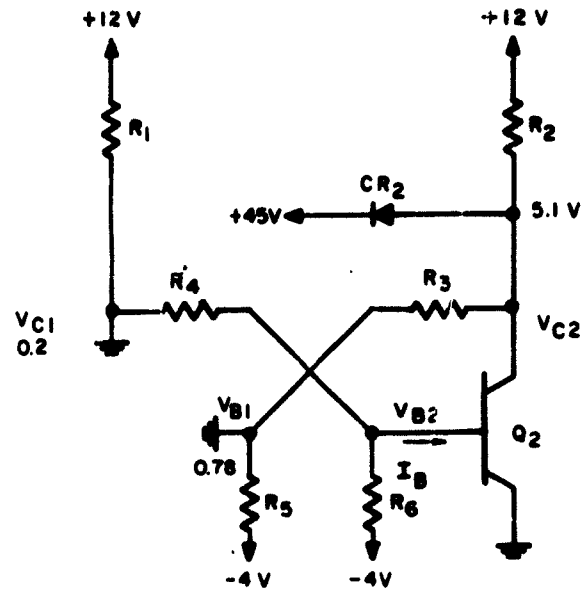

Figure 65. DC Equivalent Circuit of Flip-Flop with Q_1 off and Q_2 Non-Saturated

$$\frac{0.2 - V_{B2}}{R_4} = \frac{V_{B2} - (-4)}{R_6} + I_B \qquad (184)$$

Since the value of I_B is negligible, V_{B2} may be solved for directly and is -0.605 volts. It should be noted that the voltage V_{B2} for Q_2 non-saturated is the same as V_{B1} for Q_2 saturated, thereby pointing out that Q_2 does not operate in the non-saturated mode but is, in fact, cut off.

3.3.2 Transfer Functions of the Steering Network

The circuit analyzed in this subsection is that of a steering and logic network designed to provide the input pulse for the Microminiature Flip-Flop circuit. Each wafer contains two independent RC differentiating networks with level blocking, diode-gated outputs. Two input capacitors are provided on each gate to allow a wider variety of input pulses to be used. The schematic of this circuit is presented in Figure 66.

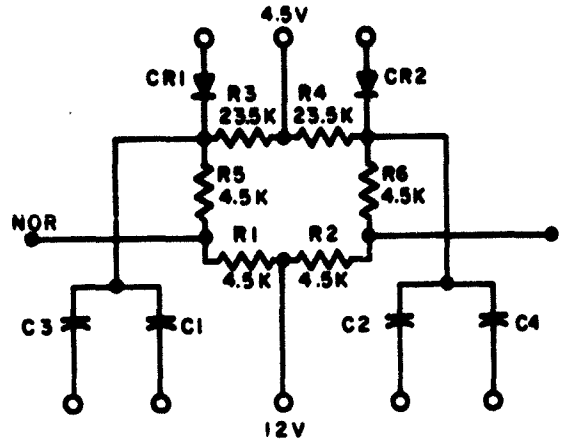

Figure 66. Microminiature Steering Network Schematic

As may be seen from the schematic, the circuit is of symmetrical nature, and therefore, an analysis of one side of the circuit is sufficient. The analysis of this circuit was made with consideration of the previous stage (e. g., in the system represented in Figure 6 the steering network is fed by a NOR circuit). Therefore, the appropriate circuitry of the NOR circuit is included into the analysis of the steering network. This approach requires that the steering network be analyzed when the NOR circuit is in the saturated and non-saturated modes. This must be done since different portions of the NOR circuit in its different modes have a significant effect on the steering network.

We will first consider the case when the NOR circuit (presented in Figure 69) is operating in the saturated state. The DC equivalent circuit for this condition is shown in Figure 67.

Referring to Figure 67(a), R_A is the resistance of the diode CR_4 and R_4' is the collector resistance of the NOR circuit. Figure 67(b) is the simplified circuit where

$$R_p = \frac{R_1 R_4'}{R_1 + R_4'} \tag{185}$$

An analysis of this circuit yields equations (186) and (187). Since there are only two unknowns, it is much easier to solve these equations

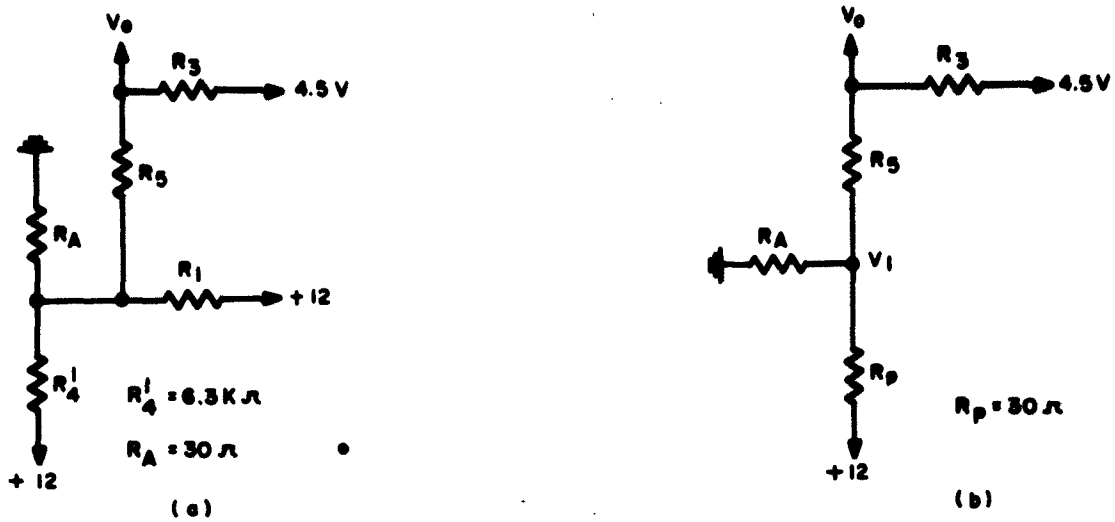

Figure 67. DC Equivalent Circuit of Steering Network when NOR Circuit is Saturated

$$\frac{12 - V_1}{R_p} - \frac{V_1}{R_A} + \frac{V_0 - V_1}{R_5} = 0 \tag{186}$$

$$\frac{4.5 - V_0}{R_3} + \frac{V_0 - V_1}{R_5} = 0 \tag{187}$$

by simple substitution rather than by the use of a computer. This type of approach gives the following relationships:

$$V_0 = \frac{V_1(R_A R_5 + R_p R_5 + R_p R_A) - 12\,R_A R_5}{R_A R_p} \tag{188}$$

$$V_1 = V_0\left(\frac{R_3 - R_5}{R_3}\right) + 4.5\,\frac{R_5}{R_3} \tag{189}$$

By substituting (189) into (188) the following expression for V_0 as a function of the circuit components is derived:

$$V_0 = \frac{4.5\,(R_A R_5 + R_p R_5 + R_p R_A) - 12\,R_3 R_A R_p}{R_A R_5 + R_p R_5 + R_p R_A - R_3 R_A - R_3 R_p} \quad . \qquad (190)$$

Once the expression for V_0 is obtained the solution for V_1 is also known by substituting the expression for V_0 into equation (189). The numerical solution is then obtained by substituting the nominal values of the components into the expressions. This procedure yields the following results:

$$V_0 = 6.34 \text{ volts}$$

$$V_1 = 5.99 \text{ volts}$$

Let us now consider the case where the NOR circuit is operating in the non-saturated mode. For this condition the equivalent circuit presented in Figure 68 applies.

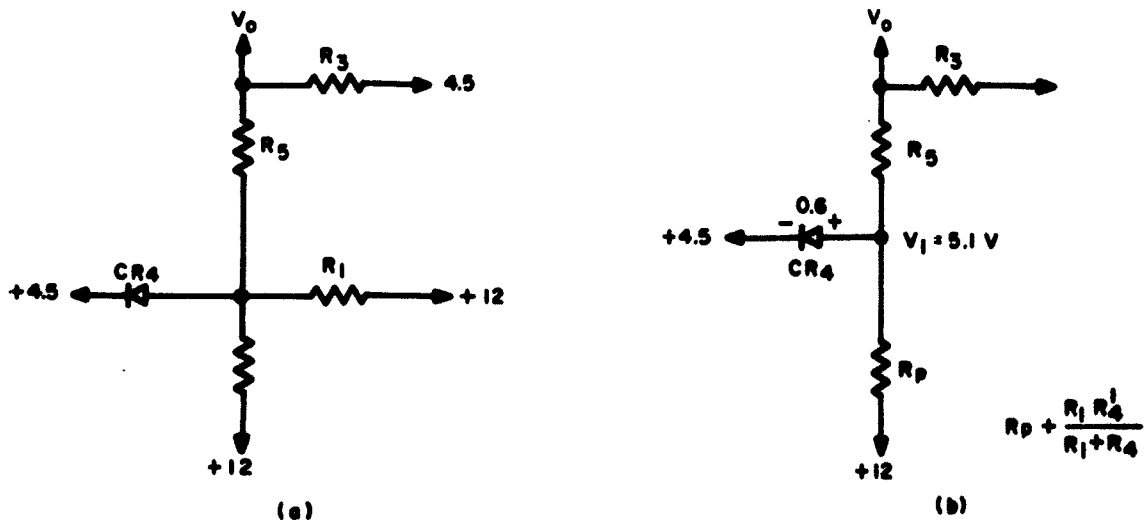

Figure 68. DC Equivalent Circuit of Steering Network when NCR Circuit is Non-Saturated

Referring to the equivalent circuit, the voltage V_1 is clamped at 5.1 volts assuming a 0.6-volt hop across the diode CR_4. It is now possible to completely

describe the voltage V_0 in terms of the circuit components by equation (191). Simplifying the expression

$$\frac{5.1 - V_0}{R_5} + \frac{4.5 - V_0}{R_3} = 0 \qquad (191)$$

and solving for V_0 yields the following relationship:

$$V_0 = \frac{4.5 R_5 + 5.1 R_3}{R_3 + R_5} \qquad (192)$$

Substituting the nominal values for the components into the expression yields the voltage V_0 when the NOR circuit is operating in the non-saturated mode.

$$V_0 = 5.0 \text{ v}$$

Thus, we have completely described the steering network in terms of its transfer functions for both internal and external effects.

3.3.3 Transfer Functions of the Microminiature NOR Circuit

The circuit to be analyzed in this sub-section is that of a NOR circuit. This circuit is simply a gate with a logic sense of plug 5 volts = False and zero volts = True. The circuit is composed of a three-input "OR" gate and an inverting transistor amplifier and a clamping diode for greater reliability. The circuit accepts a positive pulse at the input and delivers a negative pulse to the succeeding stage. The NOR circuit schematic is presented in Figure 69. The performance criteria of the circuit is shown in Table 36.

This circuit was analyzed for the transistor operating in both the saturated and non-saturated modes.

We will now consider the circuit when the transistor is operating in the non-saturated mode. The DC equivalent circuit for this condition is presented in Figure 70.

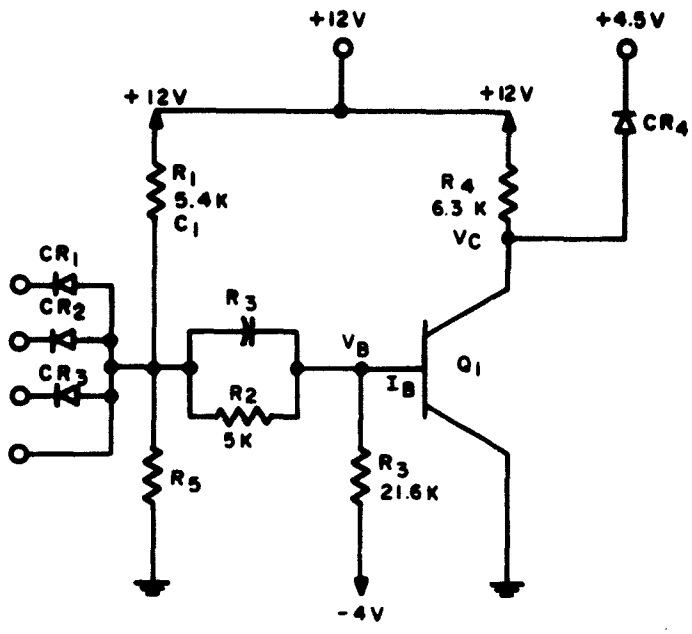

Figure 69. Schematic of Microminiature NOR Circuit

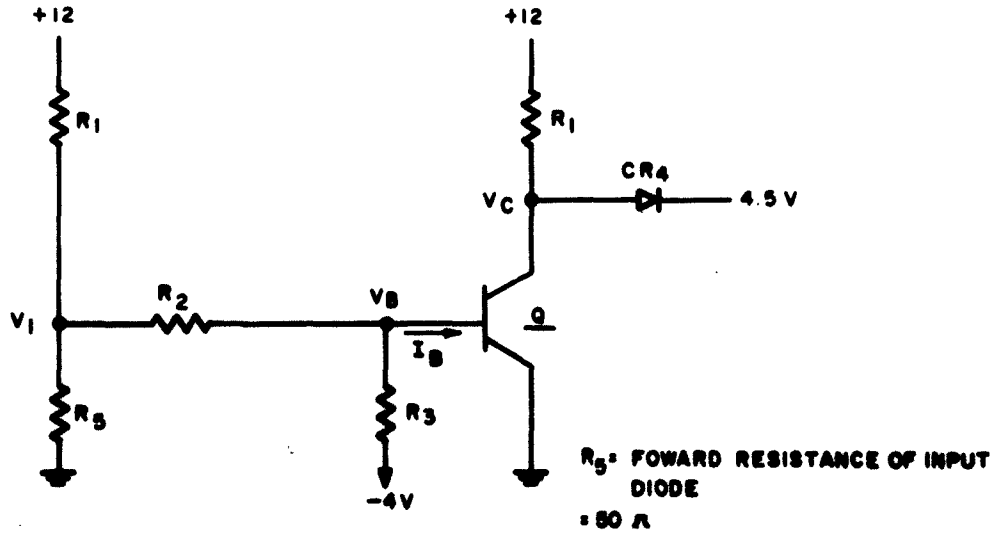

Figure 70. DC Equivalent Circuit of Microminiature NOR Circuit for the Translator in the Non-Saturated Mode

TABLE 36

PERFORMANCE CRITERIA OF MICROMINIATURE NOR CIRCUIT

INPUT REQUIREMENTS:

Maximum "Fan In" = 6 (addition of 3 diodes to pins 5 or 12)
Minimum input pulse width = 40 ns
"false" voltage level = +4.5 to + 6.0 volts
"true" voltage level = 0 to +0.5 volts

OUTPUT REQUIREMENTS:

R_L min. (Max. load to ground) = 0.5K (1 ma)
R_S min. (Max. load to V_{CC}) = 1.5K (8 ma)

Maximum DC "fan out" = 3 logic inputs or 2 level inputs (pulse level gate 37AA02)

- Max. capacitive load = 100 pf

Max. AC "Fan out" = 4 pulse inputs (pulse level gate 37AA02)
Typical output characteristics for operation with 5 volts input pulse at 25°C unloaded
Turn on time = 20 ns
Turn off time = 20 ns
Turn on delay = 10 ns
Turn off delay = 50 ns

In order for the transistor to be physically in non-saturation, one of the input diodes has to be grounded. Referring to the equivalent circuit, the analysis yields equations (193) through (195).

$$V_c = 5.1 \tag{193}$$

$$\frac{V_1 - V_B}{R_2} + \frac{-4 - V_B}{R_3} = I_B \tag{194}$$

$$\frac{12 - V_1}{R_4} = \frac{V_1}{R_5} + \frac{V_1 - V_B}{R_3} \tag{195}$$

However, in equation (194), $I_B = I_{B0} \approx 10^{-9}$; thus, since the effects of I_B are negligible, the equation may be rewritten as equation (196).

$$\frac{V_1 - V_B}{R_2} = \frac{4 + V_B}{R_3} \tag{196}$$

Utilizing the above equations the matrix equation (197) may be formed.

$$\begin{bmatrix} \frac{1}{R_2} & -\frac{1}{R_3} - \frac{1}{R_2} \\ -\frac{1}{R_4} - \frac{1}{R_5} - \frac{1}{R_3} & \frac{1}{R_3} \end{bmatrix} \begin{bmatrix} V_1 \\ V_B \end{bmatrix} = \begin{bmatrix} \frac{4}{R_2} \\ -\frac{12}{R_4} \end{bmatrix} \tag{197}$$

The solution of this matrix along with the values of the circuit parameters measured on a breadboard in the laboratory are presented in Table 37.

TABLE 37

COMPARISON OF MEASURED AND CALCULATED VALUES OF THE NOR CIRCUIT WITH THE TRANSISTOR IN THE NON-SATURATED MODE

	V_c	V_1	V_B
Measured	5.0	0.8	---
Calculated	5.1	0.73	-0.83

As may be seen from the table, the calculated and measured values of the circuit compare quite closely and thereby verify the accuracy of the transfer function.

We will now consider the case where the transistor is operating in the saturated mode. The DC equivalent circuit for the condition is presented in Figure 71. Utilizing this circuit, we may write equations (198) through (202).

$$\frac{12 - V_1}{R_1} = \frac{V_1 - V_B}{R_3} \tag{198}$$

$$\frac{V_1 - V_R}{R_3} + \frac{-4 - V_R}{R_2} = I_B \tag{199}$$

$$\frac{12 - V_c}{R_4} = I_c \tag{200}$$

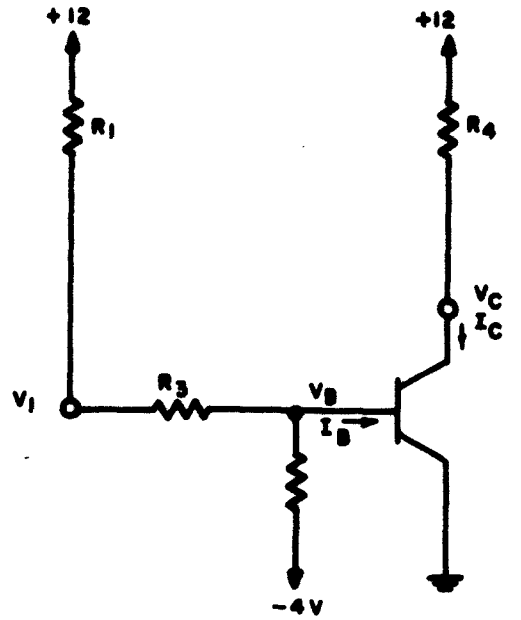

Figure 71. DC Equivalent Circuit of Microminiature NOR Circuit with the Transistor in Saturation

$$\frac{I_c}{I_B} = \beta \tag{201}$$

$$V_c = 0.2 \tag{202}$$

The above equations are then formed into the matrix equation (203).

$$\begin{bmatrix} -\frac{1}{R_1}-\frac{1}{R_3} & \frac{1}{R_3} & 0 & 0 \\ \frac{1}{R_3} & -\frac{1}{R_3}-\frac{1}{R_2} & 0 & -\frac{1}{\beta} \\ 0 & 0 & 1 & 0 \\ 0 & 0 & -\frac{1}{R_4} & -1 \end{bmatrix} \begin{bmatrix} V_1 \\ V_B \\ V_c \\ I_c \end{bmatrix} = \begin{bmatrix} -\frac{12}{R_1} \\ \frac{4}{R_2} \\ 0.2 \\ -\frac{12}{R_4} \end{bmatrix} \tag{203}$$

The matrix equation is then solved by means of a computer and the measured and calculated values are presented in Table 38.

TABLE 38

COMPARISON OF CALCULATED AND MEASURED VALUES OF THE NOR CIRCUIT WITH THE TRANSISTOR IN SATURATION

	V_1	V_c	V_B	I_c	$I_B\left(\frac{I_c}{\beta}\right)\beta = 50$
Measured	5.6	0.15	--	--	--
Calculated	5.5	0.2	-2.3	0.0018	0.00004

An examination of Table 38 reveals the close comparison between the measured and calculated values of the circuit parameters thereby confirming the accuracy of the transfer function of the microminiature NOR circuit.

SECTION IV

SYSTEMS APPLICATIONS

The procedures and applications described in this section are, to a certain extent, similar to those discussed in Section 3. The major differences in the technique as applied to systems are: (1) the added complexity and (2) the preparatory work that must be accomplished in order for the results to be both meaningful and useful.

The study has yielded three possible approaches that may be used, all of which present very useful results. The particular approach to be chosen depends upon a number of factors among which are: (1) type of information required, (2) complexity, (3) resources, (4) time and money available, etc. Therefore, the three approaches will be presented along with a discussion of the aforementioned factors. The first method that will be discussed is the most elaborate and consequently the most expensive. The second method is a modification of the first and the third and least expensive is a relatively simple but quite useful technique. The three techniques are described below.

(1) In the first approach, one obtains a complete transfer function in terms of all the components in the system. This transfer function may be derived in a number of ways. Two methods are described below:

   (a) The transfer functions of each of the subsystems may be individually obtained and then by adding, subtracting or multiplying the the individual transfer functions, depending upon the function of the subsystems, the complete transfer function may be obtained. However, if these individual transfer functions are in matrix form, the rules for manipulating matrices must be followed, i. e., in order to multiply matrices, they must be of the same order, etc. It is, therefore, quite probable that a great deal of preparatory work will be required upon the individual transfer functions prior to the task of formulating the over-all function. This method is considered to be the easier and most useful method.

(b) Another method that may be used to determine the system transfer function is to express it analytically in terms of the input and output voltages of the system. However, with this type of approach a great deal of information may be lost since many of the component parameter relationships internal to the input-output sections of the system may not appear in the transfer equation. It is, therefore, recommended that the first technique be used.

Once the system transfer function is obtained and is formed into a transformation matrix of the order N , the Monte Carlo process described in Section II of this report may be used. For this particular technique one would run the process for every component and combination of components in the matrix.

(2) The next approach that may be used is identical to that described above except that the Monte Carlo process is applied only to the critical components in the system. An example of this technique is described below:

Consider the simple amplifier shown in Figure 72. It is obvious from inspection of the circuit that the gain is given by Equation (204):

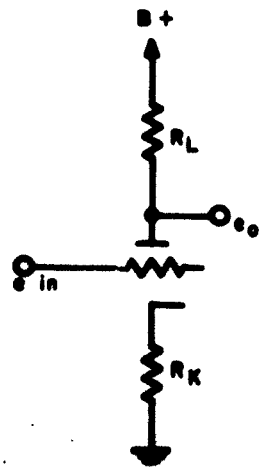

Figure 72. Amplifier Circuit

$$\text{Gain} = \frac{e_o}{e_{in}} = \frac{g_m R_K}{1 + g_m R_K} \tag{204}$$

If $g_m R_K >> 1$ it is easily seen that equation (206) may be rewritten as shown below:

$$\text{Gain} = \frac{R_L}{R_K} \tag{205}$$

It may be stated, therefore, that the critical components of the amplifier are the plate and cathode resistances R_L and R_K. The transconductance g_m may be neglected since it is common to both numerator and denominator of the gain expression. Therefore, if one determined the critical components of a system it would be possible to save a great deal of time and expense using this approach as opposed to that described in (1).

(3) The final technique to be described is one in which the Monte Carlo process is applied to the individual subsystem transfer functions. With this type of approach it is, therefore, necessary to know the input and output requirements of the individual subsystems. Once the requirements are known, the Monte Carlo process may be applied. The technique consists of Monte Carloing each of the components in the individual subsystem, and noting the effects upon the output. When and if the output does not meet the input requirements of proceeding subsystem, the values of the component or components are noted and the process is halted in the presence of a failure or continued on the next subsystem if no fialure occurs. Another useful outcome of this technique is that although the output may just fall within the input requirements of the proceeding stage, it may cause a failure at another point in the system under consideration. As an illustration of this technique, let us consider the following example:

Suppose we have two amplifiers in series

Figure 73. Illustrative Example

The gain of Amplifier #1 = Amplifier #2 = $\frac{g_m R_L}{1 + g_m R_L}$

The Amplifiers have the following Requirements:

TABLE 39

OPERATING PARAMETERS OF
ILLUSTRATIVE EXAMPLE

	Input	Output
Amplifier #1	2 ± 5% volts	10 ± 5% volts
Amplifier #2	10 ± 5% volts	50 ± 5% volts

We will assume that the input to Amplifier #1 is always at 2 volts. The next step is to perform a Monte Carlo process on each of the components in the amplifier and note the effects upon the output. From the cumulative distribution functions obtained by this procedure, it is possible to determine when the output falls outside the input requirements of the proceeding amplifier and, thus, the reliability of the amplifier is known. This process is then carried on until all of the subsystems have been analyzed.

This technique is considered to be the least expensive and requires less computer time, but as in the two techniques previously mentioned, quite time consuming. This procedure may be used on all components or only on the critical components. It is, therefore, recommended that this technique be used since it provides all necessary information.

The techniques outlined above will provide the following information:

(1) Based on the underlying frequency distribution of the components, it is possible to determine the reliability of a system at zero time and at some time or times in the future.

(2) It provides a means of improving performance, e.g., let us consider a circuit whose

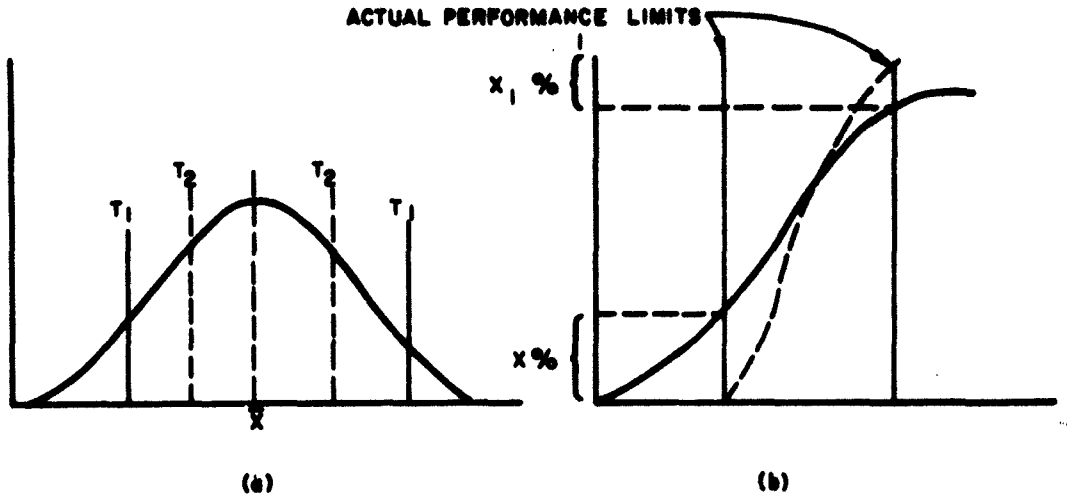

Figure 74. Illustrative Example of Application of Monte Carlo Technique

performance is plotted as the cumulative distribution function of Figure 74b. The normal distribution shown in Figure 74a represents the critical component R of the circuit. The particular tolerance limits on this component ($\pm T_1$) will yield a reliability of $1 - (X + X_1)$ for the circuit. However, it is easily seen that if a stricter tolerance (T_2) is imposed on the component R the performance of the circuit may be improved as represented by the dashed curve in Figure 74b. Therefore, by utilising the technique in this manner, the over-all performance of a circuit or system may be improved.

(3) With the information obtained from this technique, it will be possible to plan better spare parts allocation and maintainability methods.

(4) It will provide a better method for determining trouble-shooting techniques since the critical parts will be highlighted and the system degradation due to the failure of these parts will be known.

4.1 TIMING SYSTEM

It is the purpose of this subsection to present a specific application of the Monte Carlo Technique, previously described in Section IV, on a system. The system, as presented in Figure 5, generates a constant 10 microsecond pulse at a repetition rate of 100 kc in an environment where a large shift of nominal part parameters may be experienced. This treatment presents the specific application of the technique, however, in keeping with the purpose of this report, that of developing a new technique, the routine mechanics are not included. The mathematical simulation procedure is as follows:

> An oscillator is synthetically constructed utilizing the transfer function previously developed. The critical performance criteria of the oscillator is the resonant frequency and the satisfaction of this criteria will automatically ensure adequate input to the high level amplifier. Once it has been ascertained that the oscillator is operating within specifications, the second stage or high level amplifier is synthetically constructed and the process is repeated. This procedure is followed with each of the remaining stages in the system. If a failure is experienced, the process is immediately halted and the cause and location of the failure noted. The whole process is repeated 1000 times thereby yielding the reliability of the system. Referring to the test system and the waveform development shown in Figure 5, the following requirements must be satisfied by the respective subsystems in order to obtain successful operation.

Subsystem	Input	Output
Oscillator	---	0.4v - 1.0v
High Level Amplifier	0.01v - 5v	0.6v - 1000v
Trigger Circuit	6v - 10v	10v - 18v (neg)
Bistable Multi	8v - 15v (neg)	$\pm$10v - $\pm$ 18v
Monostable Multi	4v - 10v (neg)	10v - 18v
Pulse Adder	>5v unsat. operation <5v sat. operation	0 - 5v
Low Level Amplifier	0.001v - 5v	0.012v - 5v

4.2 DESCRIPTION OF THE MICROMINIATURE CIRCUITS IN THE ERROR SENSING AND READOUT CIRCUIT

In Section 3.3 the three microminiature circuits are described which compose the systems in Section IV, and detailed schematic diagrams are drawn. In this subsection these same three circuits are again described, but here in terms of their logical functions or of their general function in a configuration, as opposed to their electrical configuration. [26, 27]

4.2.1 Logical Description of a Circuit

All electrical circuits can be divided into two types, digital and analog. If a circuit is viewed as a black box, i.e., only the inputs and outputs are of interest, then analog circuits are those in which the voltages at the terminals may vary continuously over a range; whereas digital circuits are those in which the terminal voltages, both input and output, are restricted to two (or any finite number but usually only two) sufficiently separated narrow sub-ranges, say R_1 and R_2, of the total possible range R. If the voltage falls outside of R_1 and R_2 the circuit is said to have failed. If the circuit does not fail, then the voltage at each terminal must be in one and only one of two mutually exclusive sub-ranges. Different letters (a, b, ---) of the alphabet may be assigned to each terminal to indicate the presence of a voltage in one of the sub-ranges, and the negation, in the sense of symbolic logic, or Boolean algebra of this letter ($\bar{A}$, $\bar{B}$, ---) means that the voltage is in the other sub-range. An example of this is given in Figure 75.

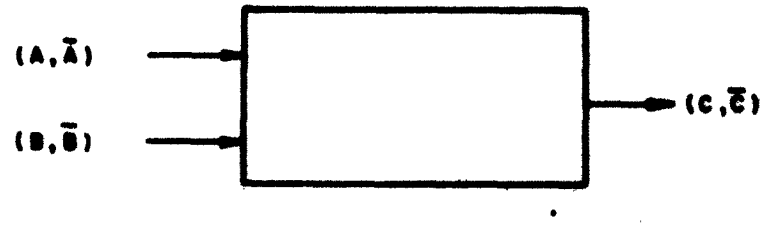

Figure 75. Symbolic Logic Block Diagram

In Figure 75 the Symbolic Logic Block Diagram, the following voltages define A B C and $\overline{A}$ $\overline{B}$ $\overline{C}$:

Input = A, when $0 \leq V_A \leq 1$

Input = $\overline{A}$, when $5 \leq V_A \leq 6$

Input = B, when $0 \leq V_B \leq 1$

Input = B, when $5 \leq V_B \leq 6$

Input = C, when $0 \leq V_C \leq 1$

Input = $\overline{C}$, when $5 \leq V_C \leq 6$

A non-sequential circuit is one in which the outputs depend only on the inputs and nothing else, e.g., internal state, past history, etc. In a non-sequential circuit the same inputs always yield the same outputs. A sequential circuit is one in which the outputs depend not only on the inputs but also on the internal state. Different internal states handle the same inputs differently, i.e., may yield different outputs for the same set of inputs. In this sense the internal state may profitably be regarded as itself another input. Sequential circuits are sometimes described as those having "memory", since they "remember" past inputs by correlating different internal states with various sequences of past inputs. A complete description of a circuit can be given by a truth table, if the inputs and outputs are represented by their respective letter symbols and arranged in the following manner. The letters are listed horizontially as column headings and each row gives each possible state of the circuit. Affirmation and negation can be described as in symbolic logic (Boolean Algebra) or numbers can be used ('one' for affirmation, 'zero' for negation). The resulting array is called a truth table (for example Table 40) and is a complete description of all possible states of a non-sequential digital circuit. A Boolean equation, or a logical truth function, is completely equivalent to this array and represents the fact that the outputs of the circuit are a certain function of the inputs. To say that a digital circuit performs a certain logical operation or that it has a certain logical description is the same as saying that its inputs and outputs satisfy a particular Boolean equation. Hence the name of some

is the same as saying that its inputs and outputs satisfy a particular Boolean equation. Hence the name of some digital circuits (e.g. NOR circuit, NAND circuit) often comes from the kind of equation which describes its operation. (e.g. $\overline{(A + B)}$ for not (A or B))

4.2.2. NOR Circuit

The NOR circuit used here has 3 inputs A, B, C and one output D. The truth table below is arranged according to the explanation given above. For all possible input configurations the output D is given as a function of this configuration (of ordered triplets of 'zero' and 'one').

TABLE 40

REPRESENTATIVE TRUTH TABLE

A	B	C	D
0	0	0	1
1	0	0	0
0	1	0	0
1	1	0	0
0	0	1	0
1	0	1	0
0	1	1	0
1	1	1	0

The equation equivalent to this truth table is given by equation (206).

$$\overline{(A + B + C)} = \bar{A}\,\bar{B}\,\bar{C} = D \qquad (206)$$

4.2.3 Flip-Flop Trigger Circuits

The combination of the flip flop and trigger circuit is designed to be used as a single unit and forms a sequential circuit.

The flip flop performs an operation which is often referred to as "remembering". It has two possible complementary outputs, called 'true' and 'false'. It can be switched from one state to another by short-duration pulses and "remembers" indefinitely the last state into which it was thrown. If the flip flop is in the condition where the 'true' output is in the 'zero' state and a pulse input is delivered to the 'true' side, the flip flop will change state so that the 'true' side goes from 'one' to 'zero'. Consequently the 'false' side goes from 'zero' to 'one'. A signal last delivered to the 'false' input will settle the flip flop so that the 'one' side goes from 'one' to 'zero', and the 'zero' side generates a 'true' signal (i.e., goes from 'zero' to 'one'). This state is maintained indefinitely and is referred to as the 'one' state of the flip flop. A second short-duration pulse delivered to the 'true' input of the flip flop does not change the state, but a pulse delivered to the 'false' input reverses the state of the flip flop so that its 'true' output terminal generates a 'zero' signal and its 'false' side a 'one' signal. The flip flop is now in the 'zero' state and remains there until an input is next delivered to the 'false' input terminal. See figure 76.

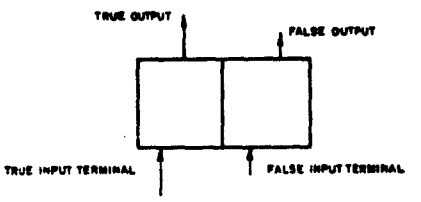

Figure 76. Logic Diagram of Flip-Flop

The trigger circuit (see Figure 77) is composed of two identical circuits.

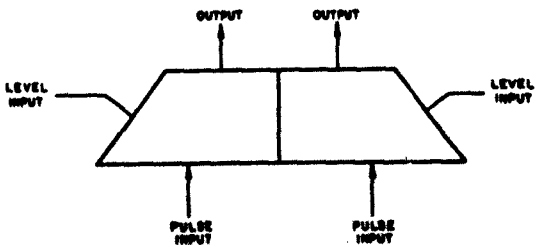

Figure 77. Logic Diagram of Trigger Circuit

Its two outputs are connected to the two inputs of the flip-flop circuit. The system clock is connected to the inputs of the trigger circuit. Clock pulses pass from the trigger input to the trigger output terminal if the level input is in state 'one'. If the level input is in state 'zero', the clock pulses do not pass through to the output.

4.2.4 Description of the System

The function of the error sensing and readout system is to monitor two inputs, each input being an output from one of two identical systems, and to compare these inputs with a reference. An indication signal is provided when

1. Either one of the two systems is in error (but only one) or
2. Both systems are in error.

The error sensing subsystem is a gating structure composed entirely of NOR circuits which has one indicator for single error, and one indicator for double error, so that correct operation of the monitored systems corresponds to an absence of such indications. Correct operation is defined as agreement with the reference signal at all times.

The readout subsystem is composed of two flip flop circuits that "remember" that an error has occurred in the time interval following the last reset of the system. These flip flops provide an indication signal at the time of malfunction and continue to supply this indication until the system is reset. Resetting clears the system of all error indications. Since these are digital systems, the signals at any time will be two valued (as has been described above). Therefore, if the two systems being monitored have different outputs at any time, one must agree with the reference and the other must disagree. If the 'true' outputs of these systems are represented by A and B then the requirement for single failure (S) can be described by the Boolean equation

$$S = \bar{A}\,B + A\,\bar{B} \qquad (207)$$

In the case of double failure (D), the two systems must agree with each other and disagree with the reference (R). The equation for this condition is

$$D = A\,B\,\bar{R} + \bar{A}\,\bar{B}\,R \tag{208}$$

It follows that correct operation (C) means that the reference and both systems agree. This can be represented by

$$C = A\,B\,R + \bar{A}\,\bar{B}\,\bar{R} \tag{209}$$

The equations for S and D can be rewritten in the following manner

$$S = A\,\bar{B} + \bar{A}\,B$$

$$S = \overline{(A\,B + \bar{A}\,\bar{B})}$$

$$S = \overline{(A\,B)}\ \overline{(\bar{A}\,\bar{B})} = \left[\overline{\overline{(\bar{A} + \bar{B})} + \overline{(A + B)}}\right] \tag{210}$$

$$D = A\,B\,\bar{R} + \bar{A}\,\bar{B}\,R + (A\,B + \bar{A}\,\bar{B})\,(\bar{R}\,A + R\,\bar{A})$$

$$D = (A\,B + \bar{A}\,\bar{B})\,(R + A)\,(\bar{R} + A)$$

$$D = \left[\overline{(A\,B + \bar{A}\,\bar{B}) + \overline{(R + A)} + \overline{(\bar{R} + \bar{A})}}\right]$$

But $\overline{(A\,B + \bar{A}\,\bar{B})} = S$ (211)

Therefore,

$$D = \left[\overline{S + \overline{(A + R)} + \overline{(\bar{A} + \bar{R})}}\right] \tag{212}$$

Expressed in this form these equations describe the error sensing NOR circuit configuration of Figure 6.

In the error readout section (also shown in Figure 6) the output of T_2 will trip flip flop F_2 on receiving the first clock pulse during the time zone in which S is present. In a similar manner, T_1 will trip F_1 on receiving the first clock pulse occurring while D is present. The flip flop drives the appropriate error indicator when S or D have occurred.

The Monte Carlo techniques described in Section 4.1 are directly applicable at this point.

SECTION V

CONCLUSIONS AND RECOMMENDATIONS

This study report has developed mathematical simulation procedures to accomplish the following:

1. Provide the designer with a specified degree of confidence that his circuit will have a particular performance criteria.

2. Provides a means of readily evaluating the sensitivity of the circuit thereby indicating the major sources of variability.

3. Tolerances for part parameters or circuit elements can be realistically specified for the selection of parts.

4. The system is optimized for a given cost.

5. The development of transfer functions require that the definition of failure be precisely specified mathematically and thus the usual decisions as to the acceptability of a circuit performance criteria is eliminated .

6. The cost of the parts purchased can be reduced as the worst case design technique is no longer required and the parts do not have to be as precise.

7. The precision of this technique is limited only by the number of iterations performed; however, this is non-restrictive because of the availability of modern day computers.

8. The technique makes possible the planning of improved allocation of spare parts.

9. It is possible to improve maintainability techniques; i. e., the information will be available to allow the optimum determination of repair crews required to maintain the system.

10. It will provide a guide for the determination of trouble shooting techniques since the critical parts will be highlighted and the system degradation due to the failure of these parts will be known.

11. Based upon the underlying frequency distribution of the components, it is possible to determine the reliability of a system at zero time and at some time or times in the future.

Thus, it is concluded that in most cases Mathematical Simulation is the only feasible solution to the reliability prediction problem.

Recommendations for future work in these areas include:

1. A hardware program be continued to further validate the predictive techniques developed in this report.

2. Additional work be continued in developing the optimum distribution of parts and components for optimizing system reliability against given constraints.

3. Research be conducted into the further application of the technique in the area of automatic circuit design.

GLOSSARY

The set of definitions presented in the RADC Reliability Notebook, dated 30 October 1959 (see reference 94 in the Bibliography) is appropriate for use in understanding this report. If an alternative definition is needed for clarity, the list below may prove useful.

FREQUENCY - The ratio of the number of events which meet a performance requirement to the total number of events.

FIRST FAILURE TIME DISTRIBUTION - The distribution of all times to the first failure.

DENSITY FUNCTION - The first derivative of the distribution function.

PART - The smallest basic element of a complete system.

MODULE - (Normally used interchangeably with component.) A module is an article which is normally a combination of parts, subassemblies, or assemblies, and is a self-contained element of a complete operating equipment, and performs a function necessary to the operation of that equipment.

CUMULATIVE DISTRIBUTION FUNCTION - (See Appendix A)

SYSTEM PERFORMANCE CRITERIA - A system performance criterion is a rule that states within what limits a system performance measure must fall. A system performance measure may be of two types, a deterministic performance measure or a probabilistic performance measure. A deterministic performance measure is a measure that can be characterized by a single number.

Some examples of this type of measure are:

a. gain
b. bandwidth
c. signal to noise ratio
d. rise time
e. fall time
f. delay time

g. noise figure

h. input impedance

i. output impedance

A probabilistic performance measure is a measure that can be characterized by a cumulative distribution function which may take any of the following forms:

1. an equation
2. a graphical curve
3. an approximating polynomial

CRITERION* - A standard of judging, a rule or test by which anything is tried in forming a correct judgment respecting it.

SPECIFICATION* - Minute description of particulars or the particular details themselves, e.g., in the terms of a contract the details of construction etc. According to the glossary in the RADC Reliability Notebook, a detailed description of the characteristics of a product and of the criteria which must be used to determine whether the product is in conformity with the description.

NOMINAL VALUE - The stated value (e.g., by the manufacturer or designer) of some characteristic or measure of performance of a piece of equipment. Note: Due to internal and external stresses, it is seldom the case that the nominal value coincides with the actual measured value of a particular characteristic.

*Definition from Webster's New Collegiate Dictionary.

BIBLIOGRAPHY

(1) Matrix Analysis of Electric Networks by P. Le Corbeiller, Harvard University Press, 1950.

(2) A Treatise on Electricity and Magnetism by J. C. Maxwell, Oxford, ed 3, 1892.

(3) Mathematical Simulation for Reliability Prediction by I. Bosinoff, et al, Final Report, 30 October 1962 (153 p) illus, Report No. F491-1, Contract No. AF30(602)-2376. Unclassified Report.

(4) Modern Mathematics for the Engineer, E.F. Beckenbach, ed., McGraw Hill, 1956. See esp. Chapt. 12 for Monte Carlo methods.

(5) Modern Probability Theory and its Applications, E. Parzen, Wiley, 1960. see esp. pp 220-1 for table of probability laws from which random numbers may be generated.

(6) Biometrika Tables for Statisticians by E. S. Pearson and H. O. Hartley, Vol. I, Cambridge University Press, 1956.

(7) Pulse and Digital Circuits by J. Millman and H. Taub, McGraw Hill, 1956.

(8) Reliable Preferred Solid-State Functional Divisions, Technical Report, RADC-TR-59-243, 15 December 1959, Job 2131, KLX-10177, Contract No. AF30(602)-1906, prepared for Rome Air Development Center, Air Research and Development Command, U. S. A. F. This contains a list of conventional circuits.

(9) IBM Machine Analysis of Network of Its Applications by F. H. Branin, Jr., March 30, 1962, TR 00.855,

(10) A Computer Application to Reliable Circuits Design by L. Hellerman, 1 TR 00.786, Development Laboratory, Data Systems Division, IBM, New York.

(11) The Nature of the Monte Carlo Method by J. Neilson, Technical report 137, November 5, 1951, Croft Laboratory, Harvard University; Office of Naval Research, Contract N5 ORI-66 Task Order 1 NR - 678-011.

(12) Vacuum Tube Oscillators by Edson, W. A., John Wiley and Sons Inc., 1953.

(13) NPN Triple Diffused Silicon Mesa Transistors 2M/89, Pacific Semiconductors, Inc., Culver City, California.

(14) Fairchild NPN Diffused Silicon Transistors SL-5/3, May 1961, Fairchild Semiconductor Corporation, Mountain View, California.

(15) Control System Synthesis by J.G. Truxal, McGraw Hill, Page 35.

(16) Reference Data for Radio Engineers, I T and T Corporation, 4th Edition, c 1949, Page 1090.

(17) The Kolmogorov-Smirnov Test for Goodness of Fit, F.J. Massey, Journal of the American Statistical Association No. 46 Pages 68-78, c 1951.

(18) Numerical Tabulation of the Distribution of Kolmogorov's Statistic for Finite Sample Size, Z. W. Birnbaum, Journal of the American Statistical Association, No. 47, Pages 425-451, c 1952.

(19) Advance in Reliability Prediction by I. Bosinoff, R. Jacobs and J. Herman, 1962 National Space and Telemetry Conference, Miami, Fla., October 2-4, 1962.

(20) Physics of Failure in Electronics, Rome Air Development Center and Armour Research Foundation, September 26-27, 1962.

(21) Wave Generation and Shaping, by L. Strauss, McGraw Hill - 1960- Page 258.

(22) Linear Signal-Flow Graphs and Application, by C. Chow, John Wiley and Sons, Inc., New York 1962.

(23) Signal Flow Graphs, by R.F. Haskins, M. Sc., Electronic and Radio Engineers, August 1959.

(24) Stabilization of Pulse Direction in Monostable Multivibrator by A. Luther, Jr. R.C.A. Review, 1955.

(25) An Analysis of the Modes of Operation of a Simple Transistor Oscillator by J.F. Gibbons, Tech report 1713-1, Proceedings of the I.R.E., Vol. 49, No. 9, pp. 1383-1390, Sept. 1961.

(26) Logical Design of Digital Computers, M. Phister, John Wiley and Sons, 1958.

(27) Design of Transistorized Circuits for Digital Computers, A.I. Pressman, John F. Rider, Publisher, Inc. 1959.

APPENDIX I

DEFINITION OF CUMULATIVE DISTRIBUTION FUNCTION

The function $F(x)$ is called the cumulative distribution function (cdf) of the random variable X if and only if $F(x)$ has the following properties:

(1) $F(x)$ lies between 0 and 1 for all values of x.

(2) $F(x)$ decreases to zero as x decreases to $-\infty$.

(3) $F(x)$ increases to 1 as the upper bound b of the interval in which x is supposed to lie increases to $+\infty$. (The probability of a value less than $+\infty$ is 1.)

(4) $F(x)$ is an increasing function in the sense that if a b, where a is the lower bound of the interval, then $F(a) \leq F(b)$. (The probability that a random value X is smaller than a is less than the probability that a random value X is smaller than the larger number b.)

(5) $F(x)$ is always continuous on the left; i.e., $F(a)$ increases to $F(b)$ as a increases to b.

Conversely, any real function $F(x)$ with the above properties defines a cumulative distribution function for a random variable X, that is

$$F(x) = Pr(X \leq x)$$

An intuitive grasp of a cumulative distribution function may be obtained from the following illustration. Suppose a thousand resistors have been made and are tested to find the exact resistance of each one. If the thousand values resulting from the test are ordered according to magnitude, starting with the smallest and ending with the largest, a graph is obtained as shown below in Figure I-1.

Here the ordinate represents the number of resistors having a value less than or equal to that shown on the horizontal scale. Depending on the scale, the ordinate is sometimes called the probability (0 to 1) or relative frequency (0 to 1) or percentage (0 to 100), but in any case, it represents the value of the cumulative distribution function $F(x)$.

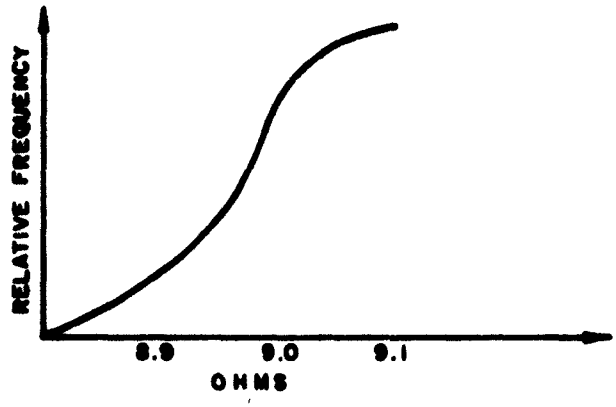

Figure I-1

The derivative of the cumulative distribution function $F(x)$ is called the density function (d.f.) $f(x)$. Since the c.d.f. is scaled to go from 0 to 1, it must be the case that the area under the d.f. is exactly equal to 1.

The items discussed above can be extended to two or more dimensions. When a process simultaneously produces two (or more) numbers at random at each trial, the collection of pairs of random numbers (X_1, X_2) can be considered. If the probability is known, with which a pair of random numbers (X_1, X_2) lie in the quadrant given by the two inequalities $X_1 \leq x_1$ and $X_2 \leq x_2$, the joint cumulative distribution function can be defined by

$$F(x_1, x_2) = \Pr \{X_1 \leq x_1 \text{ and } X_2 \leq x_2\}$$

APPENDIX II

DISCUSSION OF RELIABILITY MEASURES AS BASED ON THE CUMULATIVE DISTRIBUTION FUNCTION

The definition of reliability that has received wide acceptance in the literature is:

> The probability of performing a specified function without failure under given conditions for a specified period of time.

This can be expressed mathematically as:

$$\text{Reliability} = R(t) = e^{-\lambda t} \qquad \text{(II-1)}$$

where λ = failure rate i.e., reciprocal of mean time between failures

t = duration of mission or task

This definition of Reliability defines R as a probability which is a function of time (t) and of internal and external conditions, since λ depends on the environment as well as on internal stresses.

In this equation, the expression $e^{-\lambda t}$ gives one type of probability function which can be used as a measure of the reliability.

There may be other types of probability functions which may be used as reliability measures in addition to the type of probability function described above.

The following analysis shows how the formulation of reliability in (II-1) is related to the "Monte Carlo" procedures described in Section II. This analysis will deal first with a system having only one type of unit. To express the above reliability measure R(t) in terms of a cumulative distribution function $F_n(t)$ measuring the probability of failure let:

$$F_n(t) = 1 - R_n(t_1 = 1 - e^{-\lambda n t}) \qquad \text{(II-2)}$$

so that

$$F_n(t) + R_n(t) = 1 \qquad \text{(II-3)}$$

where $n = 1, 2 \ldots \infty$

As t approaches ∞, F_n approaches the steady state distribution function.

F_n is the particular cumulative distribution function which describes the distribution of the various intervals of time between the n^{th} and $(n+1)^{th}$ failure.

Let the cumulative distribution function of a circuit performance measure at t = 0 appear as shown in Figure II-1.

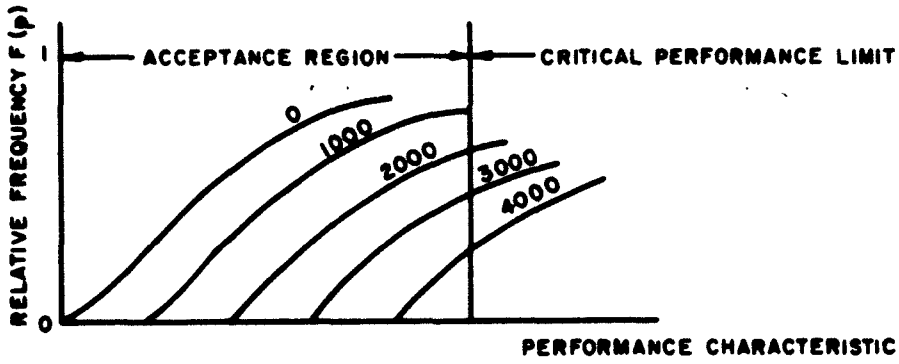

Figure II-1

Note that in Figure II-1 each of the cumulative distribution functions represents the same set of systems. A circuit is considered to have failed whenever the performance measure falls outside the preassigned limit of satisfactory operation. Therefore, any circuit or system whose performance measure falls to the right of the critical performance limit has failed (as shown by vertical line in Figure II-1). From Figure II-1 it is possible to construct Figure II-2 by noting the times at which failure occurs. These are found at the intersections critical performance limit with the time dependent cumulative distribution functions. The time-to-first-failure distribution $F_1(t)$ is defined as $1 - R_1(t)$. This is shown in Figure II-3. It is important to note here that in many instances $R_1(t)$ may <u>not</u> be in exponential form, since it is a direct function of the particular family of cumulative distribution functions curves shown in Figure II-1.

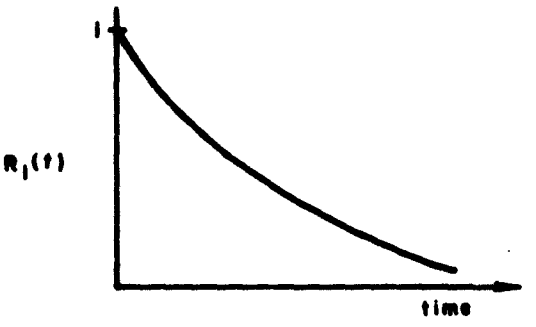

Figure II-2

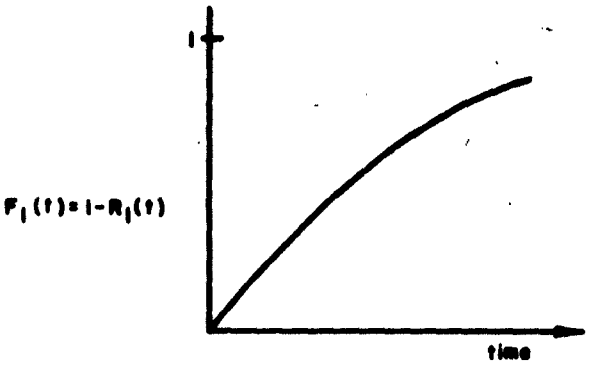

Figure II-3

The fact that one may either repair or replace units which have failed will influence the development of the mathematical models used to describe the reliability measures of the system. Furthermore, in the case of repair there will be one type of model, while in the case of replacement another type of model will be necessary.

In the case of repair, the simulated change in performance criteria is represented as shown in Figure II-4. To determine the distribution of times to first failure (i.e., F_1) and the distribution of times between the consecutive failures n and n+1 (i.e., F_n) a critical performance limit is defined (horizontal line in Figure II-4. The time to first failure is that time at which the curve describing the performance measures in time first crosses the line representing the critical performance limit.

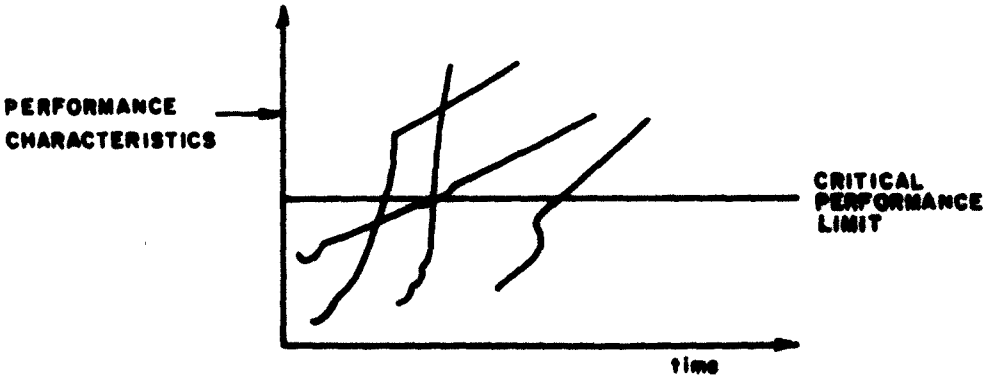

Figure II-4

If these times to first failure are ordered according to magnitude, they yield the cumulative distribution function shown in Figure II-5.

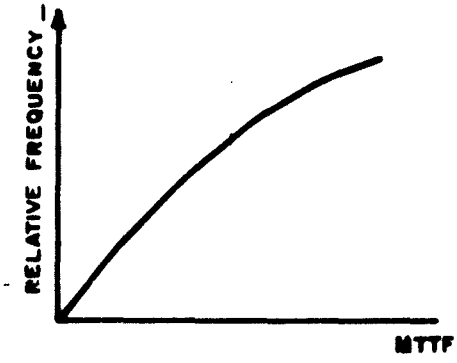

Figure II-5

Figure II-4 shows how several parts come to the time-of-first failure. Figure II-6 takes one of these parts and shows the performance of the part passing the critical performance limit at t_1 (time-to-first-failure), being repaired, rising in performance again until it passes the critical performance limit at t_2 (time-to-second-failure), and so on. Figure II-7 does this for another part. If a whole series of such graphs are imagined for each part, then a cumulative distribution function may be found for each Δt_i $[(\Delta t_i = t_i - (t_i - 1))]$ i.e., each incremental time between failures. This gives F_i (the cumulative distribution function for time from the $(i - 1)^{th}$ to the i - th failure for the type of part being tested on the basis of the performance of a large number of actual tested samples. Notice that the time required to repair a part is taken as zero on the graphs. Although this is rare in practice, this time for repair does not influence the distributions in question.

Interfailure Time Distribution with Monitoring Replacement Policy

In the case where the system is monitored and failed parts are replaced, a second mathematical model is necessary. In Figure II-8 the solid curves represent the cumulative distribution function of the original population of parts, which were subject only to degradation in time and no monitoring. If the defective parts

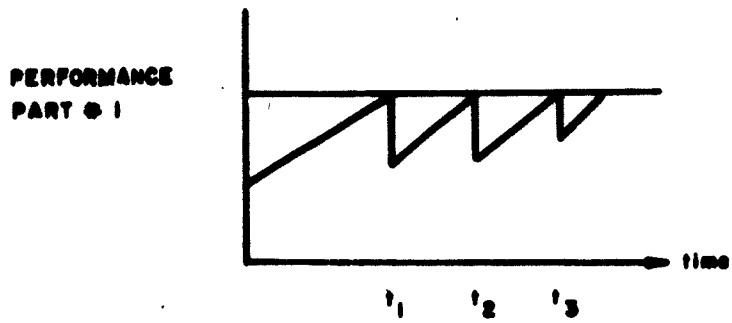

Figure II-6

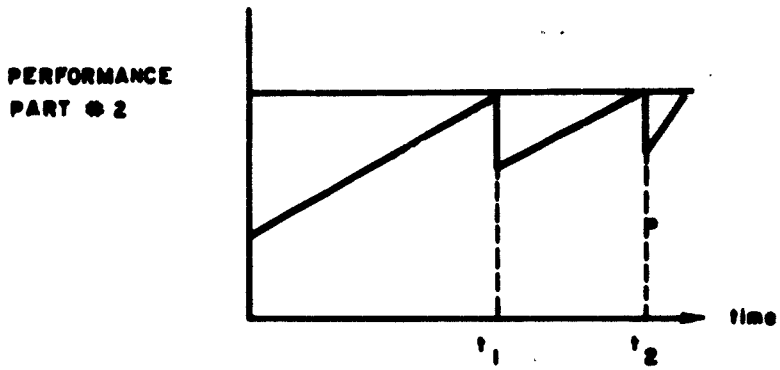

Figure II-7

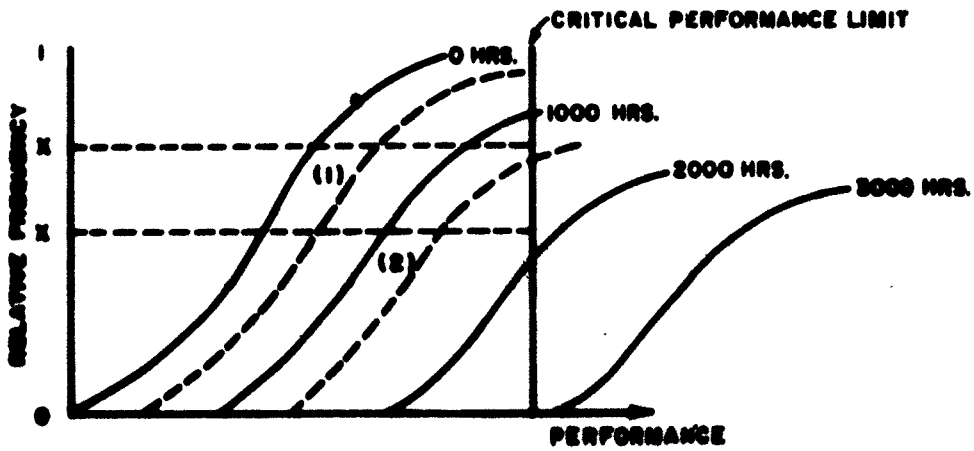

Figure II-8

are replaced at intervals when the cumulative distribution function will be described by the dotted curves, i.e., (1 - X) of the units have failed at time $t = t_n$.

(1 - X) of the units have failed at t=1000 hours; these occur because a critical performance limit is exceeded. The replacement of (1 - X) of the units taken from the population represented by the cumulative distributive function will result in the cumulative distribution function represented by the dashed curve (1) at t = 0. This replacement would, at t = 2000 hours, cause this curve to shift and be represented by the dashed curve (2). This curve would be composed of (1 - X) of the samples from the distribution at t = 1000 and X_1 of the samples from the distribution at 2000 hours. The net result would be that the reliability of the samples of the curve (2) would be increased. The increase in reliability for any point on the curve would be a maximum of (1 - X). This procedure may be repeated indefinitely as time increases.

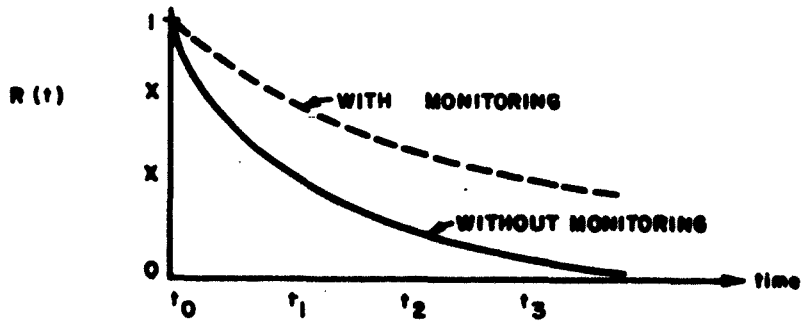

Figure II-9

Figure II-9 represents a plot of the Reliability as a function of time with and without monitoring. Figure II-10 is the corresponding plot of the failure rates.

Figures II-8, II-9, II-10 are related to each other in the same way as Figures II-1, II-2, II-3.

System with Two Types of Units

To obtain the over-all system reliability for a system with two types of units, it is sufficient to multiply the two reliabilities.

Over-all system failure occurs if any one of the two units fails. Upon failure, it is assumed that the failed unit will be restored to an operable condition. For simplicity it is further assumed that the failed unit is replaced by a new unit. To satisfy the relibility requirement, the set of distribution functions of time-to-first-failure and time-between-failures must be found. For example, if an 80% confidence limit is specified, then the lower 20% points of all failure time distributions must exceed the required value. (See Figure II-11.)

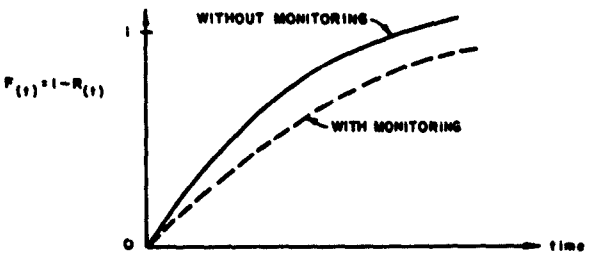

Figure II-10

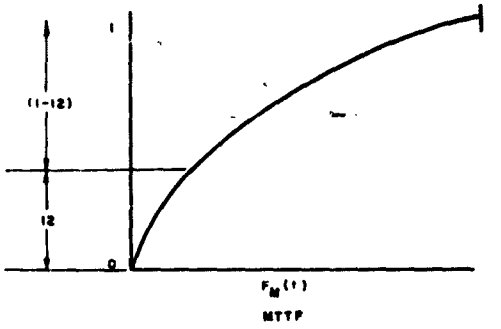

Figure II-11

To illustrate we will consider a two-unit system with given failure time distributions $F_1(t)$ and $F_2(t)$. See Figure II-12.

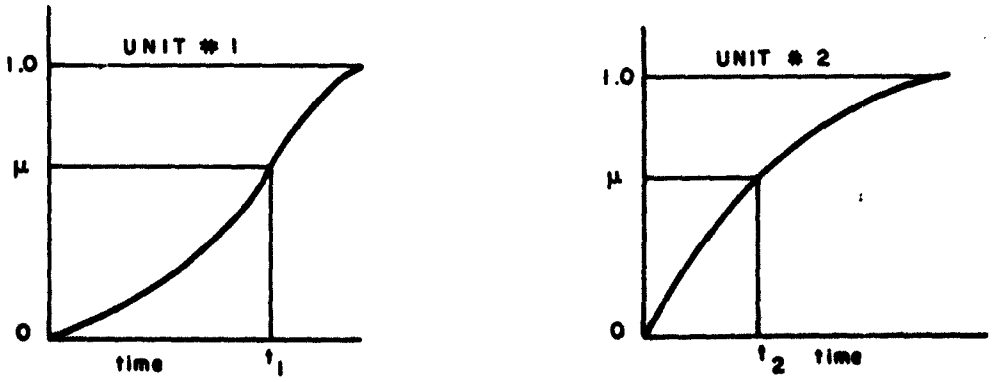

Figure II-12

To generate a sample of time-to-failure, one selects a sample value (μ) from a uniform distribution betweeon (0, 1) and determines the appropriate failure times t_1 and t_2 as shown above. System time-to-first-failure is the smaller of the two values t_1, t_2. For this example $t_2 < t_1$. At this time the second unit is replaced by a new unit. The failure distribution curve for Unit #2 is now displaced by an amount t_2, as shown in Figure II-13.

$$F_1^*(t) = \frac{F_1(t) - F_1(t_2)}{1 - F_1(t_2)} \qquad t \geq t_2$$

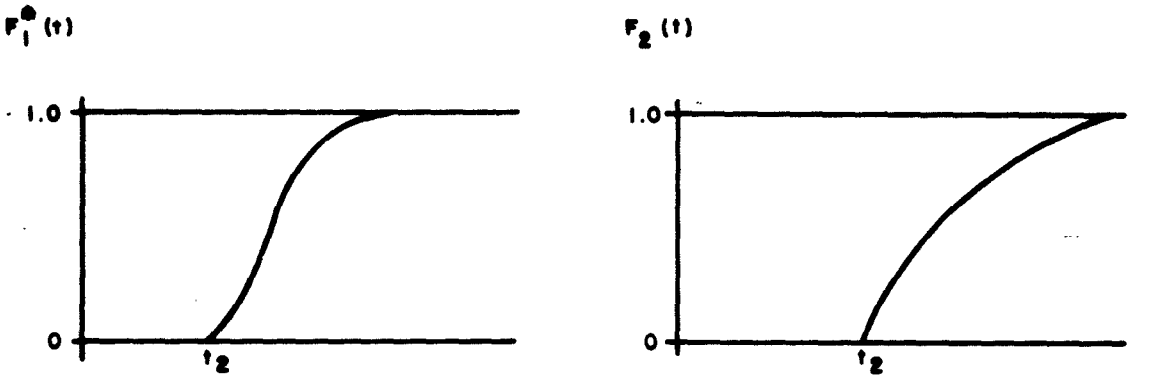

Figure II-13

The failure time distribution for Unit #1 is the conditional probability that the unit has not failed in $(0, t_2)$ and fails at t where $t < t_2$. This conditional distribution $F_1^*(t)$ is given by:

$$F_1^*(t) = \frac{F_1(t) - F_1(t_2)}{1 - F_1(t_2)} \qquad t \geq t_2$$

To obtain the time-to-second failure, we again select a deviate from a uniform distribution and proceed as above, thus obtaining a set of time-to-second-failure. The smaller of the two is the time-to-second-failure of the system. Proceeding in a similar manner times-to-third, -fourth, -fifth failures, etc., are obtained, and, accordingly, the times-between-failures. This process is repeated until a sufficient number of times to first failure, times to second, etc. are obtained. Thus, the empiric time-between-failure distributions can be determined to any desired degree of confidence. To meet the requirements, the lower 20% value of all mean-time-between-failures must exceed that value specified.

APPENDIX III

PROBABLE ERROR IN STATISTICAL SOLUTION OF AREA INTEGRAL

III. 1 MONTE CARLO MODEL FOR DETERMINING AREA

This appendix will determine the probable error resulting from a given number (n) of replications when Monte Carlo is used to ascertain an area. Figure III-1 illustrates the area (shaded) to be determined by Monte Carlo techniques.

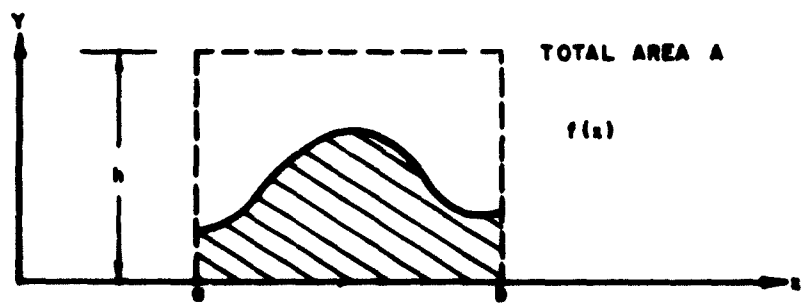

Figure III-1

Let B be the area under f(x) between the limits a and b , thus:

$$B = \int_a^b f(x)\,dx \qquad \text{(III-1)}$$

The area A under the rectangle is given by:

$$A = (b - a)\,h \qquad \text{(III-2)}$$

To determine the area under f(x) using Monte Carlo, one proceeds as follows:

From a uniform distribution select a value X_1 on the interval from a to b. In a similar manner pick Y_1 from the uniform distribution on the interval from 0 to h. These two values define a point P_1 with coordinates $P_1=(X_1, Y_1)$. This process is continued n times until one obtains $P_N = (X_N, Y_N)$. The limit of the ratio of the number n_B of points falling in B to the total number of points (n_t) defines the percentage probability as $n_t \to \infty$ or:

$$P = \lim_{n_t \to \infty} \frac{n_B}{n_t} \qquad \text{(III-3)}$$

To obtain the area B, one simply takes the product PA. If the number of points is infinite PA = B, the exact area f(x). However, since n_t is finite, a certain error is introduced. To find this probable error as a function of n, one proceeds as follows.

Define:

P = probability of falling in B

1 - P = probability of <u>not</u> falling in B

The probability of obtaining r successes in n tries can be obtained from the binomial distribution:

$$P(n, r) = C_r^N P^r (1 - P)^{n-r} \qquad \text{(III-4)}$$

The average number of successes, $\bar{r}$, is given by:

$$\bar{r} = \frac{N}{P} \qquad \text{(III-5)}$$

or

$$P = \frac{\bar{r}}{n}$$

For the binomial distribution the standard deviation σ is defined by

$$\sigma = \sqrt{nP(1 - P)} \qquad \text{(III-7)}$$

It follows that one standard deviation in $\frac{P(n, r)}{n}$ is:

$$\sigma' = \frac{\sigma}{n} = \frac{\sqrt{n(P)(1 - P)}}{n} = \sqrt{\frac{P(1 - P)}{n}} \qquad \text{(III-8)}$$

and the probable error (percent) in $P(n, r)$ is

$$\text{P. E. (\%)} = \frac{67.45\,\sigma'}{\bar{r}/n} = \frac{67.45\sqrt{\frac{P(1 - P)}{n}}}{\bar{r}/n}$$

$$= 67.45\sqrt{\frac{1 - P}{nP}} \qquad \text{(III-9)}$$

As seen from equation (III-9) the larger P and n, the smaller the probable error. Therefore, the size of the enclosing reference area should be kept as small as possible.

APPENDIX IV

DERIVATION OF THE FREQUENCY FUNCTION OF A FUNCTION OF TWO INDEPENDENT RANDOM VARIABLES

IV. 1 INTRODUCTION

This appendix considers the mathematics of a problem which arises in reliability theory, viz., the determination of the distribution of the parameters of a system given the distributions of the parameters of the components that make up the system. That is, it is the problem of determining the distribution of a function of several random variables of known distributions.

IV. 2 DERIVATIONS

Given the two random variables x and y, their joint frequency function, $p_{x,y}(\xi\,\eta)$*, and some function relating a variable z and the two variables x and y, viz.,

$$z = f(x, y) \tag{IV-1}$$

then z will also be a random variable whose distribution is determined by the distribution of x and y. We will develop methods for determining the frequency function of the distribution of z.

The distribution function of z, $F_z(\zeta)$, will simply be the integral of $p_{x,y}(\xi\,\eta)$ over that region of the ξ-η plane for which

$$f(\xi, \eta) \leq \zeta \tag{IV-2}$$

That is,

$$F_z(\zeta) = \int_{f(\xi,\eta)\leq\zeta} p_{x,y}(\xi,\eta)\, dr\, d\xi \tag{IV-3}$$

and the frequency function of z, $p_z(\zeta)$, will be the derivative of $F_z(\zeta)$ with respect to ζ; i.e.,

*Subscripts are used throughout this memorandum to identify functions; the subscripts are not to be regarded as variables.

$$p_z(\zeta) = \frac{d}{d\zeta} F_z(\zeta) = \frac{\partial}{\partial \zeta} \int_{f(\xi,\eta)\leq\zeta} p_{x,y}(\xi,\eta)\, d\eta\, d\xi \qquad \text{(IV-4)}$$

We will assume that equation (IV-1) and the Inequality (IV-2) may be solved explicitly for y and η respectively, and that the solution of equation (IV-1) for y is single-valued and differentiable; thus

$$\left.\begin{aligned} f(x,y) &= z \qquad \text{(a)} \\ f_y^{-1}(x,z) &= y \qquad \text{(b)}^* \end{aligned}\right\} \qquad \text{(IV-5)}$$

and

$$\left.\begin{aligned} &f(\xi,\eta) \leq \zeta \qquad \text{(a)} \\ \text{when} \quad &f_y^{-1}(\xi,\zeta) \gtrless \eta \qquad \text{(b)} \end{aligned}\right\} \qquad \text{(IV-6)}$$

The inequality (IV-6b), corresponding to the inequality (IV-6a), may have either sense, as noted, or it may have different senses in different regions of x.

Then Equation (IV-3) may be written:

1. If $\eta \leq f_y^{-1}(\xi,\zeta)$ when $f(\xi,\eta) \leq \zeta$

$$F_z(\zeta) = \int_{-\infty}^{+\infty} \int_{-\infty}^{f_y^{-1}(\xi,\zeta)} p_{x,y}(\xi,\eta)\, d\eta\, d\xi \qquad \text{(IV-7)}$$

2. If $\eta \geq f_y^{-1}(\xi,\zeta)$ when $f(\xi,\eta) \leq \zeta$

$$F_z(\zeta) = \int_{-\infty}^{\infty} \int_{f_y^{-1}(\xi,\zeta)}^{\infty} p_{x,y}(\xi,\eta)\, d\eta\, d\xi \qquad \text{(IV-8)}$$

*The notation f_y^{-1} is the inversion of f(x, y) with respect to y; it should not be confused with a partial derivative with respect to y.

If x and y are statistically independent, which will be assumed throughout the balance of this appendix, the joint frequency function of x and y will be simply the product of the frequency functions of x and y:

$$p_{x,y}(\xi,\eta) = p_x(\xi)\, p_y(\eta) \tag{IV-9}$$

Throughout the balance of this memorandum the following assumptions (some of which are implicit in the preceding) will be made:

1. $p_x(\xi)$ and $p_y(\eta)$ are continuous.

2. The function, $f(x, y)$, and its inversion with respect to y, $f_y^{-1}(x, z)$, are continuous, single-valued, and differentiable.

3. x and y are statistically independent.

4. x, y, and z are real.

When x and y are statistically independent, equations (IV-7) and (IV-8) reduce to

1. When $\eta \leq f_y^{-1}(\xi, \zeta)$ when $f(\xi, \eta) \leq \zeta$

$$F_z(\zeta) = \int_{-\infty}^{+\infty} p_x(\xi) \int_{-\infty}^{f_y^{-1}(\xi,\zeta)} p_y(\eta)\, d\eta\, d\xi \tag{IV-10}$$

$$= \int_{-\infty}^{+\infty} p_x(\xi)\, F_y\left[f_y^{-1}(\xi, \zeta)\right] d\xi \tag{IV-11}$$

2. When $\eta \geq f_y^{-1}(\xi, \zeta)$ when $f(\xi, \eta) \leq \zeta$

$$F_z(\zeta) = \int_{-\infty}^{+\infty} p_x(\xi) \int_{f_y^{-1}(\xi,\zeta)}^{+\infty} p_y(\eta)\, d\eta\, d\xi \tag{IV-12}$$

but for general forms of the frequency functions, $p_x(\xi)$ and $p_y(\eta)$.

1. If
$$z = x + y \tag{IV-20}$$
$$\therefore y = z - x \tag{IV-21}$$
Then $z \leq \zeta$
when $y \leq \zeta - x$ (IV-22)

Therefore
$$p_z(\zeta) = \int_{-\infty}^{+\infty} p_x(\xi)\ p_y(\zeta - \xi)\ \frac{\partial(\zeta - \xi)}{\partial \zeta}\ d\xi \tag{IV-23}$$

which is the familiar convolution integral
$$R_z(\zeta) = \int_{-\infty}^{+\infty} p_x(\tau)\ p_y(\zeta - \tau)\ d\tau \tag{IV-24}$$

2. If
$$z = x \cdot y \tag{IV-25}$$
$$y = \frac{z}{x} \tag{IV-26}$$
Then $z \leq \zeta$
when $y \leq \zeta/x$ $\quad x > 0$
$y \geq \zeta/x$ $\quad x < 0$ (IV-27)

Therefore
$$p_z(\zeta) = -\int_{-\infty}^{0} p_x(\xi)\, p_y\left(\frac{\zeta}{\xi}\right)\ \frac{\partial}{\partial \zeta}\ \frac{\zeta}{\xi}\ d\xi + \int_{0}^{+\infty} p_x(\xi)\, p_y\left(\frac{\zeta}{\xi}\right)\ \frac{\partial}{\partial \zeta}\ \frac{\zeta}{\xi}\ d\xi \tag{IV-28}$$

$$= \int_{-\infty}^{+\infty} p_x(\xi) \{1 - F_y[f_y^{-1}(\xi, \zeta)]\} \, d\xi \qquad \text{(IV-13)}$$

$$= 1 - \int_{-\infty}^{+\infty} p_x(\xi) F_y[f_y^{-1}(\xi, \zeta)] \, d\xi \qquad \text{(IV-14)}$$

Equation (IV-4) for the frequency function of $z, p_z(\zeta)$, becomes, for the two cases:

1. When $\eta \leq f_y^{-1}(\xi, \zeta)$ when $f(\xi, \eta) \leq \zeta$

$$p_z(\zeta) = \frac{\partial}{\partial \zeta} \int_{-\infty}^{+\infty} p_x(\xi) \int_{-\infty}^{f_y^{-1}(\xi, \zeta)} p_y(\eta) \, d\eta \, d\xi \qquad \text{(IV-15)}$$

$$= \int_{-\infty}^{+\infty} p_x(\xi) \, p_y[f_y^{-1}(\xi, \zeta)] \frac{\partial f_y^{-1}(\xi, \zeta)}{\partial \zeta} \, d\xi \qquad \text{(IV-16)}$$

2. When $\eta \geq f_y^{-1}(\xi, \zeta)$ when $f(\xi, \eta) \leq \zeta$

$$p_z(\zeta) = \frac{\partial}{\partial \zeta} \int_{-\infty}^{+\infty} p_x(\xi) \int_{f_y^{-1}(\xi, \zeta)}^{+\infty} p_y(\eta) \, d\eta \, d\xi \qquad \text{(IV-17)}$$

$$= \int_{-\infty}^{+\infty} p_x(\xi) \, p_y[f_y^{-1}(\xi, \zeta)] \frac{\partial f_y^{-1}(\xi, \zeta)}{\partial \zeta} \, d\xi \qquad \text{(IV-18)}$$

We will now consider a number of specific cases, that is, a number of specific forms of the function

$$z = f(x, y) \qquad \text{(IV-19)}$$

$$= \int_{-\infty}^{0} p_x(\xi)\, p_y\left(\frac{\zeta}{\xi}\right)\frac{d\xi}{-\xi} + \int_{0}^{+\infty} p_x(\xi)\, p_y\left(\frac{\zeta}{\xi}\right)\frac{d\xi}{\xi} \qquad \text{(IV-29)}$$

which reduces to the following form, which has been called the logarithmic convolution:

$$p_z(\zeta) = \int_{-\infty}^{\infty} p_x(\tau)\; p_y\left(\frac{\zeta}{\tau}\right)\frac{d\tau}{|\tau|} \qquad \text{(IV-30)}$$

3. If

$$z = \frac{y}{x} \qquad \text{(IV-31)}$$

$$y = zx \qquad \text{(IV-32)}$$

Then $z \leq \zeta$

when

$$\left.\begin{aligned} y &\leq \zeta x \qquad x > 0 \\ y &\geq \zeta x \qquad x < 0 \end{aligned}\right\} \qquad \text{(IV-33)}$$

Therefore

$$p_z(\zeta) = -\int_{-\infty}^{0} p_x(\xi)\, p_y(\zeta\,\xi)\frac{\partial}{\partial\zeta}(\zeta\,\xi)\, d\xi + \int_{0}^{+\infty} p_x(\xi)\, p_y(\zeta\,\xi)\frac{\partial}{\partial\zeta}(\zeta\,\xi)\, d\xi \qquad \text{(IV-34)}$$

$$= \int_{-\infty}^{0} p_x(\xi)\, p_y(\zeta\,\xi)(-\xi)\, d\xi + \int_{0}^{\infty} p_x(\xi)\, p_y(\zeta\xi)\xi\, d\xi \qquad \text{(IV-35)}$$

$$\therefore p_z(\zeta) = \int_{-\infty}^{\infty} p_x(\tau)\, p_y(\zeta\tau)\, |\tau|\, d\tau \qquad \text{(IV-36)}$$

4. If $$z = e^{x+y} \tag{IV-37}$$

(Obviously, $z \geq 0$ if x and y are real; the latter assumption is made throughout this memorandum.)

$$\therefore \ln x = x + y \tag{IV-38}$$

$$y = \ln z - x \tag{IV-39}$$

Then

$$\left.\begin{aligned} z &\leq \zeta \\ \text{when} \quad y &\leq \ln\zeta - x \end{aligned}\right\} \tag{IV-40}$$

Therefore, when $z \geq 0$

$$p_z(\zeta) = \int_{-\infty}^{\infty} p_x(\xi)\, p_y(\ln\zeta - \xi)\, \frac{\partial}{\partial\zeta}(\ln\zeta - \xi)\, d\xi \tag{IV-41}$$

$$= \frac{1}{\zeta} \int_{-\infty}^{\infty} p_x(\xi)\, p_y(\ln\zeta - \xi)\, d\xi \tag{IV-42}$$

$$\therefore p_z(\zeta) = \left.\begin{aligned} &0 && \zeta < 0 \\ &\frac{1}{\zeta}\,[p_x * p_y]\,(\ln\zeta) && \zeta \geq 0 \end{aligned}\right\} \tag{IV-43}$$

where, in Equation (IV-43), the usual notation for the simple convolution of the frequency functions p_x and p_y is used.

5. If $$z = x^y \qquad x \geq 0$$

(Obviously, $z \geq 0$ if x and y are real.)

$$\ln z = y \ln x \tag{IV-45}$$

$$y = \frac{\ln z}{\ln x} \tag{IV-46}$$

Then $z \leq \zeta$

when
$$\left.\begin{array}{ll} y \leq \dfrac{\ln \zeta}{\ln x} & x > 1 \\ y \geq \dfrac{\ln \zeta}{\ln x} & 0 \leq x < 1 \end{array}\right\} \qquad \text{(IV-47)}$$

Therefore, when $\zeta \geq 0$

$$p_z(\zeta) = -\int_0^1 p_x(\xi)\, p_y\left(\frac{\ln \zeta}{\ln \xi}\right) \frac{\partial}{\partial \zeta}\left(\frac{\ln \zeta}{\ln \xi}\right) d\xi + \int_1^\infty p_x(\xi)\, p_y\left(\frac{\ln \zeta}{\ln \xi}\right) \frac{\partial}{\partial \zeta}\left(\frac{\ln \zeta}{\ln \xi}\right) d\xi \qquad \text{(IV-48)}$$

$$= \frac{1}{\zeta}\int_0^1 p_x(\xi)\, p_y\left(\frac{\ln \zeta}{\ln \xi}\right) \frac{d\xi}{-\ln \xi} + \frac{1}{\zeta}\int_1^\infty p_x(\xi)\, p_y\left(\frac{\ln \zeta}{\ln \xi}\right) \frac{d\xi}{\ln \xi} \qquad \text{(IV-49)}$$

$$p_z(\zeta) = \left\{\begin{array}{ll} 0 & \zeta < 0 \\ \dfrac{1}{\zeta}\displaystyle\int_0^\infty p_x(\tau)\, p_y\left(\frac{\ln \zeta}{\ln \tau}\right) \frac{d\tau}{|\ln \tau|} & \zeta \geq 0 \end{array}\right\} \qquad \text{(IV-50)}$$

We may formalize several generalities which are suggested by the preceding:

1. Heuristically we may condense the two cases represented by equations (IV-16) and (IV-18) to a single equation:

$$p_z(\zeta) = \int_{-\infty}^{\infty} p_x(\tau)\, p_y[f_y^{-1}(\tau, \zeta)] \left|\frac{\partial f_y^{-1}(\tau, \zeta)}{\partial \zeta}\right| d\tau \qquad \text{(IV-51)}$$

Equation (IV-51) may be regarded as the generalized convolution of p_x and p_y with respect to the function f; this operation we will denote by the operator $*_f$. This convolution of p_x and p_y then becomes an operator on ζ, and equation (IV-51) may be written, in operational form:

$$p_z(\zeta) = [p_x *_f p_y](\zeta) \qquad \text{(IV-52)}$$

2. Consider a functional relation between x, y, and z of the form

$$z = h[f(x, y)] \qquad \text{(IV-53)}$$

where x and y are random variables with frequency functions p_x and p_y. We may define another random variable, w :

$$w = f(x, y) \qquad \text{(IV-54)}$$

whose frequency function, $p_w(\omega)$, will be

$$p_w(\omega) = [p_x *_f p_y](\omega) \qquad \text{(IV-55)}$$

Now

$$z = h(w) \qquad \text{(IV-56)}$$

which, we will assume, may be solved for w :

$$w = h^{-1}(z) \qquad \text{(IV-57}$$

where $h^{-1}(z)$ is a single-valued function of z .

The frequency function of z in terms of p_w will then be

$$p_z(\zeta) = p_w[h^{-1}(\zeta)] \frac{dh^{-1}(\zeta)}{d\zeta} \qquad \text{(IV-58)}$$

Therefore

$$p_z(\zeta) = \frac{dh^{-1}(\zeta)}{d\zeta} [p_x *_f p_y] [h^{-1}(\zeta)] \qquad \text{(IV-59)}$$

Example 4 above is of this type (see equation (IV-48)).

3. Consider a functional relation between x, y, and z of the form

$$z = f[g(x), h(y)] \qquad \text{(IV-60)}$$

where, again, x and y are random variables with the frequency functions p_x and p_y. Define the two new random variables:

$$\left.\begin{aligned} u &= g(x) \\ v &= h(y) \end{aligned}\right\} \qquad \text{(IV-61)}$$

and assume that equations (IV-61) can be inverted to give the single-valued functions of u and v :

$$\begin{aligned} x &= g^{-1}(u) \\ y &= h^{-1}(v) \end{aligned} \qquad \text{(IV-62)}$$

Then the frequency functions of u and v will be

$$\left.\begin{aligned} p_u(u) &= p_x[g^{-1}(u)] \frac{dg^{-1}(u)}{du} \\ p_v(v) &= p_y[h^{-1}(v)] \frac{dh^{-1}(v)}{dv} \end{aligned}\right\} \qquad \text{(IV-63)}$$

Substituting equations (IV-61) into equation (IV-60) gives

$$z = f(u, v) \qquad \text{(IV-64)}$$

and, therefore, the frequency function of z in terms of p_u and p_v is

$$p_z(\zeta) = [p_u *_f p_v](\zeta) \tag{IV-65}$$

where p_u and p_v are given by equation (IV-63). Equation (IV-65) may thus be written

$$p_z(\zeta) = \{[(g^{-1})' X\, p_x(g^{-1})] *_f [(h^{-1})' X\, p_y(h^{-1})]\}(\zeta) \tag{IV-66}$$

where:

$$\left.\begin{aligned} (g^{-1})'(\tau) &\equiv \frac{d}{d\tau}[g^{-1}(\tau)] \\ (h^{-1})'(\tau) &\equiv \frac{d}{d\tau}[h^{-1}(\tau)] \end{aligned}\right\} \tag{IV-67}$$

The operator $*_f$ defines the variables on which these operators operate. Refer to equations (IV-88) and (IV-89) with regard to the symbol X.

4. The same process may be iterated for certain types of functions of more than two variables. For example, let x, y, and w be random variables with frequency functions p_x, p_y, p_w, and let z be defined as

$$z = f[g(x, y), w] \tag{IV-68}$$

If we let

$$u = g(x, y) \tag{IV-69}$$

u will be a random variable with frequency function

$$p_u(\upsilon) = [p_x *_f p_y](\upsilon) \tag{IV-70}$$

From equations (IV-68) and (IV-70)

$$z = f(u, w) \tag{IV-71}$$

so that

$$p_z(\zeta) = [\, p_u *_f p_w \,](\zeta) \qquad \text{(IV-72)}$$

Therefore

$$p_z(\zeta) = \{[\, p_x *_g p_y \,] *_f p_w \}(\zeta) \qquad \text{(IV-73)}$$

5. Again, let x, y, u, and v be random variables with frequency functions p_x, p_y, p_u, p_v, and let

$$z = f[\, g(x, y),\ h(u, v) \,] \qquad \text{(IV-74)}$$

If we let

$$\left.\begin{aligned} s &= g(x, y) \\ t &= h(u, v) \end{aligned}\right\} \qquad \text{(IV-75)}$$

then s and t are random variables with frequency functions

$$\left.\begin{aligned} p_s(\sigma) &= [\, p_x *_g p_y \,](\sigma) \\ p_t(\tau) &= [\, p_u *_h p_v \,](\tau) \end{aligned}\right\} \qquad \text{(IV-76)}$$

z is a function of s and t:

$$z = f(s, t) \qquad \text{(IV-77)}$$

and is a random variable with the frequency function

$$p_z(\zeta) = [\, p_s *_f p_t \,](\zeta) \qquad \text{(IV-78)}$$

Therefore

$$p_z(\zeta) = \{\, [\, p_x *_g p_y \,] *_f [\, p_y *_h p_v \,] \}(\zeta) \qquad \text{(IV-79)}$$

IV. 3 SUMMARY

If we regard p_z as an operator, i.e., if we regard $p_z(\zeta)$ as the result of performing the operation p_z on ζ, we may summarize the results of the preceding in operational notation.

Let x, y, u, v, be random variables with frequency functions defined by the operators p_x, p_y, p_u, p_v, and let z be a function of the variables x, y, u, v, viz.,

$$z = f(x, y, u, v) \tag{IV-80}$$

Then z will be a random variable whose frequency function will be defined by the operator p_z. We will tabulate the form of the operator p_z for various forms of the function, $f(x, y, u, v)$ (i.e., the operator f).

First, we will define the generalized convolution operator with respect to the function f of two variables, viz., $*_f$, as :

$$[p_x *_f p_y](\zeta) \equiv \int_{-\infty}^{\infty} p_x(\tau)\, p_y[f_y^{-1}(\tau, \zeta)] \left| \frac{\partial f_y^{-1}(\tau, \zeta)}{\partial \zeta} \right| d\tau \tag{IV-81}$$

where $f_y^{-1}(x, z)$ is the inversion of $f(x, y)$ with respect to y; i.e.,

given: $z = f(x, y)$

then: $y = f_y^{-1}(x, z)$ (IV-82)

The tabulation is as follows:

1. If $z = f(x, y)$ (IV-83)

$$p_z = [p_x *_f p_y] \tag{IV-84}$$

2. If $z = h[f(x, y)]$ (IV-85)

$$p_z = \left[(h^{-1})' \times \{[p_x *_f p_y](h^{-1})\}\right]$$

$$= [D \times [p_x *_f p_y] (h^{-1})] \tag{IV-86}$$

where D is the differential operator; i.e.,

$$D[\phi(x)] \equiv \phi'(x) \equiv \frac{d}{dx} \phi(x) \tag{IV-87}$$

The cross in equations (IV-86) indicates multiplication in the following sense; Given two operators, L_1 and L_2, and the variable (or function, or operator), z, then

$$L_1 L_2(z) \equiv L_1[L_2(z)] \tag{IV-88}$$

$$L_1 \times L_2(z) \equiv [L_1(z)] \times [L_2(z)] \tag{IV-89}$$

That is, the notation of equation (IV-89) indicates the successive application of the operators L_2 and L_1: first the operation L_2 is performed on z, and then the operation L_1 is performed on the result. The notation of equation (IV-89) indicates the product of the results of performing each of the operations L_1 and L_2 on z.

3. If

$$z = f[g(x), h(y)] \tag{IV-90}$$

$$\left.\begin{aligned} p_z &= \{[(g^{-1})' p_x(g^{-1})] *_f [(h^{-1})' p_y(h^{-1})]\} \\ &= \left[\{[D \times p_x] (g^{-1})\} *_f \{[D \times p_y] (h^{-1})\}\right] \end{aligned}\right\} \tag{IV-91}$$

4. If

$$z = f[g(x, y), u] \tag{IV-92}$$

$$p_z = \{[p_x *_g p_y] *_f p_u\} \tag{IV-93}$$

5. If

$$z = f[g(x, y), h(u, v)] \tag{IV-94}$$

$$p_z = \{[p_x *_g p_y] *_f [p_u *_h p_v]\} \tag{IV-95}$$

In the following particular cases, the convolution takes the forms shown:

6. If

$$z = f(x, y) = x + y \tag{IV-96}$$

$$p_z(\zeta) = [p_x *_f p_y](\zeta) = \int_{-\infty}^{\infty} p_x(\tau)\, p_y(\zeta - \tau)\, d\tau \tag{IV-97}$$

7. If

$$z = f(x, y) = x \cdot y \tag{IV-98}$$

$$p_z(\zeta) = [p_x *_f p_y](\zeta) = \int_{-\infty}^{\infty} p_x(\tau)\, p_y\left(\frac{\zeta}{\tau}\right) \frac{dt}{|\tau|} \tag{IV-99}$$

8. If

$$z = f(x, y) = \frac{y}{x} \tag{IV-100}$$

$$p_z(\zeta) = [p_x *_f p_y](\zeta) = \int_{-\infty}^{\infty} p_x(\tau)\, p_y(\zeta\ \tau)|\tau|\, d\tau \tag{IV-101}$$

9. If

$$z = f(x, y) = e^{x+y} \tag{IV-102}$$

$$p_z(\zeta) = [p_x *_f p_y](\zeta)$$

$$= \begin{cases} 0 & \zeta < 0 \\ \dfrac{1}{\zeta} \displaystyle\int_{-\infty}^{\infty} p_x(\tau)\, p_y(\ln\zeta - \tau)\, d\tau & \zeta \geq 0 \end{cases} \tag{IV-103}$$

10.

$$z = f(x, y) = x^y \qquad x \geq 0 \tag{IV-104}$$

$$p_z(\zeta) = [p_x *_f p_y](\zeta)$$

$$= \begin{cases} 0 & \zeta < 0 \\ \dfrac{1}{\zeta} \displaystyle\int_{0}^{\infty} p_x(\tau)\, p_y\left(\frac{\ln\zeta}{\ln\tau}\right) \frac{d\tau}{\ln\tau} & \zeta \geq 0 \end{cases} \tag{IV-105}$$

The preceding is predicated on the following assumptions:

1. p_x , p_y , p_u , p_v are continuous.

2. f , g , h , and their inversions, f^{-1}, g^{-1}, h^{-1}, are continu single-valued, and differentiable.

3. x , y , u , and v are statistically independent.

4. x , y , u , v , and z are real.